Aus dem

Lubecker Institut fur Experimentelle Dermatologie

Direktor: Prof. Hauke Busch

MOLECULAR PATHOGENESIS OF PAPILLARY THYROID CARCINOMA

Inauguraldissertation

Zum Erwerb des Doktorgrades

der Universitat zu Lubeck

-Aus der Sektion Medizin-

Vorgelegt von

Asma Almansoori

UAE, 2022

1. Berichterstatterin/Berichterstatter: Prof. Dr. Hauke Busch

2. Berichterstatterin/Berichterstatter: Prof.Dr.Christian Sina

Tag der mundlichen Prufung: 13- July-2022

Zum Druck genehmigt. Lubeck, den 13-July-2022

Promotionskommission der Sektion Medizin

Dedicated to cancer patients

1 Acknowledgment

First and most Praises to God, the Almighty, for providing me strength and blessings throughout my learning Journey.

Second, I would sincerely thank His Highness Sheikh Sultan Alqasimi for his unlimited educational opportunities and support. Second, my greatest gratitude to his excellency, Dr. Hassan al alalkeem Alzaabi, Prime minister of the ministry of presidential affairs, for his encouragement and support in completing my studies. Additional gratitude is to Sheikh Khalifa Hospital management for supporting me throughout this journey.

I would also like to express my deep and sincere gratitude to my supervisor, Dr.Rifat Hamoudi, for allowing me to do cancer research and providing me with unlimited resources throughout this research. I was very fortunate to learn new methodologies under his guidance. I would also like to extend my heartful thanks to his family for the long hours taken from them for discussion and follow-ups.

I cannot express enough thanks to Dr. Riyad Bendardaf for his continued support and encouragement. I genuinely offer my sincere gratitude for allowing me to do Thyroid research.

My completion of this project could not have been accomplished without the humble care of Dr.Hauke Busch. Thank you for offering me full support and guidance. I was very fortunate to have a golden opportunity to be trained on how to do bioinformatics with your team. Without your lab and your advice, this wouldn’t happen.

Exceptional thanks to Michael Olbrich for teaching me about Next-generation sequencing and data analysis from Scratch. His innovation and creativity are something that cannot be forgotten. Additional Thanks to Axel kunstner for helping in providing guidance and troubleshooting.

Truly I was overwhelmed with the humbleness and helpfulness of my supervisors in Sharjah and Lubeck. Greatest Thanks to Dr. Saleh Ibrahim for making things happen even under challenging conditions. Million Thanks for your guidance and mentor. I also want to extend my greatest thanks to Poorna Bhamidimarri for all the great help, my lab companion Mr.Surrendra Rawat, Amena Mahdami, Thenmizhi, and other members of SIMIR.

I am also extremely grateful to my parents for their patience, support, and sacrifices to complete my education.

Finally, to my loving and caring husband, my deepest gratitude and praises for the encouragement in tough times. Much appreciated and fully noted. My deepest thanks!

2 List Of Abbreviations

Abbreviation	Definition
ATC	Anaplastic thyroid cancer
BCL2	**BCL2** Apoptosis Regulator
BRAF	Gene on chromosome 7 promotes cell functions and division
FFPE	Formalin-Fixed Paraffin-Embedded
FTC	Follicular thyroid cancer
GLOBOCAN	Cancer global observatory
GSEA	Gene set enrichment analysis
KCNN4	Potassium Calcium-Activated Channel Subfamily N Member 4
KCNQ1	Potassium Voltage-Gated Channel Subfamily Q Member
MAPK	mitogen-activated protein kinase
NGS	Next-generation sequencing
Nthy-Ori-31	normal thyroid cell
PTC	Papillary thyroid cancer
PTEN	PTEN (Phosphatase And Tensin Homolog
RAS	small GTP-binding proteins for differentiation and growth
RET	transmembrane receptor and member of the tyrosine-protein kinase family of proteins
SSGSEA	single sample gene set enrichment analysis
TC	Thyroid cancer
TPC-1	thyroid cancer cell line
UAE-NCR	UAE-National Cancer Registry
VEGFR	vascular endothelial growth factor
ViaFect	Transfection Reagent
HIST3H3	Histone cluster 3
TLX3	T Cell Leukaemia Homeobox 3
ADAM9	ADAM Metallopeptidase Domain 9

OGT	O-Linked N-Acetylglucosamine (GlcNAc) Transferase
GREB1	Growth Regulating Estrogen Receptor Binding 1
LCM	Laser-capture microdissection
PI3K	Phosphoinositide 3-kinases
Qrt-PCR	Real-Time Quantitative Reverse Transcription PCR
T3	triiodothyronine thyroid hormone
CARNIVAL	CAusal Reasoning for Network identification using Integer VALue programming
DoRthEA	Discriminant Regulon Expression Analysis
GEO	geospatial concepts
PROGENy	Pathway RespOnsive GENes for activity inference
T4	Thyroxine thyroid hormone
TF	Transcription factor
KEGG	Kyoto Encyclopedia of Genes and Genomes
NFkB	nuclear factor-kappa B
DEGs	differentially expressed genes
PTK2B	protein tyrosine kinase 2 beta
CACNA1D	calcium Voltage-Gated Channel Subunit Alpha1 D
NAG	Non-aggressive
Met	metastatic
BRCA	breast cancer gene

Table of contents

_Toc108456234

List of Tables

List of Figures

3 Thesis Summary

Thyroid cancer is the top endocrine malignancy and the second most common female malignancy in the United Arab Emirates. Since thyroid cancer is a rare disease, only a few studies have investigated the molecular pathogenesis of the disease worldwide, with no studies for the UAE populations. To our knowledge, this study is the first to provide an insight into the molecular pathogenesis of papillary thyroid cancer (PTC) in the UAE. First, an epidemiological study was conducted on data collected from local and international platforms showing a steady increase in thyroid cancer incidence in UAE and worldwide. Thyroid cancer was also a female malignancy affecting the (35 – 39 years old) group more. Second, an in-silico analysis study was performed using bioinformatics techniques on publicly available transcriptomic studies of selected populations revealed several activated pathways, most importantly, the MAPK pathway, which was activated across different stages of PTC. The study also showed that KCNQ1, CACNA1D, KCNN4, EGFR, and PTK2B genes were associated with PTC progression. In vivo-validation of these genes using UAE-clinical biopsies showed more enrichment in the metastatic stage of PTC. Third, a whole transcriptomic analysis was performed using next-generation sequencing on UAE clinical biopsies also revealed MAPK pathway (MAPK6) involvement in PTC progression. Additional validation by genomic transfection of MAPK6 into thyroid cell lines was carried out and followed by transcriptomic analysis, which revealed the putative role of (MAPK6, HIST3H3, TLX3, ADAM9, OGT, GREB1) gens and (estrogen, vitamin D)pathways in driving PTC progression.

Furthermore, the Drug bank database related to expressed genes identified a variety of FDA-approved drugs that are currently being used to treat other medical conditions and may be useful in treating thyroid carcinoma. To sum,The primary oncogenic machinery that drives thyroid carcinogenesis constitutes the cooperation of cellular pathways such as MAPK, PI3K, VEGF, vitamin D, and estrogen, which are centrally driven by altered components. Therefore, a clearer understanding of the

underlying mechanisms and drivers of TC pathogenesis may lead to promising opportunities for novel drug discoveries and clinical strategies for treatment and management.

4 Zusammenfassung der Arbeit

Schilddrüsenkrebs ist das häufigste endokrine Malignom und das zweithäufigste Malignom bei Frauen in den Vereinigten Arabischen Emiraten. Da es sich bei Schilddrüsenkrebs um eine seltene Erkrankung handelt, haben nur wenige Studien weltweit die molekulare Pathogenese der Erkrankung untersucht, wobei es keine Studien für die Bevölkerung der VAE gibt. Nach meinem Kenntnisstand ist diese Studie die erste, die einen Einblick in die molekulare Pathogenese des papillären Schilddrüsenkrebses (PTC) in den VAE gibt. Zu diesem Zweck wurde zunächst eine epidemiologische Studie mit Daten von lokalen und internationalen Plattformen durchgeführt, die einen stetigen Anstieg der Schilddrüsenkrebsinzidenz in den VAE und weltweit zeigten. Es wurde auch festgestellt, dass Schilddrüsenkrebs ein weiblich prävalentes Malignom ist, das vor allem die Gruppe der 35- bis 39-Jährigen betrifft. Zweitens wurde eine In-silico-Analysestudie mit Hilfe von Bioinformatiktechniken an öffentlich zugänglichen Transkriptomstudien ausgewählter Populationen durchgeführt. Die Studien zeigten mehrere aktivierte Signalwege auf, vor allem den MAPK-Signalweg, der in verschiedenen Stadien von PTC aktiviert war. Die Studie zeigte auch, dass die Gene KCNQ1, CACNA1D, KCNN4, EGFR und PTK2B mit dem Fortschreiten von PTC in Verbindung stehen. Die In-vivo-Validierung dieser Gene anhand von klinischen UAE-Biopsien ergab eine stärkere Anreicherung im metastasierten Stadium des PTC. Drittens wurde eine vollständige Transkriptomanalyse mittels Next-Generation-Sequenzierung an klinischen Biopsien aus den Vereinigten Arabischen Emiraten durchgeführt, die ebenfalls eine Beteiligung des MAPK-Signalwegs (MAPK6) an der PTC-Progression ergab. Eine zusätzliche Validierung durch genomische Transfektion von MAPK6 in Schilddrüsenzelllinien, gefolgt von einer Transkriptomanalyse, zeigte die mutmaßliche Rolle von (MAPK6, HIST3H3, TLX3, ADAM9, OGT, GREB1) Genen und sowie von Östrogen und Vitamin D bei der Progression von PTC. Darüber hinaus wurden in einer pharmakogenetischen Analyse die sich auf exprimierte Gene bezieht, verschiedene von der FDA zugelassene Arzneimittel identifiziert, die derzeit zur Behandlung anderer Erkrankungen eingesetzt werden und auch für die Behandlung von Schilddrüsenkarzinomen nützlich sein könnten. Zusammenfassend lässt sich sagen, dass die primäre onkogene Maschinerie, die die Schilddrüsenkarzinogenese antreibt, eine enge Verbindung von zellulären Signalwegen wie MAPK, PI3K, VEGF, Vitamin D und Östrogen darstellt, die durch veränderte Komponenten zentral gesteuert werden. Ein besseres Verständnis der zugrundeliegenden Mechanismen und Triebkräfte der TC-Pathogenese könnte daher zu vielversprechenden Möglichkeiten für die Entdeckung neuer Medikamente und klinischer Strategien für die Behandlung und das Management führen.

5 Research Aims

Due to the absence of recent national studies on thyroid cancer in UAE, to our knowledge, this study is the first to provide an insight into the molecular pathogenesis of papillary thyroid carcinoma in UAE and selected populations. To do so, we undertook the following:

- Carried out an epidemiological study by analyzing the incidence of thyroid cancer among UAE populations by ethnicity, gender, and age and compared them to worldwide statistics to identify epidemiological trends of the malignancy. Additionally, we projected thyroid cancer estimates for the upcoming thirty years, which may help establish cancer baselines and monitoring strategies to address future epidemics.
- Performed an in-silico analysis of publicly available data that identified activated genes and pathways involved in papillary thyroid cancer pathogenesis across the biopsies of selected populations (i.e., Ukraine, South Korea, and Brazil). This was undertaken using bioinformatics techniques and validating them with an independent cohort of TC samples.
- Conducted a next-generation sequencing and bioinformatics analysis on UAE clinical biopsies of thyroid cancer patients to identify molecular markers and pathways involved in PTC pathogenesis.
- Executed an in vitro validation of genes of interest (MAPK6) identified in the previous aims to validate their expression in normal and malignant cell lines, using functional genomics transfection techniques.
- Highlighted the gaps in the current estimates that are worth addressing for future studies to establish an accurate epidemiological profile for a strong health information system that fits with international health agendas.

6 Study Workflow Summary

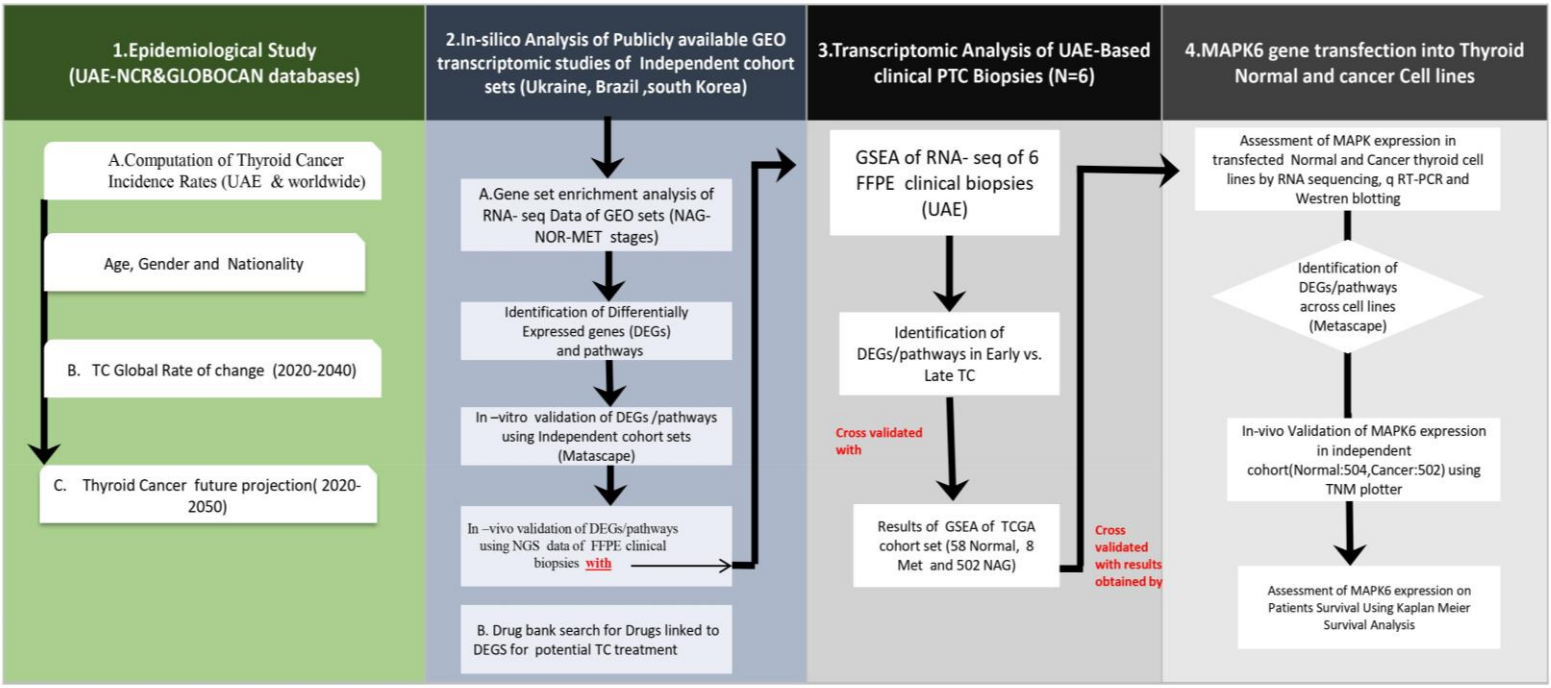

Figure 1.Work-Flow chart of study's design. Abbreviations: TC;thyroid cancer,GEO;gene expression omnibus, NAG;non aggressive,NOR;normal,MET; metastatic,DEGs; differentialy expressed genes,FFPE;formalin fixed paraffin embedded, GSEA;gene set enrichment analysis; TCGA ;the cancer genome atlas.

7 List of scientific publications

Our study is based on the content of the following papers:

1. Almansoori et al. **Identifying Diagnostic and Prognostic targets for Papillary Thyroid Carcinoma through mining Gene Expression BIG Datasets using Adaptive Filtering and Advanced Bioinformatics Algorithms**.Published 14th International Conference on Developments in eSystems Engineering (DeSE), 2021. https://ieeexplore.ieee.org/document/9719384

2. Almansoori et al. **In silico Analysis of Publicly Available Transcriptomic Data Identifies Putative Prognostic and Therapeutic Molecular Targets for Papillary Thyroid Carcinoma**. International Journal of General Medicine, Published 18 March 2022, **DOI** https://doi.org/10.2147/IJGM.S345336

3. Almansoori et al. **Thyroid cancer incidence in the United Arab Emirates is associated with younger age and gender: A retrospective study**. F1000 Research. , published on March 2022, https://doi.org/10.12688/f1000research.76121.1

4. Almansoori et al. **Transcriptomic analysis from archival tissue of UAE patients reveals the involvement of MAP kinase-related pathways in papillary thyroid carcinoma pathogenesis**. European Journal of Medical Research. In review

8 INTRODUCTION

8.1 Thyroid Gland (TG)

8.2 Embryology and Anatomy

The thyroid gland is a small, butterfly-shaped bi-lobular gland located at the anterior side of the neck and below the larynx. The two lobes are connected by a narrow strip called an isthmus. Thyroid tissue appears as small lobules enclosed by connective tissue. Each lobule contains small follicules that act as a primary site for thyroid hormone storage (Figure 2). In healthy adults, the thyroid gland is hardly palpable. A swollen or enlarged thyroid gland can indicate a pathological condition or iodine deficiency(3). At approximately the sixth or seventh week of gestation, the thyroid gland is the first endocrinal organ to develop. It originates embryologically from the neural crest and the primitive pharynx (4). The bulk of the gland originates from the primitive pharynx, whereas the dorsolateral sides of the gland arise from the neural crest. The TG becomes functionally mature by the end of the twelfth gestational week (5, 6).

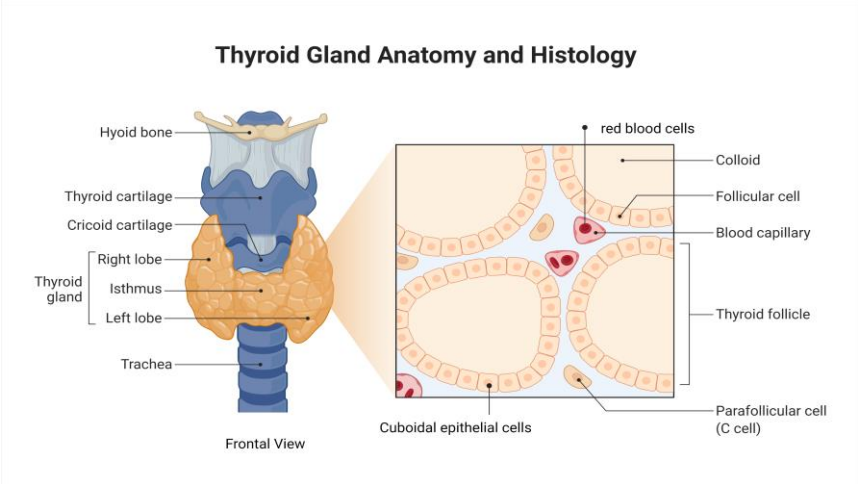

Figure 2. Thyroid Gland Anatomy. Thyroid gland is composed of two types of cells: follicular and parafollicular cells. Medullary thyroid cancer originates from parafollicular cells. Papillary and follicular thyroid cancers originate from follicular cells

8.2.1 Physiology

The thyroid gland is a hormone-producing gland that controls the metabolism, growth, and development of many tissues in the human body(Tablel 1)(7). It regulates many functions by releasing hormones such as triiodothyronine (T3), calcitonin, and tetraiodothyronine/thyroxine (T4). Together, the thyroid gland, hypothalamus, and anterior pituitary gland form a hypothalamic-pituitary-thyroid axis responsible for releasing the thyrotropin-releasing hormone (TRH), T4, and the thyroid-stimulating hormone (TSH) that establish the self-regulatory circuits needed for homeostasis. Thyroid hormones are usually bound to protein transporters; less than 0.2% of thyroid hormones (such as free T4) are active and unbound. (T4) are transported by thyroxine-binding globulin (TBG), while a transthyretin transporter transfers thyroxine and retinol. Upon reaching the targeted site, T4 and thyroxine dissociate from their transporting protein and enter cells through mediated transport or diffusion. T4 or thyroxine then binds to either the nuclear α or β receptor in the targeted tissue, activating the specific transcription factor and its corresponding genes and cellular pathways(8). Transcription factors specific to thyroid receptors have a higher affinity for T3 than T4; thus, T4 is typically found to be inactive and unbound(7). Thyroid hormones are finally degraded by glucuronidation and sulfation in the liver and excreted through the bile. Thyroid Hormone biosynthesis is illustrated in (Figure 3).

Table 1 . Thyroid Hormones Functions

Summary of Thyroid Hormones Physiological Functions
Increasing basal metabolism
Promoting lipid synthesis required for metabolism
Stimulation of carbohydrates metabolism
Protein anabolism/catabolism
Catecholamines permissiveness
Synergistically bone growth stimulation in early childhood
Neural maturation in prenates
Regulation of ovulation, menstruation, and fertility

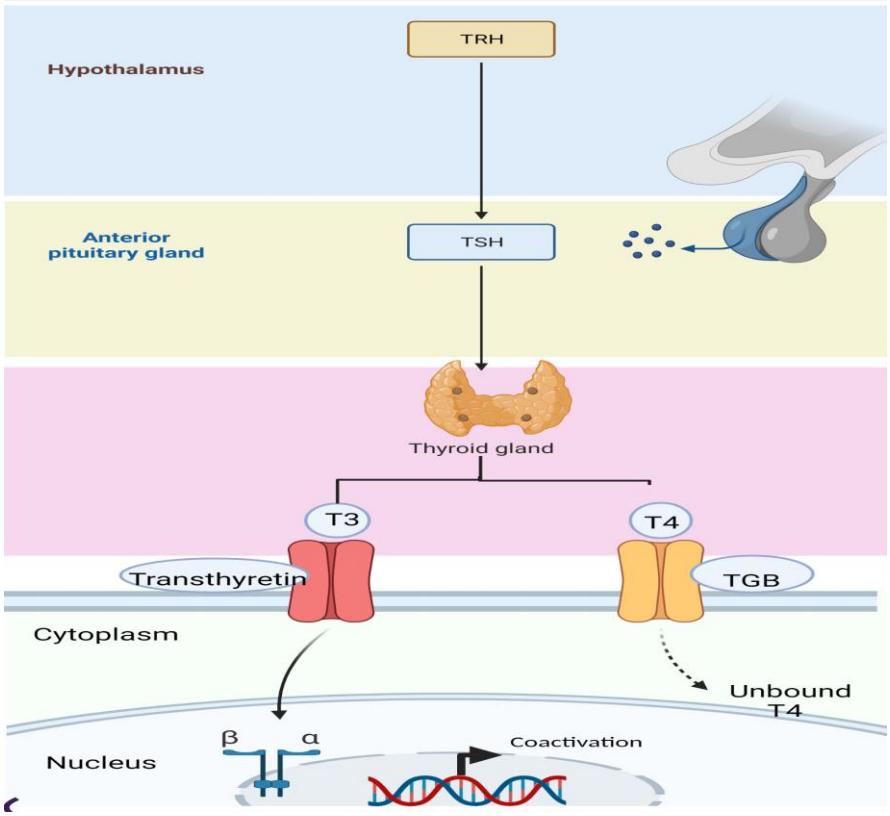

Figure 3. Thyroid Hormone (TH) Biosynthesis. TH synthesis starts when hypothalamus produces thyrotropin-releasing hormone (TRH) which stimulates pituitary gland to secrete thyroid-stimulating hormone (TSH).TSH stimulates Thyroid gland to produce thyroid hormones triiodothyronine (T3) and thyroxine (T4).This mechanism is regulated by negative feedback by thyroid hormones itself by acting on pituitary gland and Hypothalamus .Arrows indicates hormone release.Created with Biorender.com.

8.2.2 Pathophysiology

Most thyroid disorders arise from the deregulation of the hormones that the thyroid gland produces. Disorders can vary from a small, benign goiter to life-threatening thyroid cancer. Thyroid disorders associated with hormone imbalance include hypothyroidism(e.g., Graves' disease, sub-acute thyroiditis) and hypothyroidism (e.g., Hashimoto's thyroiditis) (Table 2)(9), but the true association between thyroid hormone imbalance and thyroid cancer development is still under investigation. Previous in-vitro studies and animal models have investigated the role of T3 and T4 in promoting tumor genesis in breast, prostate, gynaecological, renal, and colorectal cancers with only minor reference to thyroid cancer (Table 2) (10). An in vitro study by Mousa et al. revealed that T3 and T4 promote proliferation and a Ras/MAPK signaling pathway in thyroid cancer (11). Another in vivo study conducted by Yeh et al. demonstrated that patients with hyperthyroidism due to the overproduction of thyroid hormones are at a higher risk of

developing thyroid cancer(12). Furthermore, a study conducted by Yalcin et al. on the effect of tetraiodothyroacetic acid (tetrac) and L-thyroxine analog on human medullary thyroid cancer samples revealed that tetrac has an inhibitory effect on angiogenesis induced by fibroblast growth factor (FGF) and vascular endothelial growth factor (VEGF)(13). Additionally, tetrac blocked angiogenesis and cancer cell proliferation initiated by the thyroid hormone on alpha v beta3 integrin at hormone receptor (14). Another updated study conducted by Yalcin et al. on human follicular thyroid cancer cell line (FTC-236) and xenograft mouse models demonstrated that tetrac and tetrac nanoparticles (NP) had arrested tumor growth and associated angiogenesis, suggesting its inhibitory effect on follicular TC(15).

Table 2. Preclinical Investigations of Thyroid Hormones in selected cancers(10).

Cancer Type	Studies Type	Thyroid Hormones involved	Receptors Involved/	Hormone Effect
Breast	In Vitro	T3 (10–13) and T4 (14)	Integrin avb3, ER, TR, and membrane receptor	T3 promoted cell migration, proliferation, chemosensitization, and apoptosis.
Prostate	In Vitro	T 3&T 4	integrin avb3, downregulated BTG2 and upregulated c-fos	T3 Promoted proliferation, and T4 enhanced cell migration
Gynaecological(cervix)	In Vitro	T4	Membrane receptors	T4 activated MAPK pathway
Renal	In vitro	T3 & Tetrac	TR & integrin avb3	T3 promoted cell proliferation
Colon	In vitro	T 3&T 4	integrin avb3	T3 stimulated differentiation and growth. T4 promoted PDL1 expression and cell proliferation
Thyroid	In vitro	T 3&T 4	integrin avb3	T3&T4 promoted proliferation

Table 3. Thyroid Gland Disorders (16-18).

Disorder	hyperthyroidism	Hypothyroidism
Causes	Overproduction of T3 and T4 and decrease of TSH. Other causes: include Grave's Disease and thyrotrophic adenoma, which leads toT3/T4 increase and TSH decrease.	Primary Hypothyroidism: decreased T3/T4 levels production and increased TSH. Secondary Hypothyroidism: decreased TSH and T3/T4 due to pituitary disorders. Tertiary hypothyroidism: decreased TRH, TSH, and T3/T4 levels. Due to hypothalamus dysfunction. Other causes: Hashimoto Thyroiditis
Symptoms	▪ Increased thermogenesis due to increased Na+/K+-ATPase. ▪ Cardiac output increases. ▪ Tachycardia ▪ Musculoskeletal tremors ▪ Neuropsychiatric symptoms ▪ Diffuse goitre ▪ Onycholysis	• Decreased metabolic rate(Bradycardia, Poor appetite, Myopathy, Cold intolerance, etc. • Generalized myxoedema(voice hoarseness, puffy appearance, Myxedematous heart disease)
Associated conditions	▪ Excess Iodine syndrome ▪ Thyrotrophic pituitary adenoma ▪ Toxic multinodular goitre ▪ Jod-Basedow phenomenon.	▪ Postpartum thyroiditis ▪ Subacute thyroiditis ▪ Iodine deficiency ▪ Riedel thyroiditis ▪ Wolff-Chaikoff effect
Treatment	▪ Antithyroid drugs(19): • Lithium, Propylthiouracil, Amiodarone. ▪ Beta-Blockers for thyrotoxicosis	Thyroid hormone replacement therapy

8.3 Thyroid Cancer Overview

Cancer, the ancient disease-causing human body cells to grow irrepressibly, is considered among the top chronic illnesses that cause death and disability worldwide. The earliest evidence of cancer was discovered among fossilized bones of ancient Egyptian human mummies; an old textbook dated 3000 BC referred to as the "Edwin Smith Papyrus" described eight cases of breast tumours removed by fire drill cauterization (20). Most interestingly, ancient Egyptians annotated cancer in their manuscripts as "there is no treatment''!

8.3.1 Definition and Classification

Thyroid cancer (TC) refers to malignant neoplastic cells arising from follicular or parafollicular cells of the thyroid gland. TC can be classified into several distinct types, including differentiated (e.g., papillary, follicular, or Hürthle cell cancer), undifferentiated (anaplastic), medullary, and primary thyroid lymphomas(Table 4)(21). Papillary, follicular, and anaplastic variants of TC arise from follicular cells, whereas the medullary variant arises from parafollicular cells of the thyroid gland. Well-differentiated TC (follicular and papillary forms) are usually curable with a good prognosis. In contrast, poorly differentiated TC (anaplastic form) is more aggressive, less common, and associated with a poor prognosis. Neuroendocrine medullary TC has an intermediate prognosis compared to well- and poorly-differentiated TCs (Table 4)(22, 23).

Table 4 .Thyroid cancer classifications with recommended treatments (2, 22)

Tumor Subtype(24)	Cellular Origin	Occurrence %	Overall Survival (25)	Treatment(5)
Papillary	Follicular thyroid cells	80	10-year survival: 74–93%	thyroidectomy/^{131}I therapy/TSH suppression with thyroxine
Follicular	Follicular thyroid cells	10-15	10-year survival 43–94%	thyroidectomy/^{131}I therapy /TSH suppression with thyroxine
Medullary	Parafollicular thyroid cells- C cells	2	65–89%(26)	Total Thyroidectomy /palliative chemotherapy and doses of L-thyroxine

Tumor Subtype(24)	Cellular origin	Occurrence %	Overall Survival (25)	Treatment(5)
Anaplastic	Follicular thyroid cells	2	4–5 months from diagnosis	Surgery: tracheostomy/Chemotherapy
Follicular Thyroid Adenoma	Follicular thyroid cells	Benign	-	Thyroid lobectomy and isthmusectomy
Poorly differentiated thyroid cancer (PDTC)	Follicular thyroid cells	5-10	-	surgery, radioactive iodine, and radiation therapy
Thyroid Primary Lymphoma	Lymphocytes	<1	80%(27)	Chemotherapy/radiation therapy
Metastasis to the Thyroid gland from other organs	Non-thyroid cells	<1	-	total thyroidectomy and L-thyroxine doses

8.3.2 Papillary Thyroid Carcinoma

Histology and Classification: One of the most common forms of thyroid cancer is papillary thyroid carcinoma (PTC), accounting for more than 80% of all thyroid cases. It is associated with a good prognosis. PTC is an epithelial malignancy-exhibiting follicular cell differentiation with distinguishing nuclear aspects such as altered nuclear dimensions, fragmentation, and overlapping chromatin migration and clearing(Figure 4)(28). Histologically, the tumor appears as an irregular solid mass with 2-3cm lesions that tend to grow slowly but may present as cystic features in rare circumstances. The most common identifier of PTC is its capability to invade adjacent lymphatic structures, causing regional node metastasis and multi-focal lesions. However, venous invasion and cervical metastasis are rarely occurring. According to the WHO classification of endocrine tumors, PTC has sixteen variants, all with different histological features. The most common histotypes include classic papillary, follicular, microcarcinoma, and tall cell variants. Less common variants include columnar cell, oncocytic, solid, and diffuse sclerosing (29) (Table 5).

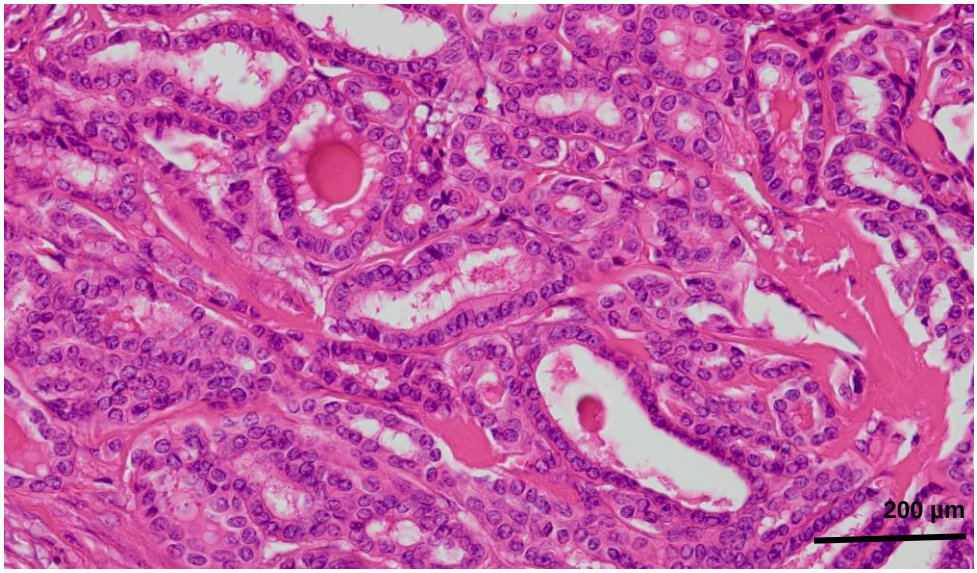

Figure 4.Microscopic features of classic PTC (H&E x40).Typical nuclear features include: nuclear overlapping ,enlargement ,irregularity of nuclear membrane ,nuclear clubbing, chromatin Migration and papillae fibro vascular cores

Table 5. Papillary thyroid carcinoma variants (29).

Variants	
Follicular variant	Columnar cell
Oncocytic	Solid
Diffuse sclerosing	Cribriform morula
Macrofollicular	Clear cell
Tall cell	prominent hobnail PTC
Papillary microcarcinoma	fasciitis-like stroma PTC
Conventional	Combined PTC and Medullary forms/Combined PTC with Anaplastic

8.3.3 Epidemiology

Thyroid cancer is the most common endocrine malignancy worldwide. In 2021, an estimated 44,280 adults in the United States were diagnosed with thyroid cancer, making it the most rapidly increasing cancer in the US. The overall incidence of thyroid cancer has increased significantly in both genders. The increased incidence can be attributed to improved detection by highly sophisticated and sensitive screening ultrasounds. TC is diagnosed earlier than most adult cancers, and females are three times more likely to develop the disease than males(30).

Over the last few decades, thyroid cancer incidence has steadily increased, although the mortality rate remains stable. In 2021, TC was found to be the fifth most common cancer among both men and women and the seventh most common malignancy in females in the United States. Researchers explained that the increase in incidence might be caused by over-diagnosis resulting from highly sensitive diagnostic tools used to detect small cancers. The rate of increase was approximately 1.9% over the last ten years, with an annual mortality rate of 0.7% between 2007 and 2016. According to National Cancer Institute statistics, thyroid cancer accounts for 3.0% of all cancer types, with an annual prevalence rate of 15.8 per 100,000 among males and females. The highest incidence rate was observed among those aged 45 to 54, with a median of 51 years at onset of diagnosis; the highest mortality rate was observed among those aged 75 to 84, with a mortality rate of 27.4% and a median of 73 years at death. In the United Arab Emirates, thyroid cancer follows the global trend of being the top endocrine malignancy and the second most common female cancer(31,32). According to the Ministry of Health and Prevention (MOHAP) and the National Cancer Registry (UAE-NCR), TC is the third most common cancer in both genders, aside from breast and colorectal cancers. A significant increase in incidence was observed between 2011 and 2017, when the TC rate peaked from 4.37% to 9.99% among all newly diagnosed cancer cases. Additionally, the Global Cancer Observatory (GLOBOCAN) declared a total of 405 (8.4%) per 100,000 thyroid cases were diagnosed in UAE, with a mortality rate of 1.7% in 2020(30, 33). Age-standardized rate (ASR) per female was 12.5/100,000 for females and 2/100,000 for males in UAE. In the neighboring Gulf Cooperation Countries (GCC),

thyroid cancer is the fifth most common cancer in both genders and the second most common female malignancy. Between 1998 and 2007, a total of 5587 (5.9%) newly-diagnosed TC cases were registered with an overall (ASR) incidence rate of 1.8/100,000 in males and 5.9/100,000 in females. Additionally, it was projected that the incidence of TC will continue to rise by 63% in females and 24% in males in the upcoming decade(34-36).

8.3.4 Risk factors

According to the American Cancer Society, developing thyroid cancer is associated with age, gender, genetics, radiation exposure, a low-iodine diet, race, and pre-existing breast cancer(37). Females are three times more likely to develop cancer than males for unclear reasons. The onset of TC in females begins at an earlier decade of life than in males(38, 39). TC can occur at any stage of life, but females tend to develop it in their thirties and forties, while men are most at risk in their sixties and seventies. Other risk factors include genetics and inherited diseases in families(40). Although TC's hereditary predisposition is high, over 90% of diagnosed cases are sporadic due to somatic mutations(16).

8.3.4.1 Familial Predisposition

In familial medullary thyroid cancer (FMTC), two out of ten diagnosed cases are due to inheriting an abnormal RET gene(41). FMTC may manifest on its own or with other tumors, forming multiple endocrine neoplasia type 2 (MEN 2). Patients with the inherited familial disease are more likely to develop thyroid cancer, such as familial adenomatous polyposis (FAP), Cowden disease, Carney complex, Type 1, and familial nonmedullary thyroid carcinoma (42)(Table 6).

Table 6. Familial medical conditions associated with thyroid cancer development(43-46).

Inherited medical condition	Mutations	Remarks
Familial adenomatous polyposis (FAP)/Gardner syndrome	APC gene	• Carriers may develop colon polyps/cancer and are at higher risk of developing papillary thyroid carcinoma.
Cowden disease	PTEN gene	• Patients are at increased risk of developing hamartomas, breast, uterine, and thyroid cancers.
Carney complex, type I	*PRKAR1A*	• Patients at risk of hormonal deregulations and developing papillary and follicular TC.
Familial non-medullary thyroid carcinoma/ papillary histotype (FPTC)	Mutations of genes on Chromosome 1 and chromosome 9	• It runs in some families mostly at an earlier age.
Medullary cancer-associated multiple endocrine neoplasia type 2 (MEN 2) & MEN 2b subtypes	RET gene	• The more common Subtype, MEN 2a, occurs in adrenaline-producing pheochromocytomas and parathyroid tumors. • MEN 2b occurs within pheochromocytomas and neuromas of the tongue.

8.3.4.2 Radiation Exposure

Over the last two decades, increased attention has been directed toward thyroid cancer due to Ukraine's Chornobyl nuclear plant accident in 1986. Belarus and the western region of Russia were also affected. There was a significant increase in reported cases among children and adolescents exposed to radioactive iodine isotopes near the nuclear plant. Between 1992 and 2000, a total of 3000 cases of TC were observed among children aged 0 to 14, making them among the most affected group due to ^{131} contaminated cow's milk (47, 48). Radiation therapy used in treating breast cancer or Hodgkin's disease is associated with a higher risk of TC, especially if the treatment protocol involves radiation to the head and neck region. Conversely, dental x-rays, routine mammograms, and chest x-rays are not highly associated with TC development, yet radiation exposure should still be minimized and used only for medical necessities (49). A diet low or high in iodine is another risk factor for developing TC. The element iodine is not only vital for thyroid hormone synthesis (T3 and T4) but also critical in the prevention of mental retardation and impaired cognitive development in newborns (50). Diets higher in iodine increase the likelihood of developing papillary thyroid cancer, whereas an iodine-deficient diet increases the risk of developing follicular TC, goitre, hypothyroidism, and myxedema coma (51). The history of iodine-fortified salt started in the early 1930s when David Marine (US) first introduced the connection between thyroid problems and iodine deficiency and developed the innovative approach of using salt to increase iodine uptake(50). In the United States, for example, most people get enough iodine in their diet due to strict consumer laws that enforce the use of iodized salts in the food industry. In France, on the other hand, using iodized salt in food processing is prohibited; consequently, the general population may be deprived of their potential iodine needs. Despite the recent progress in the iodized salt food industry in India, health reporters claim that more than 350 million individuals will face iodine deficiency (Figure 5). Interestingly, the selected populations in our study: Ukraine (Insufficient intake) and South Korea (excess), are considered to have inadequate iodine intake (less or more than 100-299 ugL/L)(Figure5); this can draw a putative link to iodine intake and TC in Ukraine and South

Korea, but not for UAE and brazil where no association was found between iodine intake and TC development.

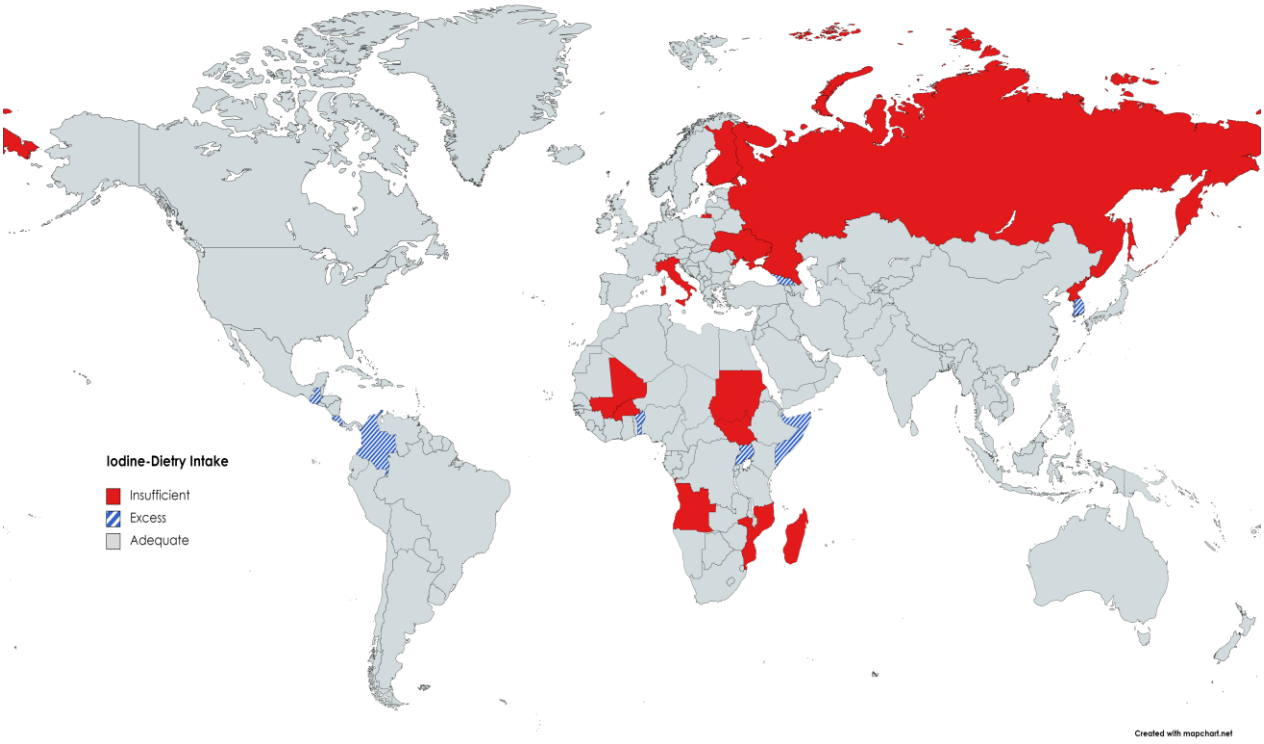

Figure 5. World map representations of Iodine diet status. Our study populations represent the following: UAE has an Adequate Iodine intake, Ukraine has insufficient intake, and South Korea has an Excess Intake. Created with mapchart.net.(50)

*8.3.4.3 **Race Risk factor***

Race may be a risk factor for developing several types of cancer, including thyroid cancer. TC risk is highest in Caucasians, followed by Pacific Islanders/Asians, Native Americans (Indians/Alaskans), and Blacks. Additionally, TC incidence is higher in non-Hispanic males and females than in Hispanics (Table 7) (52, 53).

Table 7. Thyroid cancer incidence per Race between 2007- 2011(52)

Race	Incidence for both genders/100.000
Caucasian/Whites	26.7
African Blacks	14.6
Pacific Islanders/Asians	24.2
Native Americans (Indians/Alaskans)	15.2

A recent study by Lal et al. revealed the association between TC and radiation therapy in breast cancer survivors. Researchers have suggested that patients with invasive ductal carcinoma are at a higher risk of developing TC within the first five years after their initial diagnosis. These patients are urged to employ screening measures for early detection. The study has also shown no difference in the risk of developing TC between receptor-positive or metastatic forms. Furthermore, the investigators showed that TC that develops subsequent to breast cancer is usually more aggressive, smaller type, and occurs at an older age than in patients who had TC only (62yrs versus 45)(54).

8.3.5 Clinical Presentation, Diagnosis, and Staging

PTC usually presents as an asymptomatic, painless thyroid nodule in the neck that may arise from the thyroid gland itself (67%), from both cervical nodes and thyroid (13%), or nodes only (20%). Patients may also present with hoarseness, dysphagia, or trouble breathing. Many cases of TC are accidentally diagnosed when performing imaging for different medical conditions involving the head and neck region. In geriatric populations, a sudden onset of hoarseness coupled with rapid nodule growth is an early sign of anaplastic TC if other conditions are ruled out. (16, 17, 39, 40, 51, 55, 56).

Thyroid nodule evaluation follows a standard principle that starts with a medical history review, clinical examination, and biochemical testing of TSH and T4. Based on the results obtained, fine-needle aspiration cytology is chosen as a gold standard for TC diagnosis when coupled with ultrasonography. Cytology results are often classified by the Bethesda system for reporting thyroid cytopathology. Other factors that influence TC diagnosis include age, family history of TC, and radiation exposure. Medical diagnostics that can be used in thyroid cancer are illustrated in (Table 8) (21, 57).

Table 8 . Thyroid cancer Diagnostics.

Thyroid cancer test	Remarks([5](), [16](), [17](), [21](), [24](), [28](), [39](), [40](), [51](), [58](), [59]())
Physical Examination	• Examination of the thyroid gland, neck, and lymph nodes for unusual swelling or growth. Laryngoscopy might be recommended before interventional surgery.
Blood tests	• Molecular markers test can be performed if FNA results are unclear. BRAF/ NTRK and RET/PTC are primarily investigated. • Thyroid T3&T4 and TSH levels test. • Tg and TgAb test to measure thyroglobulin levels after radioactive treatment or surgery. A higher level of Tg indicates residual cancer activities. • Carcinoembryonic antigen (CEA) and calcitonin levels test if medullary TC is suspected. • *RET* proto-oncogenes test in the familial history of medullary TC.
Ultrasonography	• To differentiate between solid (cancerous mass) and benign fluid-filled sacs(cysts)
Biopsy	• The gold standard for actual diagnosis (FNA). • More invasive procedures, including Core Biopsy and Lobectomy, might be helpful if the FNA diagnosis was unclear.

Thyroid cancer test	Remarks
Radioiodine scanning	• Whole-body scan using radioactive iodine I-123 or I-131. Identified thyroid regions with low radioactivity can be benign or cancerous.
x-ray	• It helps in detecting metastasis to the lungs, especially in Follicular TC.
Computed tomography (CAT /CT)	• Complimentary 3-dimensional imaging is used to detect tumorous tissues omitted by ultrasound and metastasis to the lung and liver. • Patients with MTC have a higher risk of developing abdominal endocrine tumours; thus, abdominal CT scan is also recommended.
Positron emission tomography scan (PET)	• An alternative to radioiodine scan and found to be useful when coupled with CT scan. • Injected radioactive sugars are consumed more by cancer cells, therefore, determining tumour's location and size.

8.3.6 Survival

Fortunately, PTC is curable and usually associated with a good prognosis if diagnosed early. The prognosis is generally better for patients below 45 than those over 45 years old. SEER-stage five-year relative survival rate reported between 2011 and 2017 by the American Cancer Society and the National Cancer Institute reveals promising estimates that may help understand the likelihood of treatment success. (Table 9)(23, 25, 28, 55, 60-62)

Table 9. PTC SEER-stage five-year relative survival rates(63, 64).

PTC SEER staging	Relative survival Rates (5 years)
Localized	approximately 100%
Regional	99%
Distant	75%
Accumulative SEER stages	Near 100%

8.3.7 Treatment

8.3.7.1 Surgery

For the best outcome, treatment should involve multidisciplinary strategies and efforts. Treatment options are best tailored to the type and stage of thyroid cancer, the patient's health and overall preference, and the likelihood of potential side effects. Although TC is curable with most classical methods in the early stages, useful treatment options become less beneficial as the disease progresses. Surgery is the primary option for TC treatment. The goal of surgery is to remove tumor tissues and marginal healthy tissues. The most common surgical options include lobectomy, subtotal thyroidectomy, and total thyroidectomy (Table 10). (5, 15, 16, 22, 25, 28, 45, 51, 57, 65-77).

Table 10. PTC common surgical treatments (22, 28, 77)

Common surgical interventions	Remarks
Lobectomy.	Removal of cancerous thyroid nodule
Subtotal thyroidectomy	Removal of the entire gland but a small portion of the gland
Total thyroidectomy	Removal of the entire gland
Classic thyroidectomy	A conventional method of basal or medial incision for direct access to TG.
Endoscopic thyroidectomy	Same as classic, but scope assisted and under the surveillance of video monitors.
Robotic thyroidectomy.	Less recommended. -Indirect access to the thyroid gland via armpits or hairline with a robotic tool to excise tumour's tissues.

8.3.7.2 Targeted therapies

Generally, thyroid cancers are well known to respond poorly to chemotherapy. While standard chemotherapy attacks all rapidly growing cells, there have been promising discoveries of targeted drugs that can attack specific sites on cancer cells, limiting damage to vital, healthy cells. The latest FDA-approved targeted drugs for papillary thyroid and follicular carcinomas include sorafenib (Nexavar),lenvatinib (Lenvima,E7080), larotrectinib(Vitrakvi),entrectinib (Rozlytrek), pralsetinib (Gavreto), and selpercatinib (Retevmo) (Table11) (39, 78).

Table 11. Recent FDA-approved drugs for Thyroid cancer treatments (79-82)

FDA Approved Drugs	Year approved	Remarks	Common Side effects
Sorafenib (Nexavar),	2013	For recurrent or later stage DTC	Skin reactions, fatigue, HBP, diahrrea ,weigh loss
Lenvatinib (Lenvima, E7080),	2015	later stage DTC when iodine I-131 therapy has failed.	HBP, nausea, weight loss, reduced appetite
Larotrectinib (Vitrakvi)	2018	For PTC and FTC with *NTRK* fusion mutations	Dizziness, diarrhoea, constipation, vomiting, fatigue, and nausea
Entrectinib (Rozlytrek)	2019	For PTC and FTC with *NTRK* fusion mutations	Taste problems, shortness of breath, memory problems, dizziness, fever, and visual problems
Pralsetinib (Gavrecto)	2020	For Metastatic advanced *RET* fusion TC	Hypertension, constipation, fatigue, muscular pain, neural pain.
Selpercantinib (Retevmo)	2020	Metastatic advanced PTC with *RET* fusions	Dry mouth, fatigue, cholesterolemia, constipation and swelling, platelets, and enzymes imbalance

9 Materials and Methods

9.1 Materials

9.1.1 Devices and Consumables

- 30-300 µL Multichannel micropipette (Thomas Scientific, United States).
- NanoDrop 2000 spectrophotometer (Thermo Scientific, United States)
- Leica LMD 6 Laser Capture Microdissection (LCM) system (Leica Microsystems CMS GmbH, Germany)
- Centrifuge 5804R (Eppendorf, Germany)
- DFC7000 T camera for the LCM system (Leica, Germany)
- ScanVac Maxivac Beta evaporator (LABOGENE, Denmark)
- Ion S5™ System (Thermo Fisher Scientific, United States).
- Ion OneTouch™ 2 Instrument (Thermo Fisher Scientific, United States).
- QuantStudio 3 real-time PCR (Applied Biosystems, United States)
- Olympus BX43 microscope (Olympus Corporation, Japan)
- Olympus IX53 inverted microscope (Olympus Corporation, Japan)
- Olympus DP75 camera (Olympus Corporation, Japan)
- S1 Pipet Filler (Thermo Scientific, United States)
- 200 µL PCR tubes (Axygen, Corning, United States)
- 96 Well PCR plates and caps (Axygen, Corning, United States)
- T75 cell culture flasks (Thero Scientific, USA)
- Qsonica (coleparmer,USA)

9.1.2 Chemicals and Reagents

- AMPHOTERICIN B UG/ML 50ML (ISRAEL)
- Trypsin-EDTA (0.05%), (Thermo Scientific; United States)
- Xylene (Thermo Scientific; United States)
- Trypan blue solution (Sigma-Aldrich, Germany)
- Ethanol (Honeywell, Germany)
- Nuclease-free water (Sigma-Aldrich, Germany)
- 0.25 g agarose powder (Sigma-Aldrich, USA)
- Syber safe (New England Biolabs,USA)
- Glycine (Sigma-Aldrich, Germany)
- Tris-borate-EDTA buffer (Thermo Scientific; United States)

9.1.3 Kits

- Plasmid Maxiprep system (Qiangen)/ Qubit quantification kit (Invitrogen, USA)
- PCR kit (Biosystem, USA)
- TRIzol RNA Isolation kit ((Thermo Scientific; United States)
- RecoverAll FFPE RNA Isolation kit
- SYBER green qPCR primers (e-oligos, United States)
- SYBR® safe DNA gel stain (Invitrogen, United States)

9.1.4 Solutions

Solution/Mixture Name	Composition
FACS buffer	▪ 2% fetal bovine serum ▪ Phosphate buffer saline
Agarose Gel 1%	▪ 0.25 agarose powder ▪ 4 ul syber safe ▪ 25 ml TBE buffer
10x Transfer buffer (1 L at 5C):	▪ 30.27 g of Tris-base ▪ 144 g of glycine ▪ Up to 1 L of distilled water o (pH equivalent to 8.60)
1.5 M Tris-chloride (150 mL) (stored at 4˚C)	▪ 27.23 g of Tris-base ▪ Approximately 150 mL of distilled water ▪ (pH equivalent to 8.8)
10% Ammonium persulfate (stored at -20˚C,1 ml)	▪ g of ammonium persulfate ▪ 1 ml of distilled water
10x Running buffer (1 L):	▪ 30.3 g of Tris-base ▪ 144.1 g of glycine ▪ 10 g of sodium dodecyl sulfate ▪ 1 L of distilled water (pH adjusted to 8.3)
1x Tris borate EDTA (TBE) buffer (1L, stored at room temperature)	▪ 100 ml of 10x Tris borate EDTA buffer ▪ - 900 ml Distilled water
10x Tris-buffered saline (TBS) buffer (1L) (store at 4˚C):	▪ 24.23 g of Tris-base ▪ 80.06 g of sodium chloride ▪ - Up to 1 L of distilled water (pH :7.6)
1.5 M Tris-Chloride (150 mL at 4 C):	▪ 27.23 g of Tris-base ▪ 150 ml of distilled water (pH adjusted to 8.8)

0.5M Tris-chloride (150 ml, pH at 4°C , ph adjusted to 6.8)	▪ g of Tris-base/150 ml of distilled water (pH adjusted to 6.8)
Complete RPMI medium (500 mL):	▪ RPMI supplemented with L-glutamine ▪ 5 mL Penicillin/streptomycin ▪ 50 mL fetal bovine serum
Na-Citrate Buffer (0.1 M, pH 6.0)	▪ 1L of distilled water ▪ 3.358 g of Citric Acid ▪ 0.1N HCl (pH ≈ 6.0).
Tris-EDTA buffer at 4C	▪ 1.21 g of Tris-base ▪ 0.37 g of EDTA ▪ 1L of distilled water (pH adjusted to 9.0) ▪ 0.5 ml of Tween 20
1x Running buffer	▪ 450 ml of distilled water ▪ 50 ml of 10x running buffer
Mild Stripping Buffer	▪ 1 liter. ▪ 15 g glycine. ▪ 1 g SDS. ▪ 10 ml Tween20. Adjusted pH to 2.2
10x Tris borate EDTA (TBE) buffer (1L, stored at room temperature)	▪ Approximately 1 L of distilled water ▪ 108 g of Tris-base ▪ 55 g Boric acid ▪ 9.3 g EDTA

9.1.5 Cell lines/ Plasmids

- NTHY-ORI 3-1 human thyroid follicular epithelial cell lines (Sigma-Aldrich, USA)
- TPC-1 Human Papillary Thyroid Carcinoma Cell line (MilliporeSigma, USA)
- MAPK6 (NM_002748) Human Tagged ORF

9.1.6 Tumor Samples

Our study recruited six well-characterized PTC FFPE samples from the University Hospital Sharjah (UHS). Ethical approval was obtained from their Ethics and Research Committee on June 10, 2019 (reference number: UHS-HERC- 011-105 10062019). Tumor samples were chosen based on TNM staging and confirmed clinicopathological diagnosis. All investigations in our study were conducted in compliance with the ethical standards of the declaration of Helsinki (Table 12).

Table 12. Clinicopathological characteristics of FFPE papillary thyroid cancer (n=6)(2)

Patient's Code	Gender	Age	Diagnosis	Stage	Nationality	TNM stage
T1	Female	43	Papillary Thyroid Carcinoma (prototypic conventional / classic)	Early	Egyptian	-
T2	Male	65	Papillary Thyroid Carcinoma (prototypic conventional / classic)	Early	UAE	-
T3	Female	60	Papillary Thyroid Carcinoma (prototypic conventional / classic)	Early	UAE	-
T4	Female	33	Follicular Variant of Papillary Thyroid Carcinoma	Early/severe	Tunisian	PT2N0aMx
T5	Male	43	Papillary Thyroid Carcinoma (prototypic conventional / classic)	Severe	Egyptian	PT2N1Mx
T6	Female	33	Papillary Thyroid Carcinoma (prototypic conventional / classic)	Severe	Philippines	PT1bN1Mx

9.2 Methods

9.2.1 Thyroid Cancer Incidence, Demographics, and Future Predictions

9.2.1.1 Data collection

The present study collected local and global data from GLOBCAN(83) and UAE's National Cancer Registry (UAE-NCR). The latest local TC data collected between 2011-2017 provides population-based incidence rates in compliance with the international coding and staging system (ICD-10 and ICD-0). The data provided were exclusively obtained from the health informatics system of the ministry of health (UAE), pathology reports, and HAAD central and DHA cancer registries. Incidence rates were expressed as an annual mean per 100,000 (age-adjusted) using the total population of UAE computed by the population division of the united nations (33). Further estimates and predictions of global future cancer incidence were conducted using a web-based software adapted by the international agency on cancer research (https://gco.iarc.fr/tomorrow/en) (84, 85). The malignancies predictive model for 2011-2017 was constructed by applying a linear regression equation ($y = m * x + c$) to the data collected from UAE-NCR. The annual rate of change of thyroid cancer was computed via an application of gradient analysis to the data yielded from linear regression equation utilization. The age-standardized rate was also computed using data from the UAE Federal Competitiveness and Statistics Centre (https://fcsc.gov.ae/en-us) and US Census Bureau (https://www.census.gov).

9.2.1.2 Statistical Analysis

In the current study, continuous variables were presented as standard deviation means ($\pm$); categorical variables were reported as percentages and counts. A student t-test was used for group comparison, and Pearson and Rank correlations were assessed where applicable. Euclidean distance measure and average linkage were used for unsupervised hierarchical clustering. Additionally, a combination of R and SPSS was used to conduct the statistical analysis; $P < 0.05$ was considered statistically significant.

9.2.2 In silico Analysis of Publicly Available Papillary Thyroid Carcinoma Transcriptomic Data

9.2.2.1 Independent Discovery Cohort Set

Gene expression omnibus (GEO) was used to retrieve gene sets associated with PTC. Only gene sets from the Affymetrix Human Genome U133 plus 2.0 Array platforms, inclusive of control thyroid samples, were selected for analysis. Gene sets GSE6004, GSE60542, and GSE3678 were retrieved, and a total of 95 cases and their associated raw CEL files were identified and further subjected to Gene Set Enrichment Analysis (GSEA).

9.2.2.2 Independent Validation Cohort Set

Three independent sets from various populations were selected to validate genes and pathways identified in the discovery cohort, including Ukraine GSE35570, South Korea GSE129562, and Brazil GSE50901. All investigations were conducted with ethical approval from the Research Ethics Committee of UHS (reference number: UHS-HERC- 011-10062019).

Table 13. In-silico discovery and validation cohort sets Independent(2)

No.	Gene Set ID	Country	PTC stage			Remarks
			Normal	Non-Aggressive	Metastatic	
1	GSE6004	Ukraine	4	7	7	Discovery set
2	GSE60542	Belgium and France	30	14	19	
3	GSE3678	USA	7	7	0	
		Total	41	28	26	Grand Total = 95
4	GSE35570	Ukraine	51	32		Validation set
5	GSE50901	Brazil	4	61		
6	GSE129562	South Korea	8	8		

9.2.2.3 ***Adaptive Filtering and Raw Microarray Normalization***

Microarray normalization of 95 PTC patients' raw files was performed using Affymetrix Microarray Suite 5 (MAS5) and Gene Chip Robust Multiarray Averaging (GCRMA) packages in R scripts to remove data turbulence. Adaptive filtering was performed using an R script where invariant probes were eliminated, and non-specific filtering was executed to identify common variant probe sets. Probes with a variation coefficient of 10–100% and MAS5 value >50 in GCRMA across normal, non-aggressive, and metastatic sets were intersected to yield sets with common variant probes. Identified probes were further mapped to gene sets found in Broad Institute software http://software.broadinstitute.org/gsea/downloads.jsp). The maximal expression of probes was considered significant as an expression value for the corresponding gene, while probes with no association with genes or those associated with housekeeping genes were excluded (Figure 6)(86, 87).

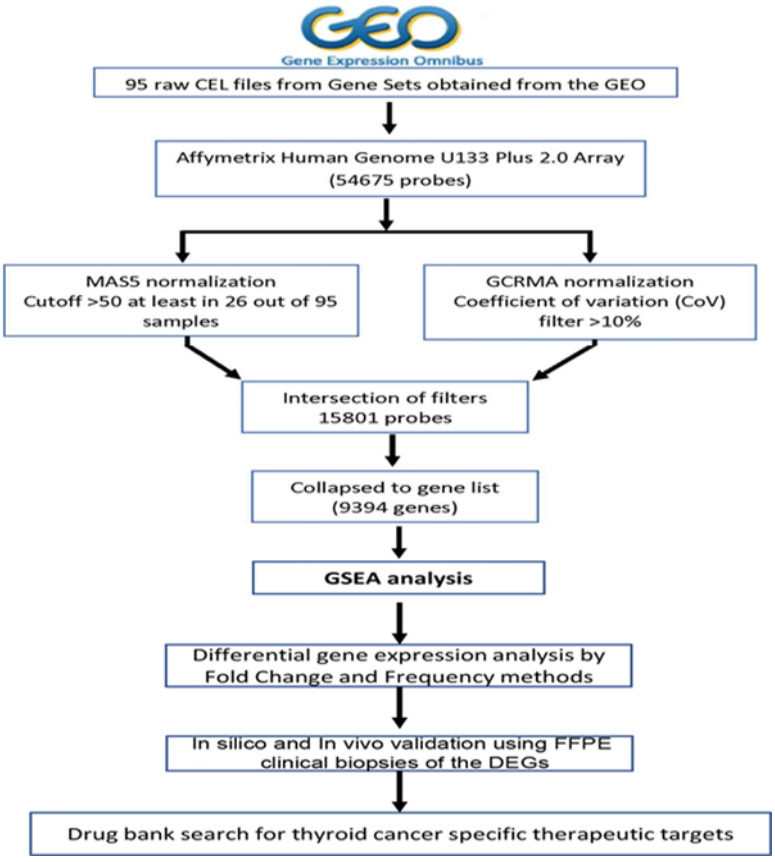

Figure 6. Flow chart of transcriptomic data normalization and gene set enrichment analysis (2).

9.2.2.4 Differential Gene Expression Analysis in PTC versus Normal Thyroid Samples

Using R scripts, genes frequent among activated pathways across all PTC samples were identified. Furthermore, statistical analysis with a cut-off of the 95th percentile was computed for each sample. The average expressions of each gene set,and fold change value were computed to obtain differential expressed genes in metastatic and non-aggressive PTC samples. Upregulated genes were identified as having a fold change >1.5, and down-regulated genes a fold change of <0.5.

9.2.2.5 Pathway Enrichment using Gene Set Enrichment Analysis

A mapped gene list obtained through adaptive filtering was further analysed using GSEA to identify pathways activated in cellular pathways or biological processes associated with metastatic papillary thyroid carcinoma and non-aggressive PTC against normal thyroid samples. GSEA was performed on expression values of seven well-annotated gene sets (C1 to C7) from Broad Institute's database (https://www.gsea-msigdb.org), with approximately 20,500 annotated cellular pathways. The enrichment of activated pathways was considered significant if $P < 0.05$ and FDR < 0.25; pathways were further analysed to identify genes enriched within these pathways.

9.2.3 In-vitro Validation of Genes and Pathways identified by GSEA in Independent Sets

9.2.3.1 Metascape analysis

To validate the pathways enriched by GSEA in discovery and cohort samples, their highly frequent genes among NAG and metastatic PTC were analysed using Metascape software (https://metascape.org/) to identify and validate their corresponding enriched cellular pathways.

9.2.4 Drug Bank Therapeutics Search

A Drugbank database search was conducted using the most differentially expressed genes obtained via GSEA among non-aggressive and metastatic PTC samples. Potential drug targets

related to upregulated genes were identified and listed as putative therapeutic agents for papillary thyroid carcinomas.

9.2.5 Transcriptomic Analysis of Papillary Thyroid Carcinomas and Archival FFPE Biopsies of UAE Patients (Early versus Late Stage)

9.2.5.1 Sample Description

A total of six well-characterized PTC FFPE samples were recruited from UHS. Ethical approval was obtained from UHS's Ethics and Research Committee on June 10, 2019 (reference number: UHS-HERC- 011-105 10062019). Samples were chosen based on TNM staging and a confirmed clinicopathological diagnosis. FFPE biopsies were subjected to microdissection, RNA isolation, and transcriptomic analysis. All investigations were conducted in compliance with the ethical standards of the declaration of Helsinki.

9.2.5.2 RNA Sequencing

RNA isolated from FFPE thyroid tissues was subjected to next-generation sequencing using AmpliSeq Whole Transcriptome on S5 System (ThermoFisher, USA). The Ion AmpliSeq Transcriptome Human Gene Expression Kit (Thermo Fisher Scientific) was used to prepare RNA-seq targeted libraries that were further sequenced using an Ion 540 Chip on the Ion S5 XL Semiconductor sequencer.

9.2.5.3 Tumor Tissue Preparation

All PTC Biopsies were sectioned to 3 um slides using a standard microtome (Leica) and further screened for diagnosis by an experienced clinical histopathologist. FFPE blocks of confirmed PTC with more than 40% tumor content were selected for transcriptomic analysis. For each patient, ten slides (of approximately 2–6 mm^2 surface area) were prepared where one section was used for hemotoxylin and eosin (H&E) staining; the rest underwent molecular analysis.

9.2.5.4 Laser Capture Microdissection

Using the LCM system, pure tumor cell populations from FFPE were microdissected under direct visualization using an LMD6 microscope to enrich the regions of interest (LEICA, USA). Enriched regions were isolated via the direct placement of a thermoplastic film cap over the tissues and irradiated by a low-power laser to melt the film into the selected cells. Upon the removal of the cap, the cellular regions of interest remained attached to be utilized in the transcriptomic analysis. Due to the small tumor content found in each slide, multiple laser captures were performed on consecutive slides from the same patient to capture an optimal number of cells. Microdissected tumor tissues were mounted on slides covered with polyethylene-naphthalate (PEN) membrane to dry out at room temperature and be stained later via H&E staining. All steps were conducted under RNase-free conditions (Figure 7 B).

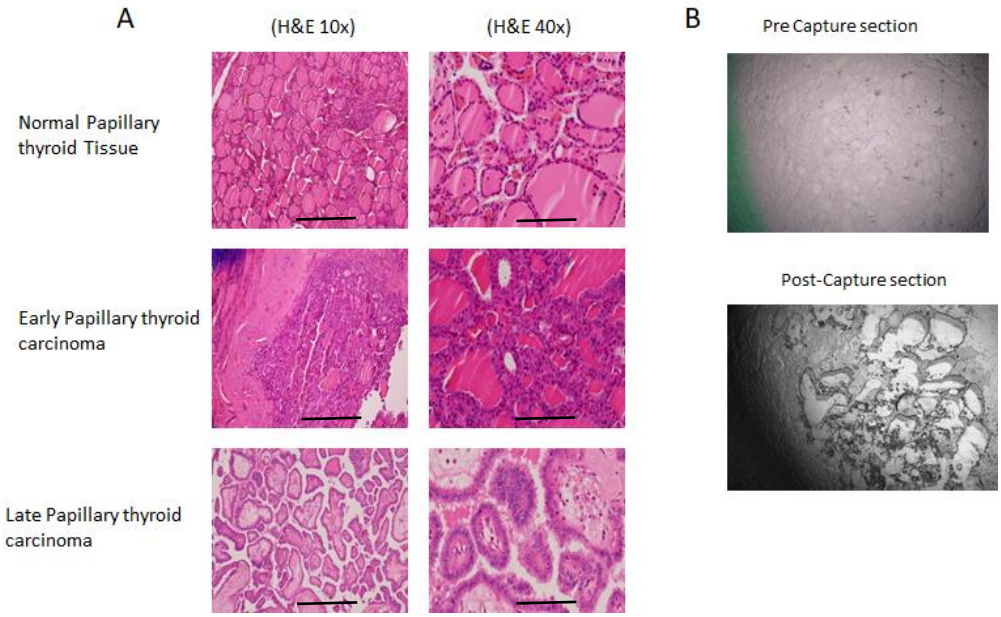

Figure 7 Histopathological slides of papillary thyroid carcinoma tissue exhibiting nuclear alterations in early and late stages (stained with Haemotoxylin and Eosin). (B) laser capture microdissection sections of PTC showing areas before extraction of tumor tissue and after .Bar scale for 10x: 250 µm , bar scale for 40x:100 µm.

9.2.5.5 RNA Isolation/ Quantification

RNA was extracted from laser capture microdissected slides using the Recover All FFPE RNA Isolation Kit per the manufacturer's protocol. Microdissected sections (3 um with a tissue surface area of approximately 0.5 mm^2) were incubated directly using a digestion buffer and protease at 50 C for 3 hours. Released RNA was purified using an on-filter nuclease treatment and elution in RNase-free water. To ensure the purity of the nucleic acid, turbo-DNase was used to eliminate any remnant DNA that might interfere with the results. The Qubit Quantification Kit (Invitrogen, USA) and Nanodrop (ThermoFisher, USA) were used for quantification purposes.

9.2.5.6 Library Preparation and cDNA Synthesis

RNA extracted from microdissected FFPE TC blocks was subjected to next-generation sequencing using AmpliSeq Whole Transcriptome on S5 System 165 (ThermoFisher, USA). The Ion AmpliSeq 166 Transcriptome Human Gene Expression Kit (Thermo Fisher Scientific) was then used to prepare targeted RNA-seq libraries. cDNA was synthesized using the SuperScript VILO cDNA Synthesis Kit (Invitrogen), followed by an amplification process using Ion Ampliseq gene expression primers per the manufacturer's protocols. The concentration of cDNA was then determined using the Nanodrop 2000 spectrometer (ThermoFisher, USA) to be used further in Qrt-PCR.

9.2.5.7 Real-time Quantitative Reverse Transcription PCR (QRT-PCR)

Quantitative real-time PCR was performed in triplicates using the Superscript First-Strand Synthesis System (Invitrogen) and SYBR green (Solis BioDyne) on Quant 189 Studio 3 (Applied Biosystems). A total of 40 PCR cycles were performed with an initial denaturation of 15 sec at 95 C, combined with an annealing/extension cycle of 10 min at 60 °C. The 195-threshold cycle value (Ct) was normalized against the expression value of the housekeeping gene (18s rRNA) to identify the relative expression of MAPK6 in the transfected cell lines.

MAPK6 and the housekeeping gene (18s rRNA) were amplified using primer sets MAPK6_sense: CATTGACATGTGGGCTGCAG, MAPK6_Antisense: AGCTGCATCTGTTCAAGTTCA, TGACTCAACACGGGAAACC, and 18s rRNA_antisense: TCGCTCCACCAACTAAGAAC.

9.2.5.8 Immunoblotting

Using the western blot technique, MAPK6 (63kDa) and the protein of interest were separated by gel electrophoresis and blotted to a nitrocellulose membrane. Transferred membranes were blocked for 1 hour. By adding 5% skimmed milk (dissolved in 1X TBST), the non-specific binding of the antibodies added in the subsequent steps was avoided. Blocked membranes were probed with primary antibodies, including Anti ERK3/MAPK6 (1:2000) (Abcam, UK) and Anti 204 β-actin (1:5000) (Abcam, UK). β-actin was used as a loading control and left for incubation overnight. Washing buffer 1X 206 TBST was used the next day three times for 10 mins to unbound reagents and reduce background noise. Secondary antibodies, including anti- Rabbit IgG, Anti Horseradish peroxidase, and anti-Mouse IgG (Cell Signaling), were dissolved in 5% skimmed milk in 1X TBST and added to the washed membrane for another cycle of incubation. Three subsequent washes of the membranes were followed by the addition of an ECL detection reagent substrate (Thermo Fisher, USA). Chemiluminescence was analyzed using a Chemidoc membrane visualizing system (BioRad, USA).

9.2.5.9 Cross-validation of Targeted Biomarkers in larger Cohort Sets

To overcome the small sample size of FFPE biopsies, RNA-seq analysis data of a larger cohort set was retrieved from the Cancer Genome Atlas Program (TCGA). The cohort set compromised 58 normal thyroid samples: eight metastatic and 502 non-metastatic PTC samples. The analysis involved the employment of a TNM plotter (https://tnmplot.com/analysis/) and a statistical comparison via a Kruskal–Wallis test. Only results with $P < 0.05$ were considered significant.

9.2.6 MAPK6 Transfection in Normal and Thyroid Cancer Cell Lines

9.2.6.1 Plasmid Extraction

To investigate the role of MAPK6 overexpression in TC, MAPK6 (NM_002748) Human Tagged ORF (OriGene) (Figure 8) was cloned into a pCMV6-Entry Expression Vector, forming plasmid pCMV6-mapk6. Plasmid extraction was performed using a Maxiprep kit (QIAGEN). In brief, bacterial plasmids were grown in 5 ml of LB broth with Amphotericin B for expansion; 2 ml out of 5 ml of Pcmv6-MAPK6 and Amphotericin B solution were transferred and subcultured overnight. Bacterial cells were centrifuged at 6,000 for 10 mins at 5° C, followed by resuspension using a suspension buffer (lysed by lysis buffer) and incubation on ice for 15 mins. Subsequent centrifuging at 20,000 g led to the supernatant formation, which was transferred to a QIAGEN column and allowed to penetrate the resin by gravity. The QIANGEN column was further washed using the QC buffer. The QF buffer and isopropanol were added to isolate the DNA pellet eluted by isopropanol and allowed to air dry. The dried DNA pellet (plasmid) was washed using 15 ml of nuclease-free water for further use in transfection (Figure 9).

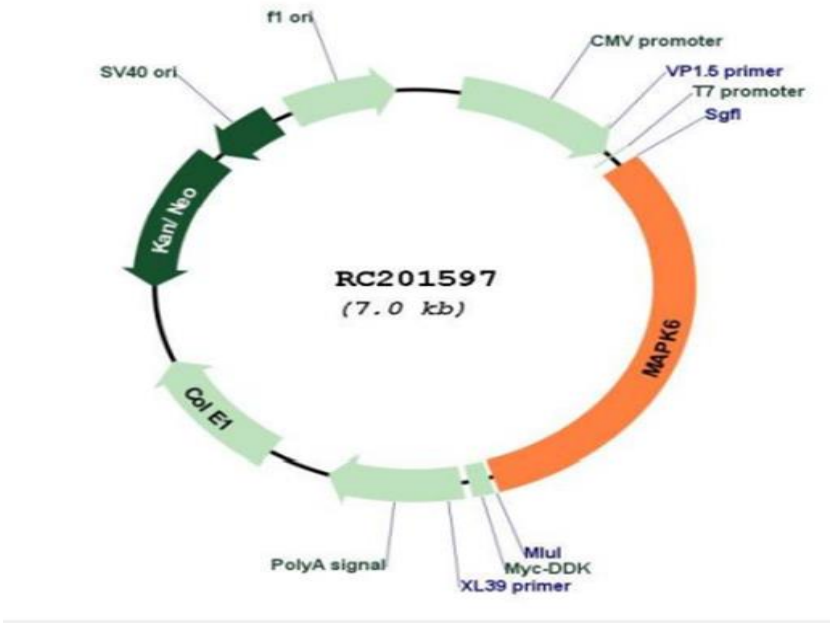

Figure 8 schematic diagram of pcDNA-MAPK6 plasmid map. Orange segment represents the transfection site of MAPK(gene of interest) into the vector and cell line.

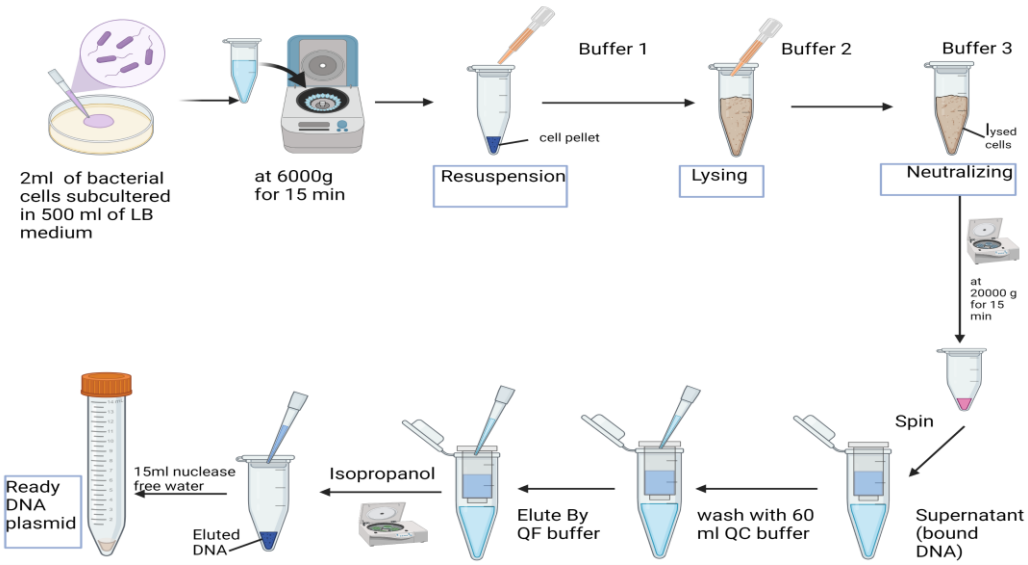

Figure 9.MAPK6 plasmid extraction process. Created by Biorender.com

9.2.6.2 Cell Culture/ Cell Lines Transfection

Thyroid cancer (TCP-1) and normal Nthy-ORI-3-1 (Nthy) cell lines were cultured in T75 flasks containing Dulbecco's Modified Eagle Medium (Sigma-Aldrich, USA), supplemented with L-glutamine, 10% FBS, 1% penicillin/streptomycin, and 1% amphotericin B at 37 C of 5% humidified CO_2 atmosphere. Cultured Nthy and TPC-1 cells with a 70-80% confluency were transfected with a MAPK6 vector. Nthy and TPC-1 cells with a size of 2.5 x 105 cells were seeded at 37 C overnight in six-well plates (well size: 34.8 mm). Cells were transfected transiently with MAPK6 plasmid DNA using Viafect reagent (Promega, USA). Four of the six wells were labeled (untransfected, Viafect, mock transfection, and MAPK6 transfection). Each well received 250 µl of transfection media (serum-free, antibiotic-free DMEM media), 5 µl Viafect reagent, 224 2.5 ng pcDNA-MAPK6 plasmid DNA, and 5 µl Viafect reagent (transfection mixture). Plates were incubated for 15 mins to facilitate lipid-DNA complex formation. Mock transfection was conducted using a pcDNA empty vector. Prepared transfection mixtures were added to the four wells at 24-hour and 48-hour time intervals, except for the control well, where only a transfection media free of plasmids was added. Following 24-48 hours of incubation, transfected Nthy and

TPC-1 cells were harvested for mRNA extraction and subsequent MAPK6 expression using Western blotting, qRT-PCR, and transcriptomic analysis.

9.2.6.3 Transfection Optimization of pcDNA-MAPK6 Vector into (TPC-1) Thyroid Cancer and Normal Nthy-Ori-3-1 (Nthy) Cell lines using RT- qPCR

Different concentrations of a high-performing, low toxicity transfecting agent (Viafect) were used to optimize the transfection efficiency while maintaining a constant plasmid DNA concentration. Viafect was added in two different volumes: 3 µl and 4 µl. Viafect efficiency increased with concentration without exhibiting any toxicity on cells. Conversely, transfection potency was not enhanced with time increase. Figures 10 A and 10 B show that the Viafect time point after 24 hours and a concentration ratio of 4:1 (Viafect: MAPK6 vector) showed the best expression of the MAPK6 transfected gene in both normal and cancerous thyroid cells.

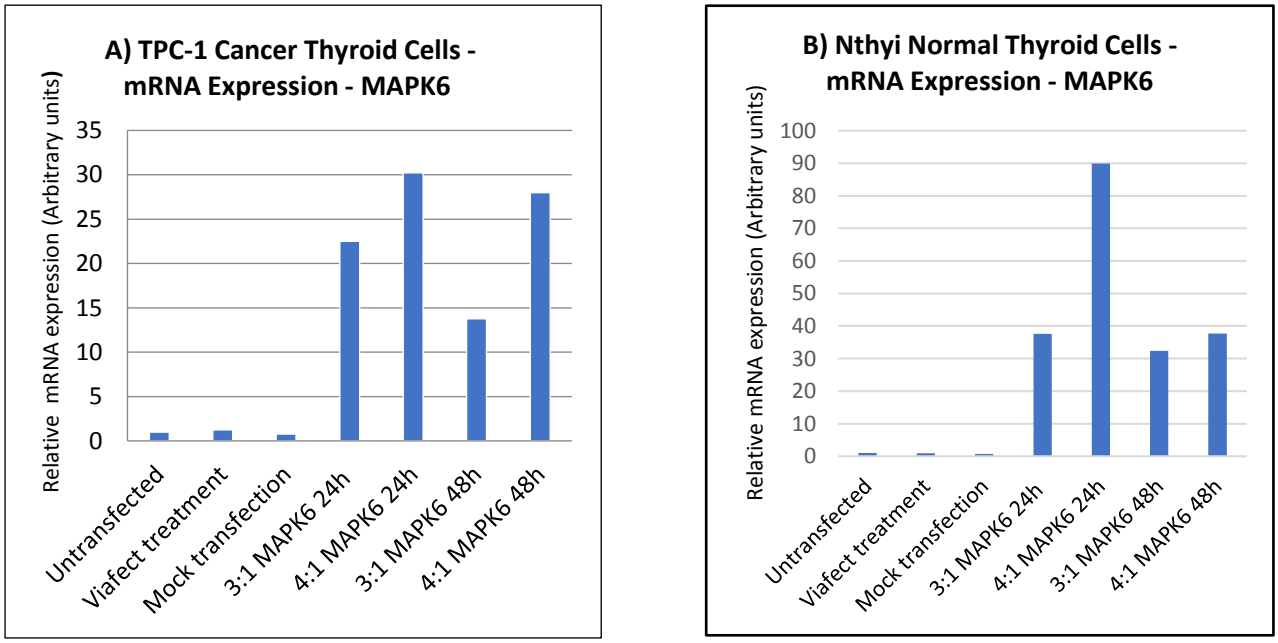

Figure 10 **Transfection Optimization of TPC- and Normal Nthyi thyroid cells lines using Viafect: A) mRNA expression of MAPK6 in TPC-1 with different time intervals and Viafect concentrations obtained by RT-qPCR; B) mRNA expression of MAPK6 in normal thyroid cells with different time intervals and Viafect concentrations; y-axis: relative mRNA expression; x-axis: concentrations of Viafect with time points.**

9.2.6.4 RNA Sequencing

RNA isolated from FFPE thyroid tissues was subjected to next-generation sequencing using AmpliSeq Whole Transcriptome on S5 System (ThermoFisher, USA). Furthermore, the Ion AmpliSeq Transcriptome Human Gene Expression Kit (Thermo Fisher Scientific) was used to prepare RNA-seq targeted libraries that were further sequenced using the Ion 540 Chip on the Ion S5 XL Semiconductor sequencer.

9.2.6.5 Bioinformatics and Statistical Analysis

Bioinformatics analysis of the RNA-seq data was conducted using Ion Torrent Software Suite version 5.4 (Ion S5 XL Semiconductor sequencer, Thermifischer, USA). In contrast, differential gene expression (DGE) analyses were performed using R/Bioconductor package DESeq2 with raw read counts and a significance of $P < 0.05$. Read counts of less than ten normalized read counts were excluded from the analysis. Visualization and data annotation was conducted using the Database for Annotation, Visualization, and Integrated Discovery (DAVID) (https://david.ncifcrf.gov/).

9.2.6.1 Data Clustering/ Pathway Analysis

Identified differentially expressed genes ($P < 0.01$) among early and late papillary thyroid cancer were subjected to unsupervised hierarchical clustering with Euclidean Ward distance and average linkage measures. These methods help stratify patients according to their transcriptomic profile and identify potential biomarkers associated with PTC progression.

Differentially expressed genes produced by RNA-seq analysis were subjected to pathway analysis. Pathway-responsive genes for activity inference (PROGENy), DoRthEA, and CARNIVAL Pipeline were employed to infer sample-wise and transcription factor (TF) activity scores and identify protein networks associated with PTC pathogenesis. Pathway activity scores of 286 transcription factors were evaluated for 14 signaling pathways(PI3K, VEGF, Trail, WNT, EGFR, Hypoxia, TGFb, MAPK, TNFA, Androgen, NFkB, Estrogen, JAK. STAT, and p52) using (PROGENy). Differential changes in transcription factor activity were then analyzed using DoRothEA.Combined pathway activity scores

obtained by PROGENy and DoRothEA were analyzed further for potential protein interaction using CARNIVAL(P-value cut-off used for the active/inactive nodes of gene sets <0.05).

Furthermore, using limma, statistical tests were performed to determine significantly differentially active TFs. The pathways identified using the methods above were cross-validates with Metascape Analysis.

10 Results

10.1 Global Thyroid Cancer Incidence Demographics and Predictions

The data in Figure 10 indicates a global increase in thyroid cancer cases, except for Europe, where the incidence shows a steady rate from 2020 to 2040. The highest increase in thyroid cancer cases can be observed in the Asian continent, and the lowest increase in Oceania (Figures 11A and 10B). In Figure 11C, UAE shows a steady rise in TC incidence following the global trend of thyroid cancer incidence.

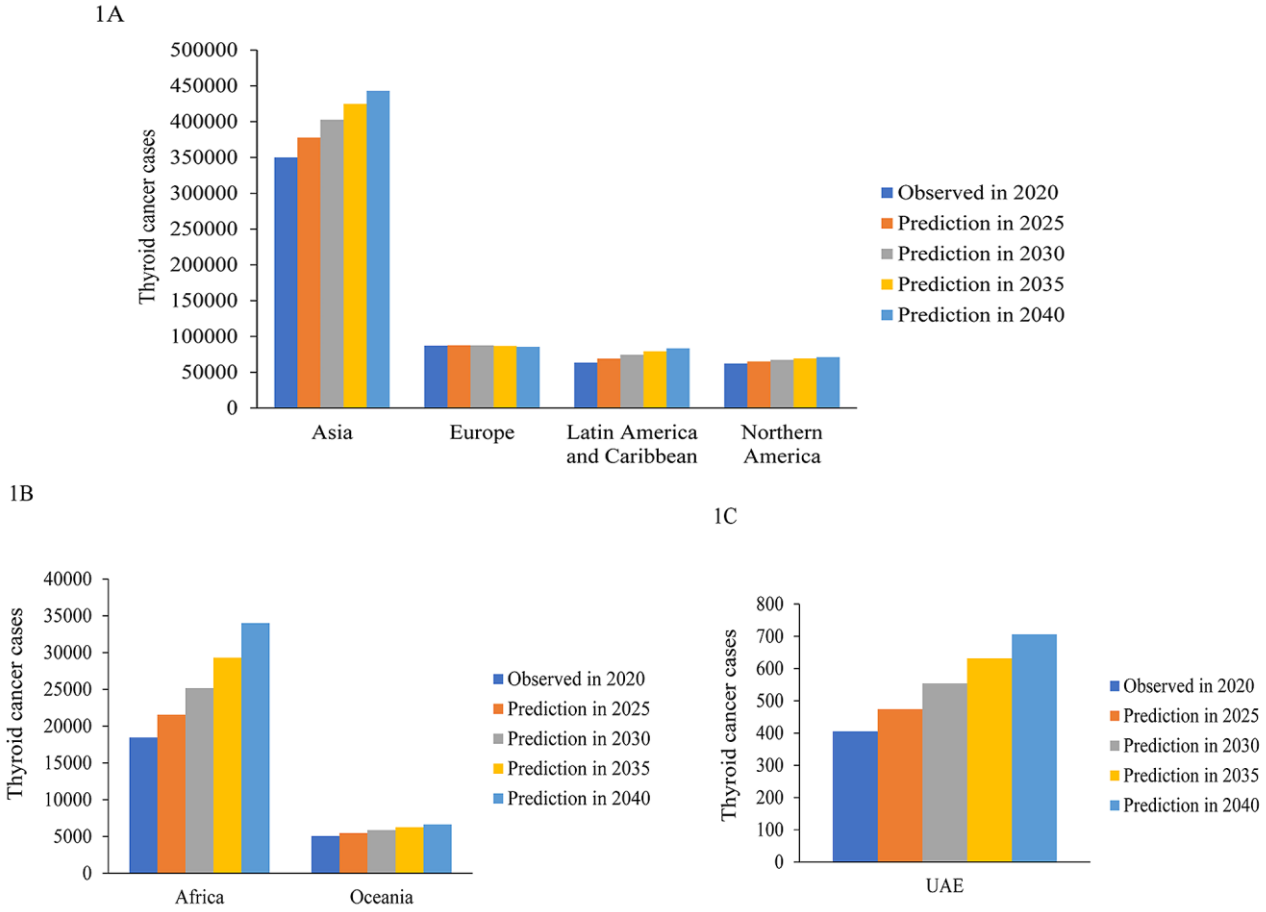

Figure 11 **Global Thyroid Carcinoma Demographics by using Predictive Models based on GLOBOCAN data between 2020 and 2040 (1).**

10.1.1 Unsupervised Hierarchical Clustering of Future Incidence of Thyroid Carcinoma using Predictive Models

To predict thyroid cancer incidence from 2020 to 2040, we used a predictive model based on Euclidean distance measure and average linkage. The predicted data shows a steady increase in thyroid cancer incidences globally, except for Europe, where cases increase rapidly between 2020 and 2030 and decrease gradually until 2040 (Figure 12).

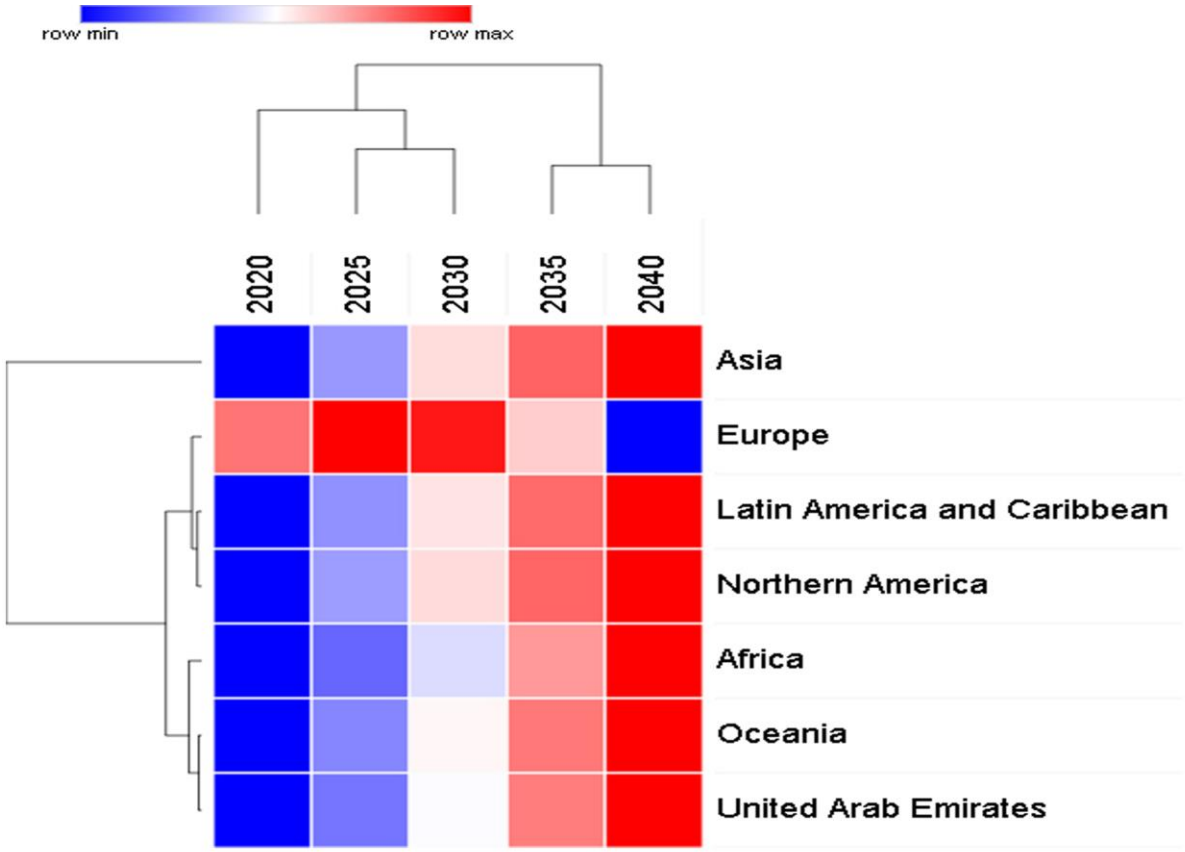

Figure 12.Two-way unsupervised hierarchical clustering of predicted data for Global thyroid cancer incidence from 2020-2040(1). Red colour represents high frequency; blue colour: represents low frequency.

10.1.2 Global Rate of Change in Thyroid Cancer Incidence between 2020-2040

To compute the total global thyroid malignancies from 2020 to 2040, we used a predictive model applying a linear regression equation (y = m * x + c) to the data collected from UAE-NCR and GLOBCAN. The data yielded were used to construct a gradient analysis representing

the TC incidence rate change. Overall, the data indicate a relatively small rate of increase in comparison to other cancers. Additionally, it confirms that the Asian continent will be the most affected by the increasing rate, followed by the continents of Africa and South America. UAE has the lowest rate at 15.2, whereas Europe has a negative rate of increase, supporting the decreasing incidence obtained by the predictive model from 2030 to 2040 (Table 14).

Table 14. Rate of change of thyroid cancer incidences globally between 2020 and 2040 using a predictive model of a linear regression equation (y = m * x + c).m; gradient of the line,c; y-intercept (1).

Region	Rate of Change of Thyroid Cancer cases
Asia	4665
Africa	3885
Latin America	1002.8
North America	438.6
Oceania	78.7
UAE	15.2
Europe	-84.3

10.1.3 Thyroid Cancer Prevalence in the UAE from 2011 to 2040

Table 15 shows that thyroid cancer prevalence can increase to 6 by 2040, with an average increase of 4.02. Therefore, suggesting a steady increase in prevalence between 2011 and 2040.

Table 15. Prevalence of thyroid cancer in UAE (2011 to 2040)(1).

Year	Prevalence*	Incidence per 100.000
2011	1.18	98
2012	2.18	188
2013	3.16	282
2014	3.42	314
2015	3.7	344
2016	4.22	398
2017	4.32	412
2020 ***	4	405
2025 ***	5	474

*Prevalence: describes the percentage of patients previously and newly diagnosed

**Incidence: describes only newly diagnosed cases.

*** Predicted values obtained by using linear regression models

Year	Prevalence*	Incidence per 100.000
2030 ***	5	554
2035 ***	6	632
2040 ***	6	706

Table 15 continued. Prevalence of thyroid cancer in UAE (2011 to 2040)(1).

10.1.4 Actual and Predicted Thyroid Cancer Incidence in the UAE from 2011 to 2040

A linear regression model was used to calculate the predicted values of all cancer cases, including thyroid cancer. Data from the regression model were compared against data collected from UAE-NCR between 2011 and 2017. Table 16 shows that the linear regression model of predicted total malignancies matches closely by a significant correlation ($r = 92.5$, $p = 0.003$) with the actual total malignancies between 2011 and 2017 obtained by UAE-NCR. Additionally, the data presented in percentages of predicted thyroid cases show an increase of 6.6% between 2011 and 2017, dropping to 3.3% in total thyroid cases between 2011 and 2040 in UAE (Table 16)(1).

Table 16. Actual and predicted TC incidence in UAE between 2011 and 2040

Year	Predicted** total malignancies(all cancer)	Actual* total malignancies (all cancer)	Actual TC (n=patients)	Predicted TC (n=patients)	predicted TC %	Actual TC %
2011	2688	2284	98	138	3.65	4.37
2012	2954	3094	188	189	6.36	6.29
2013	3221	3574	282	240	8.76	7.89
2014	3221	3610	314	291	9.75	8.7
2015	3487	3744	344	342	9.87	9.19
2016	3754	3982	398	393	10.60	9.99
2017	4020	4123	412	443	10.25	9.99
2020 *	4820	-	-	494	8.40	-
2025 *	6153	-	-	749	7.70	-
2030 *	7485	-	-	1003	7.40	-
2035 *	8818	-	-	1257	7.17	-
2040 *	10151	-	-	1766	6.95	-

10.1.5 Thyroid cancer incidence per Nationality in the UAE between 2011 and 2017

Table 17. shows that between 2011 and 2017, a total of 2,036 newly diagnosed thyroid cases were recorded by UAE-NCR. Out of those (n = 1,402) were expats and (n = 634) were Emirati.

Table 17. Thyroid Cancer incidence per Nationality in UAE (1).

Year	Total Malignancies	Thyroid Cancer cases (n=2036)	Emirati patients	Expat patients	Total %	Emirati %	Expat %
2011	2284	98	39	59	4.29	1.71	2.58
2012	3094	188	63	125	6.08	2.04	4.04
2013	3574	282	87	195	7.89	2.43	5.46
2014	3610	314	88	226	8.70	2.44	6.26
2015	3744	344	110	234	9.19	2.94	6.25
2016	3982	398	124	274	9.99	3.11	6.88
2017	4123	412	123	289	9.99	2.98	7.01

10.2 Gender Analysis of Thyroid Cancer Incidence

10.2.1 Global Female to Male Ratio of TC per 100,0000

Thyroid cancer incidence rates for 2020 were extracted per gender from GLOBCAN and are represented in Figure 13. The data show that the female: male ratio is higher across all continents, with an average of three times higher incidence in females than in males (11.6: 3.5). The highest incidence of TC was observed in Polynesia, and the lowest was observed in Africa.

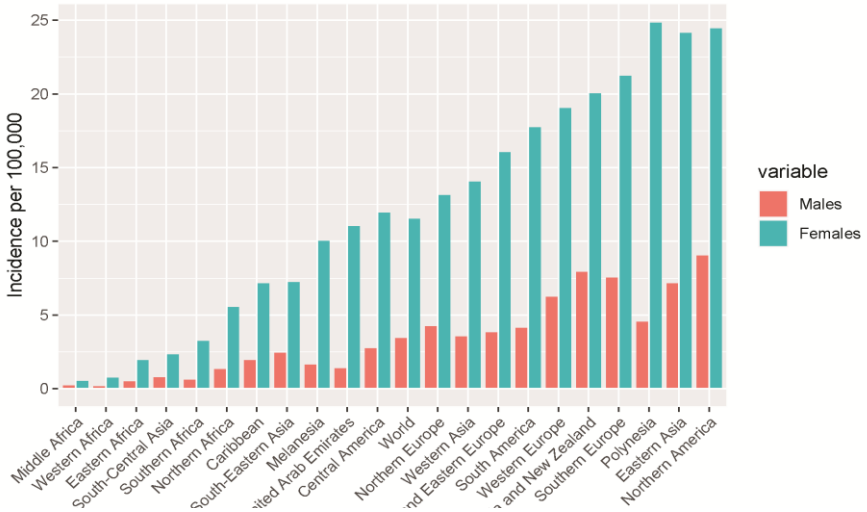

Figure 13.Global Male to female ratio of thyroid cancer incidence per 100.000 based on Global Cancer Observatory for 2020(1).

10.2.2 UAE Female to Male Ratio of TC per nationality

Table 18. shows that 2011 scored the highest female: male ratio of 12.0 for Emiratis and 2016 for expats with a ratio of 3.92. An independent Student's t-test confirmed the significance of the female: male ratio for both Emiratis ($P < 0.0001$) and expats ($P < 0.001$). The data demonstrates that thyroid cancer incidence is higher in females than in males, not only in UAE populations but worldwide, as shown in Figure 12(1). UAE gender distribution of thyroid cancer incidence from 2011 to 2017

Table 18. UAE gender distribution of thyroid cancer incidence from 2011 to 2017

Year	Emiratis				Expats			
	Total	Males	Females	Female: Male ratio	Total	Males	Females	Female: Male ratio
2011	39	3	36	12.00	59	12	47	3.92
2012	63	6	57	9.50	125	35	90	2.57
2013	87	10	77	7.70	195	69	126	1.83
2014	88	15	73	4.87	226	65	161	2.48
2015	110	27	83	3.07	234	61	173	2.84
2016	124	21	103	4.90	274	70	204	2.91
2017	123	24	99	4.13	289	86	203	2.36

10.3 Thyroid cancer Age-Distribution in the UAE between 2011-2017

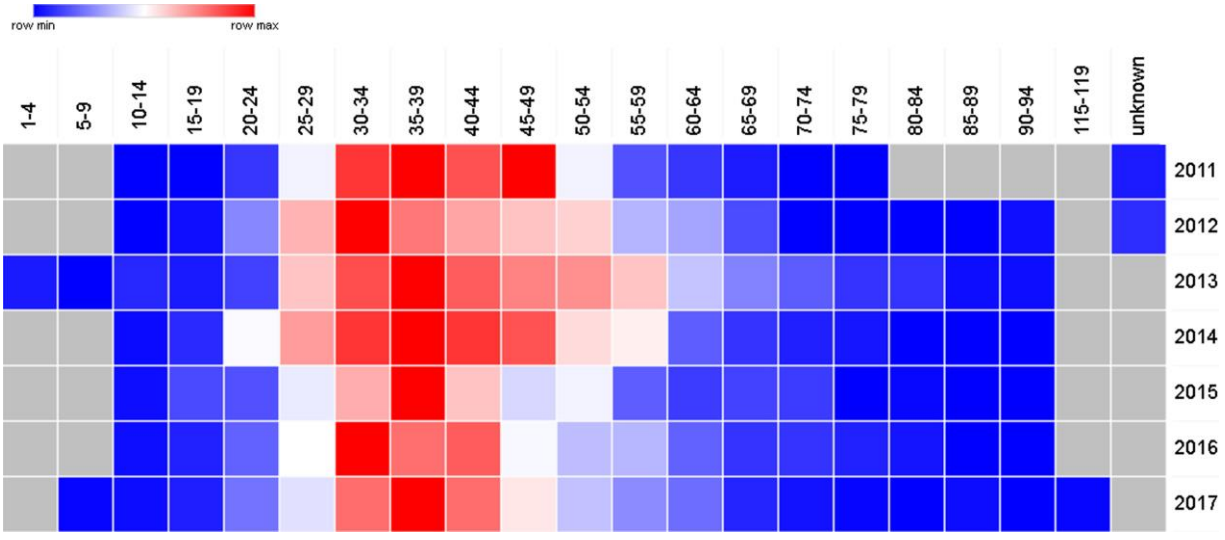

Figure 14.Heatmap representation for age distribution of thyroid cancer in UAE from 2011 to 2017. Red color represents high frequency and blue low frequency(1).

As shown in Figure 14, the peak of thyroid cancer cases is observed among those aged 35-39 years (P = 0.03), compromising 17.5% of all thyroid cancer patients diagnosed. This was followed by the 30-34 age group, comprising 15.9% of all thyroid cases. Figure 14 also confirms that the highest occurrence of thyroid cancer was found in those aged 30-34 and 35-39, respectively.

10.4 In silico Analysis of Publicly Available Transcriptomic Data to identify Key Differential Molecular Pathways and Genes in Papillary Thyroid Carcinoma

10.4.1 Identification of Differentially Expressed Cellular Pathways (Non-aggressive and Metastatic) compared to Normal Thyroid using Gene Set Enrichment Analysis

Using absolute GSEA on normal thyroid sets versus non-aggressive sets, 1,795 significantly differentially expressed pathways were identified in relation to biological processes and molecular functions ontology gene sets (Table 19). The most observed enriched pathways among normal versus non-aggressive sets include phosphatase regulator activity, protein tyrosine phosphatase activity, calcium-dependent protein kinase activity, transforming growth factor-beta receptor binding, and protein kinase activity (Supplementary Table 1). Insulin-like growth factor receptor signalling pathways, negative regulation of peptide hormone secretion, regulation of MAPK cascade, activation of MAPK activity, transmembrane receptor protein tyrosine kinase signalling pathways, and regulation of protein serine-threonine kinase activity were enriched in normal versus metastatic PTC sets (Supplementary Table 2). Pathways with nominal $P < 0.05$ and a false discovery rate (FDR) < 0.05 cut-off were considered significant, as represented in Table. The output representation of GSEA for a singular dataset is shown in Figure 15.

Table 19. Significant pathways enriched in non-aggressive and metastatic PTC compared to normal thyroid samples by GSEA. The highest enrichment was observed in pathways related to biological processes and immunological signatures. P < 0.05 and FWER values <0.05 were considered significant(85).

GENE SET ID	Description	Total Number of pathways	GSEA pathways for Non-aggressive	GSEA pathways for Metastatic
C2	Curated gene sets e.g., KEGG REACTOME	6229	447	294
C5.bp	Ontology Gene set: biological processes	7573	998	728
C5.mf	Ontology Gene set: molecular functions	1697	207	100
C6	Oncogenic signature	189	124	117
C7	Immunologic signature	4872	788	730

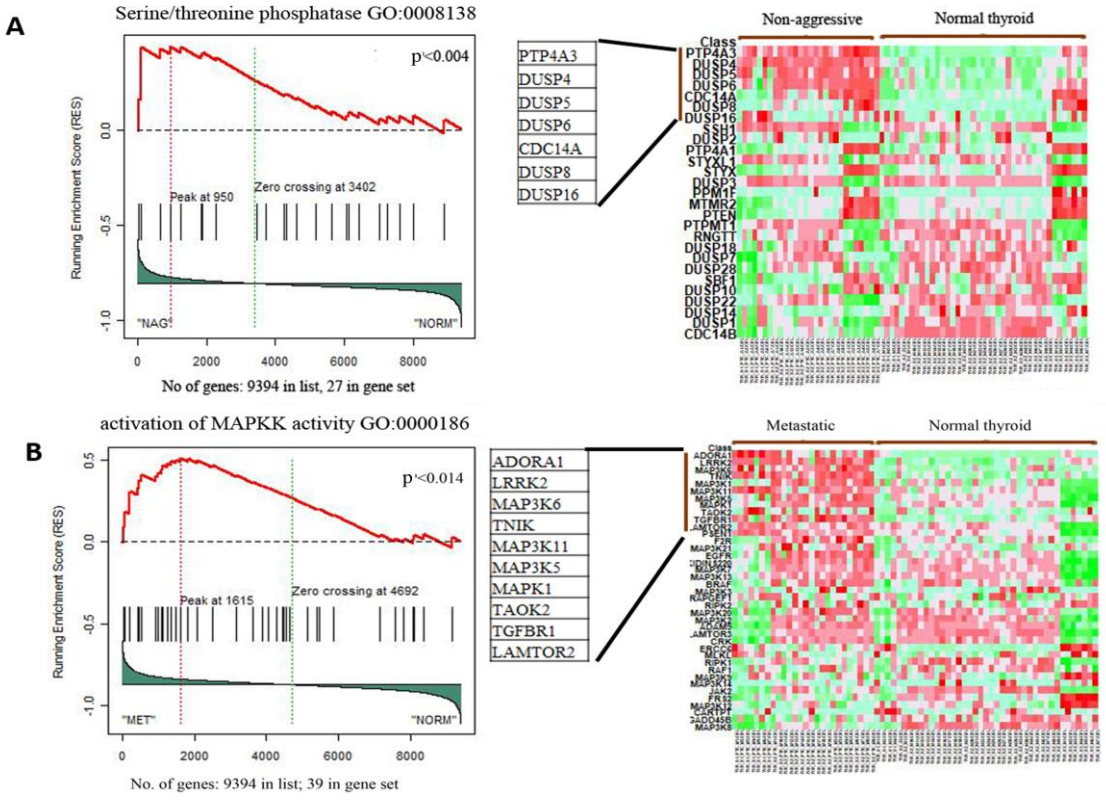

Figure 15 . Example of Graphical representation for Gene set enrichment scores of significant pathways in PTC (A) Enrichment scores graph for normal versus non-aggressive PTC shows that Serine/threonine phosphate is enriched more in non-aggressive state. b)Heat map of enrichment score for normal versus metastatic PTC shows that MAPK activation is highly enriched in metastatic stages.

10.4.2 Differentially Expressed Cellular Pathways of NAG/Metastatic compared to Normal Thyroid using Absolute Gene set Enrichment Analysis (GSEA)

Upon employing a stringent gene frequency cut-off using the 95th percentile on enriched pathways from GSEA, a total of 355 NAG and 280 genes in metastatic samples were identified to be more frequent in corresponding pathways. The top 40 hub genes based on the 95th percentile cut-off is shown in (Tables 20 and 21). Additionally, 144 genes were upregulated, and 27 were downregulated in non-aggressive. In metastatic samples, 138 genes were upregulated, and 20 genes were downregulated. InteractiVenn (http://www.interactivenn.net) was used to display the intersection between non-aggressive and metastatic samples, where 144 upregulated genes were commonly observed as intersecting (Figure 16& Table 22).

The genes most frequently retrieved from microarrays were plotted using fold change expression, where nominal P-values < 0.05 and < 0.001 were considered significant. When comparing the differential expression obtained for MET (n = 26) and NAG (n = 28) against normal thyroid tissues, three genes showed the highest differential expression: KCNN4 (P < 0.001), EGFR (P < 0.05) and PTK2B (P < 0.001), as shown in Figure 17.

Table 20.Top 40 most frequent genes in normal against Non-aggressive sets(95-percentile cutoff)(2)(86).

Gene symbol	Frequency	Gene symbol	Frequency
KCNQ1	38	CACNA1A	29
CACNA1D	37	EDN3	29
PTK2B	35	EGFR	29
EDN1	34	KCNAB1	29
SFRP1	33	KCNE4	29
ABAT	32	RYR2	29
KCNJ2	32	KCNE3	27
KCNJ5	32	KCNJ8	27
KCNS3	32	KCNK1	27
ADRA2A	31	KCNMA1	27
ANO1	31	KCNQ3	27
BCL-2	31	SCN4B	27

Gene symbol	Frequency	Gene symbol	Frequency
FKBP1B	31	CXCL12	26
GPER1	31	GRIN2C	26
AGT	30	PTEN	26
CACNB3	30	RGS4	26
HCN4	30	AKR1C3	25
ITPR1	30	GRIK2	25
KIT	30	ITPR3	25

Table 21.Top 40 Hub Genes most frequent in Normalversus Metastatic PTC samples((95-percentile cutoff)(2).

Gene	Frequency	Gene	Frequency	Gene	Frequency
EGFR	26	ITPR1	20	ANXA6	17
PTK2B	25	RGS2	20	CACNA2D1	17
RYR2	24	SRC	20	FGF13	17
BCL-2	23	ANK2	19	KCNJ5	17
CACNA1D	23	CRABP2	19		
SFRP1	23	FYN	19		
CXCL12	22	AGT	18		
GPER1	22	AKT1	18		
KCNJ2	22	CACNA1A	18		
KCNQ1	22	CAV1	18		
RYR1	22	CX3CL1	18		
ABL1	21	EFEMP1	18		
ADRA2A	21	FGFR3	18		
SLC8A1	21	HBEGF	18		
CDK5	20	INHBB	18		
DMD	20	KIT	18		
EDN1	20	PSEN1	18		
FKBP1B	20	ADRB2	17		

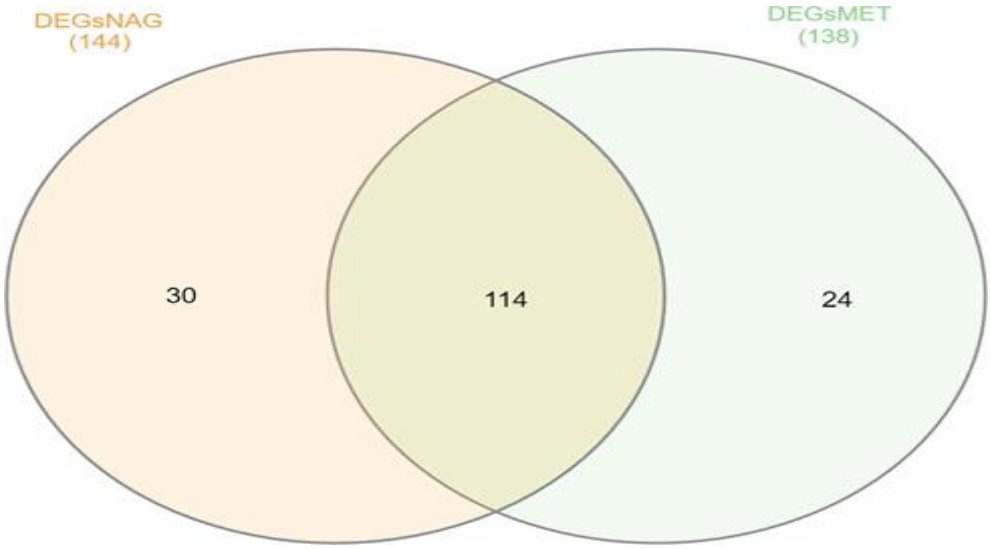

Figure 16.InteractiVenn representation of upregulated genes intersection among non-aggressive/metastatic in comparison to normal Thyroid samples.

Table 22. List of Intersected upregulated DEGs among NAG/metastatic versus normal thyroid sample(86)

DCSTAMP	LEMD1	LINC02555	MIR31HG	AGR2	ABTB2	CRLF1
KLK10	FAXC	ABCC3	TMEM163	GLT1D1	MIR100HG	CLDN1
GABRB2	FAM230B	KCNJ2	SPTBN2	GALE	TUSC3	KRT19
RXRG	SYT12	KCNN4	SLC34A2	CLDN16	LRRK2	NAT8L
SYTL5	GOLT1A	EGFEM1P	ADTRP	HLA-DQB2	TMEM79	IL17RD
CLDN10	LAMP5	RAB27B	ADORA1	NOD1	NOX4	TNFRSF 12A
PRSS2	ZCCHC12	NMU	THRSP	NR2F1-AS1	DOCK9-DT	
HMGA2	KLHDC8A	TRDC	ALOX15B	DPP4	B3GNT3	
PRR15	CITED1	CD1A	CHI3L1	LPAR5	CORO2A	
LRRC52-AS1	NGEF	BRINP1	GLDN	ULBP2	HPCAL4	
PDZK1IP1	LRRK2-DT	LIPH	STK32A	MMP16	ECM1	
ARHGAP36	GDF15	FAM20A	CTXND1	KISS1R	NRCAM	
TMPRSS4	RIMS2	TENM1	ALDH1A3	EVA1A	PLAU	
AHNAK2	KCNQ3	KLK11	TIAM1	NFE2L3	TACSTD2	
ST6GALNAC5	SCEL	PDZRN4	SYT1	CCL13	PCSK1N	
GAP43	LCN2	CDKN2B	COMP	MAMLD1	LINC00891	
LAMB3	CDH3	RYR1	SHROOM4	CYP1B1	NHSL2	
METTL7B	SLC27A6	LRP4	CEACAM6	IGSF1	INAVA	

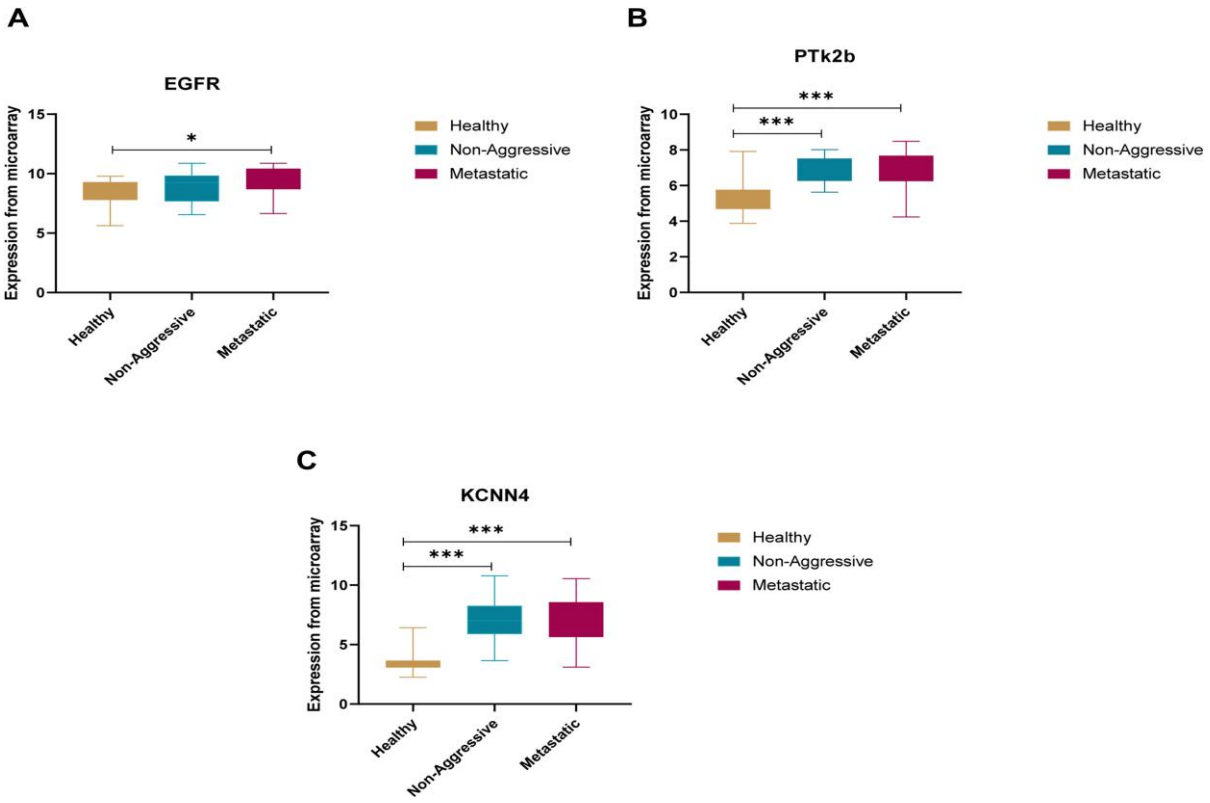

Figure 17. Box plot representation of microarray log fold expression analysis of DE genes between normal, non-aggressive and metastatic PTC. A) EGFR differential expression ($p < 0.05$) B) PTk2b differential expression($p < 0.01$) and C)KCNN4 differential expression($p < 0.01$)(2).

10.4.3 In-Vivo Validation of Deferentially Expressed Genes by Next-Generation Sequencing

Three genes showed the highest differential expression. KCNN4 ($P < 0.001$), EGFR ($P < 0.05$), and PTK2B ($P < 0.001$) were validated using our cohort set of six well-characterized PTC patients' biopsies from UAE. Cohort samples were subjected to next-generation sequencing and analysis, which confirmed our in-silico findings concerning the higher expression of PTK2B, KCNN4, and EGFR. All three genes revealed higher differential expression in late PTC compared to early PTC. Interestingly, PTK2B ($P < 0.001$) showed the highest expression in late PTC among KCNN4 ($P < 0.001$) and EGFR ($P < 0.05$) genes, as shown in Figure 18.

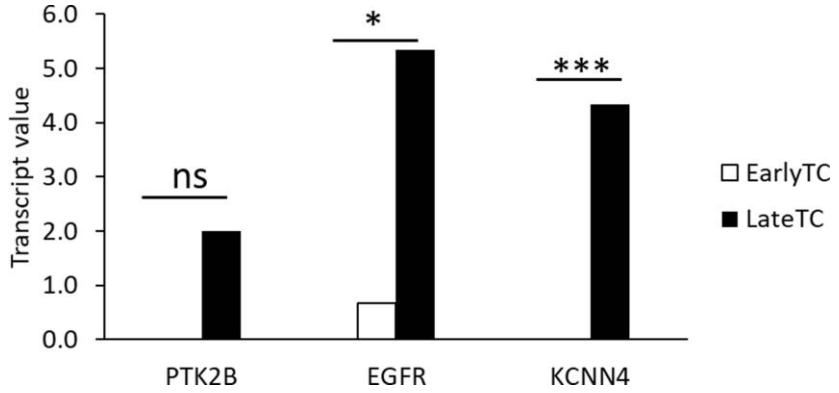

Figure 18. Differential expression of EGFR, PTK2B, KCNN4 genes using Next generation sequencing on UAE-clinical biopsies.EGFR genes shows highest expression among other genes (P < 0.05)(2)

10.4.4 In-vivo Validation of Differentially Expressed Genes using TNM Plotting

Using an independent validation cohort RNA-seq data of 502 thyroid cancer cases, the differential expression of PTK2B, KCNN4, and EGFR was obtained via in-silico analysis (microarray) was further examined. The validation process revealed that KCNN4 ($P < 0.0001$), EGFR ($P < 0.01$), and PTK2B ($P < 0.0001$) all exhibited higher expression in non-aggressive and metastatic samples compared to normal samples. Thus, the findings for the independent cohort set matched the results from both the in-silico analysis and the UAE patients' biopsies used in NGS (Figure 18).

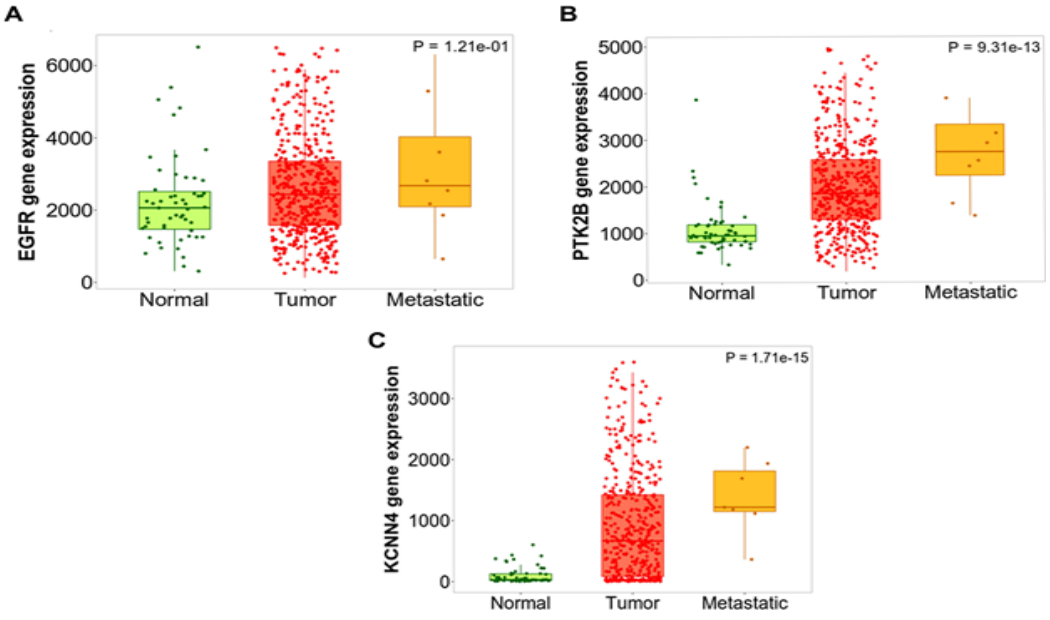

Figure 19 .Differential expression of PTK2B, KCNN4, and EGFR in Independent cohort PTC samples(n=502).Figure 18A, 18B, and 18C show higher expression of corresponding genes in metastatic stage (2).

10.4.5 In silico Validation of GSEA using Metascape Analysis for non-aggressive and Metastatic PTC versus Normal.

10.4.5.1 Metascape Analysis of Enriched Pathways

Validation of enriched pathways obtained by GSEA was carried out using the Metascape analysis tool. Based on gene ontology annotation, the validation analysis revealed key cellular pathways such as the regulation of ion transmembrane transport, calcium ion transport, regulation of system processes, regulation of hormone levels, positive regulation of protein phosphorylation, and signaling by receptor tyrosine kinase in non-aggressive PTC (Figure 20A). In metastatic samples, validation analysis showed enrichment in the regulation of cation transmembrane transport, regulation of membrane potential, positive regulation of protein phosphorylation, MAPK cascade, signaling by receptor tyrosine kinases, potassium ion transport, and regulation of growth and apoptotic signaling pathways. Interestingly, MAPK cascade was present in both NAG and MET but came up triple times in the metastatic stage (Figure 20B).

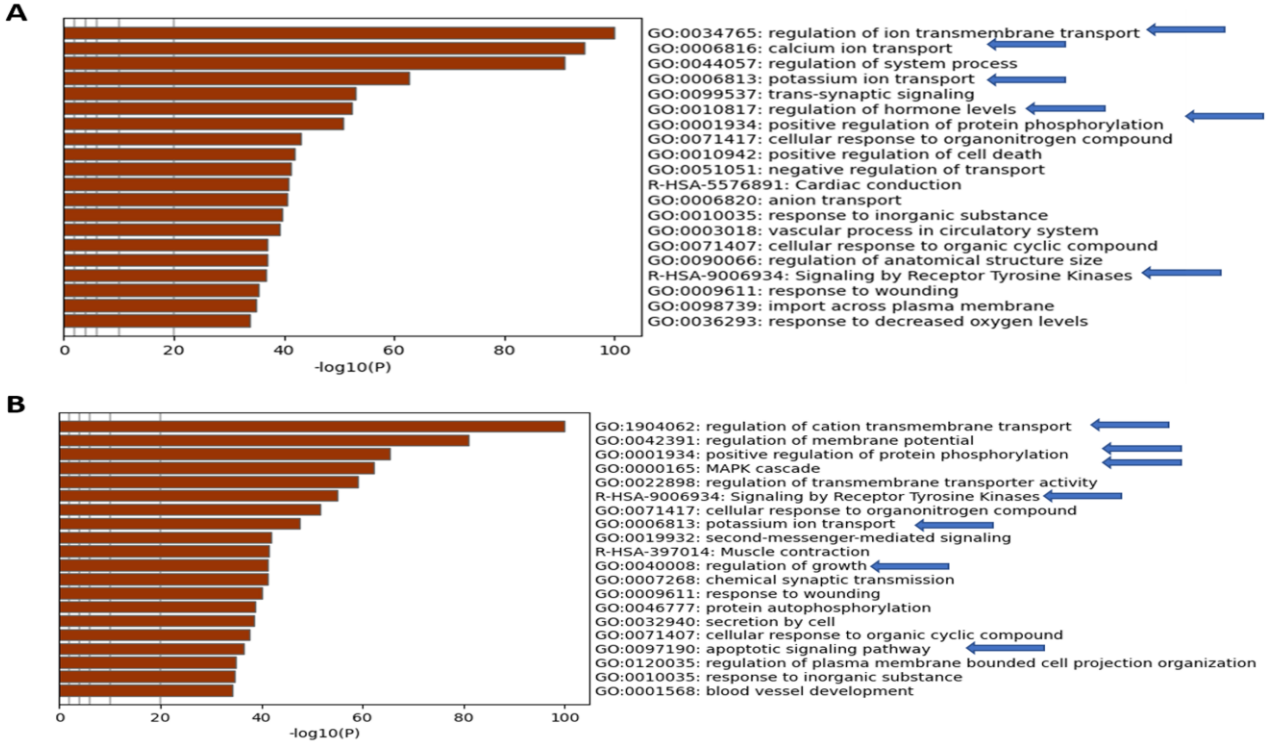

Figure 20 .Heatmap of Metascape analysis of highly frequent DEGs between healthy, non-aggressive and metastatic cohort samples. a) Healthy Thyroid versus non-aggressive PTC sets. b) Healthy versus metastatic PTC sets. Arrows indicate putative enriched pathways for PTC.

10.4.5.2 Metascape Analysis of Upregulated Gene Sets

To determine the link between the upregulated gene sets (Table 22) obtained by GSEA and their corresponding biologic pathways, frequently upregulated gene sets were input into Metascape for analysis. The most interesting pathways were extracellular matrix organization, positive regulation of protein phosphorylation, neuropeptide signalling pathways, and transforming growth factor-beta stimulus pathways (Figure 21).

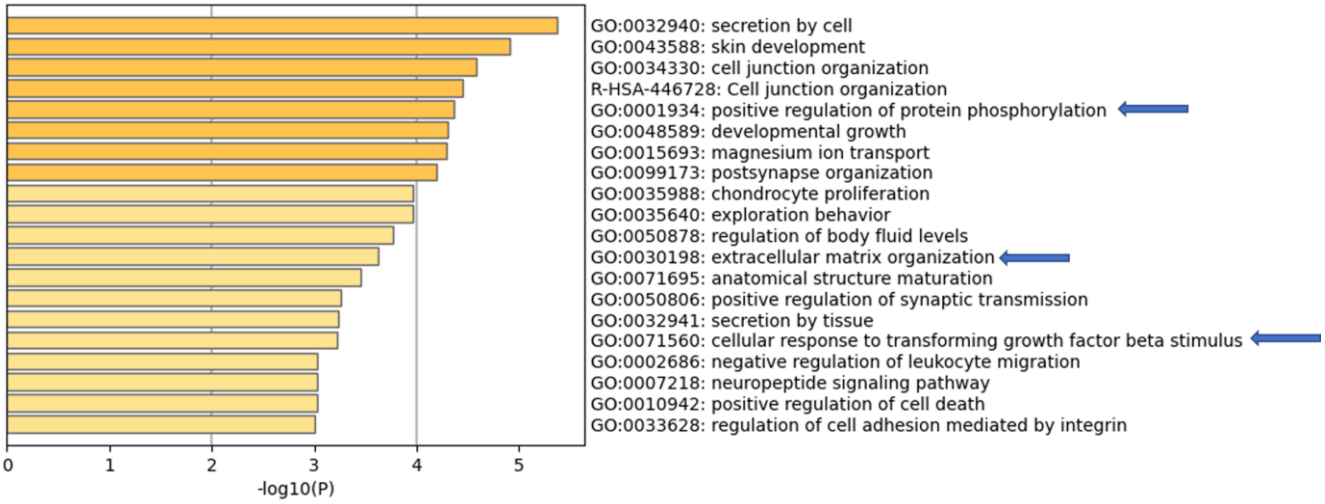

Figure 21.Heatmap representation of GSEA for upregulated pathways. Arrows represent potential pathways of interest. Orange color indicates a higher pathway enrichment score; Yellow color indicates a low enrichment score.

10.4.5.3 Metascape Analysis of Immunologic Component of non-Aggressive and Metastatic Papillary Thyroid Carcinomas

Enriched genes obtained from GSEA related to immunologic processes were subjected to Metascape analysis. The findings showed that the inflammatory component in non-aggressive PTC is higher than in metastatic PTC. In non-aggressive PTC, increases in fractions of macrophages M0, dendritic cells resting, NK cells activation and resting, and memory naïve B-cell ratios were observed. In metastatic samples, there was an increase in monocyte activity, lower macrophage activity, and no NK involvement compared to non-aggressive PTC (Figure 22).

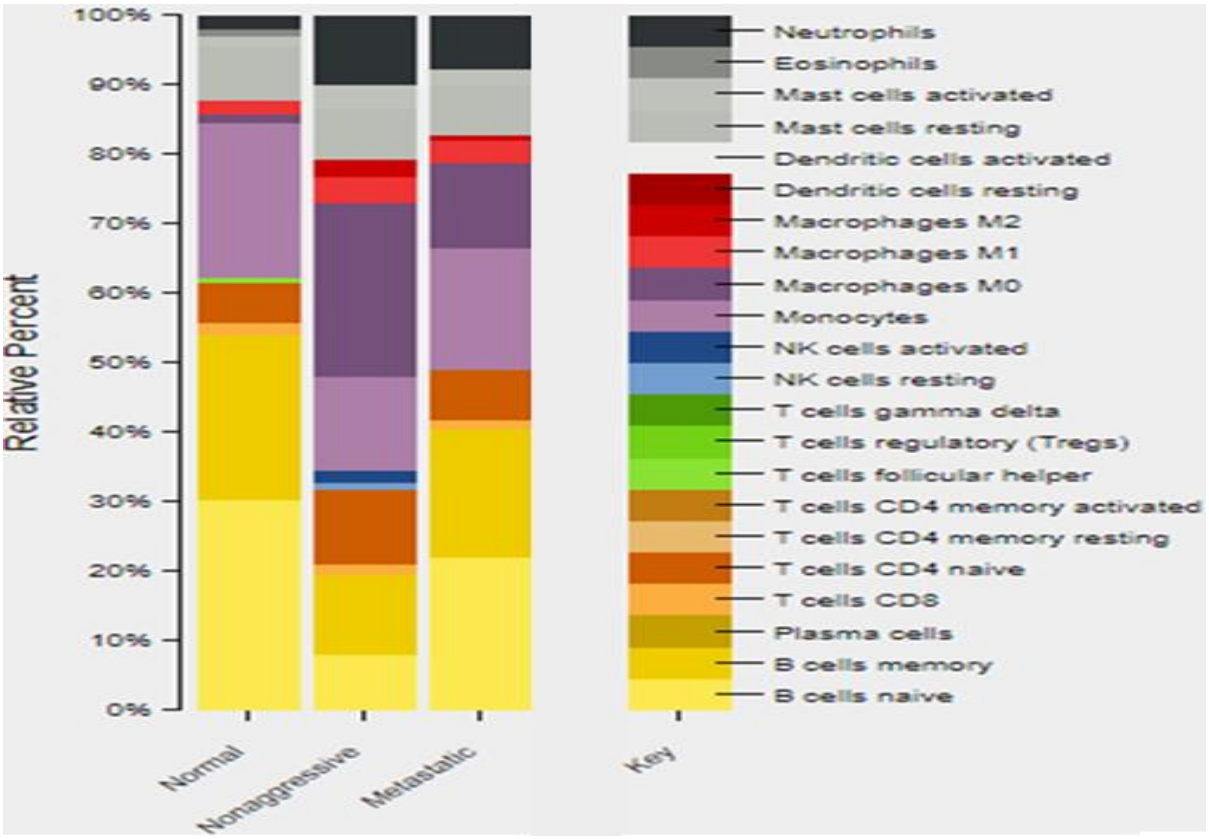

Figure 22.Metascape analysis of immunologic components of non-aggressive and Metastatic PTC. Representation reflects the relative percent of enrichment scores of immunologic components in PTC.

10.4.5.4 Overall Survival of Independent Cohort of PTC Samples

Differentially enriched genes obtained by GSEA were subjected to Kaplan-Meier analysis. The top genes that contributed to poor survival among an independent cohort of 502 PTC patients were PTK2B, CACNA1D, and BCL2 (Figure 23)(2).

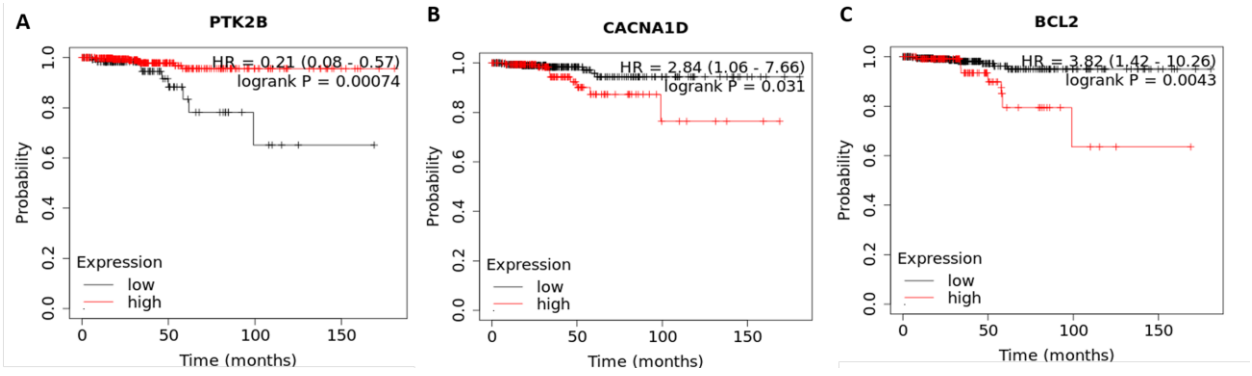

Figure 23. Kaplan Meier analysis of overall survival related to PTK2B, CACNA1D, and BCL2 overexpression.

10.4.5.5 Identification of Differentially Expressed Genes and Pathways of Thyroid Cancer across Selected Populations (Brazil, South Korea, and Ukraine)

Normalized microarray data obtained from GEO were mapped to differentially expressed gene sets. Metascape performed further analyses of gene sets to estimate the most enriched pathways of thyroid cancer between the Ukrainian, Brazilian, and South Korean populations. Key pathways identified across the three populations mainly were related to MAPK pathways, such as tyrosine metabolism, MAPK family signalling cascade, phosphatidylinositol 3-kinase signalling, and regulation of MAP kinase activity. In Ukrainian populations, the most significantly enriched pathways were NABA CORE MATRISOME, hormone metabolic processes, tyrosine metabolism, and regulation of MAP kinase activity (Figure 24). In Brazil, pathways related to response to an inorganic substance, bicarbonate transport, MAPK family signalling cascades, and regulation of small-molecule metabolic processes were enriched (Figure 25). In the South Korean population, enrichment was observed in wound healing, cell adhesion molecules (CAMs), positive regulation of apoptotic processes, and viral entry into the host cell. (Figure 26)

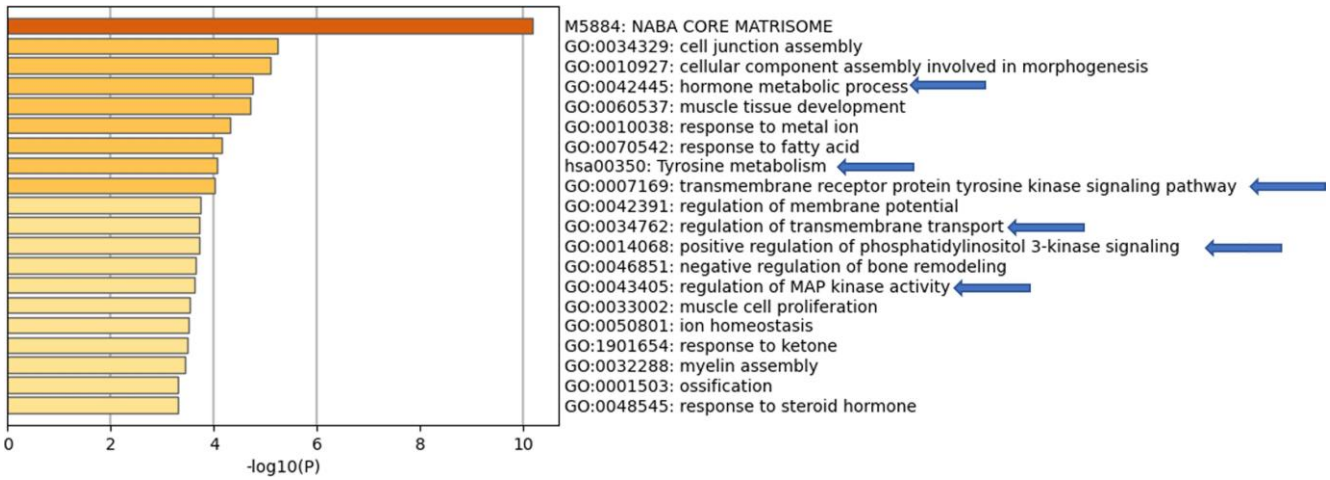

Figure 24. Pathway analysis using Metascape on Ukrainian thyroid cancer samples. The dark orange color represents higher enrichment scores than yellow (low enrichments score).

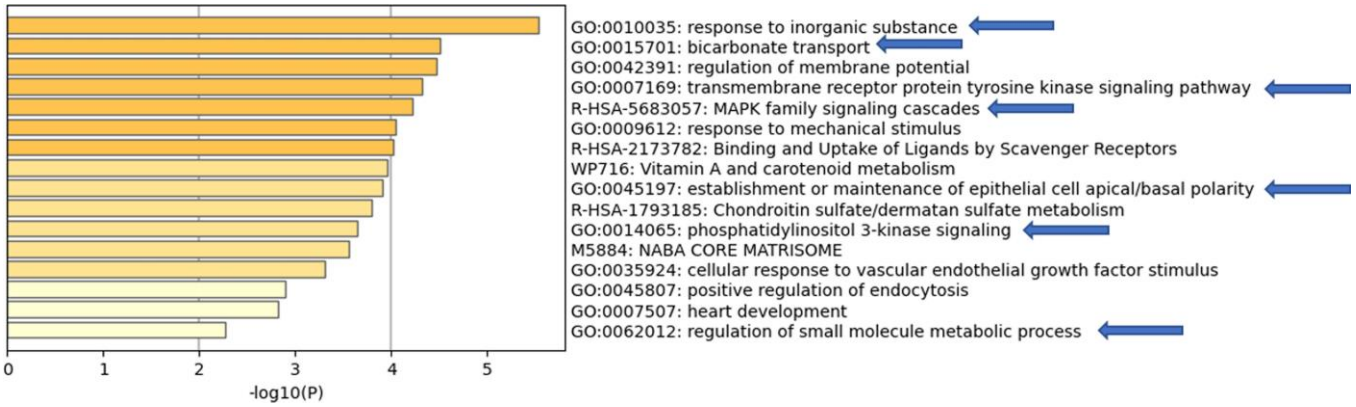

Figure 25.Pathway analysis using Metascape on Brazilian thyroid cancer samples. Dark yellow represents high enrichment pathway score, yellow represents low enrichment score.

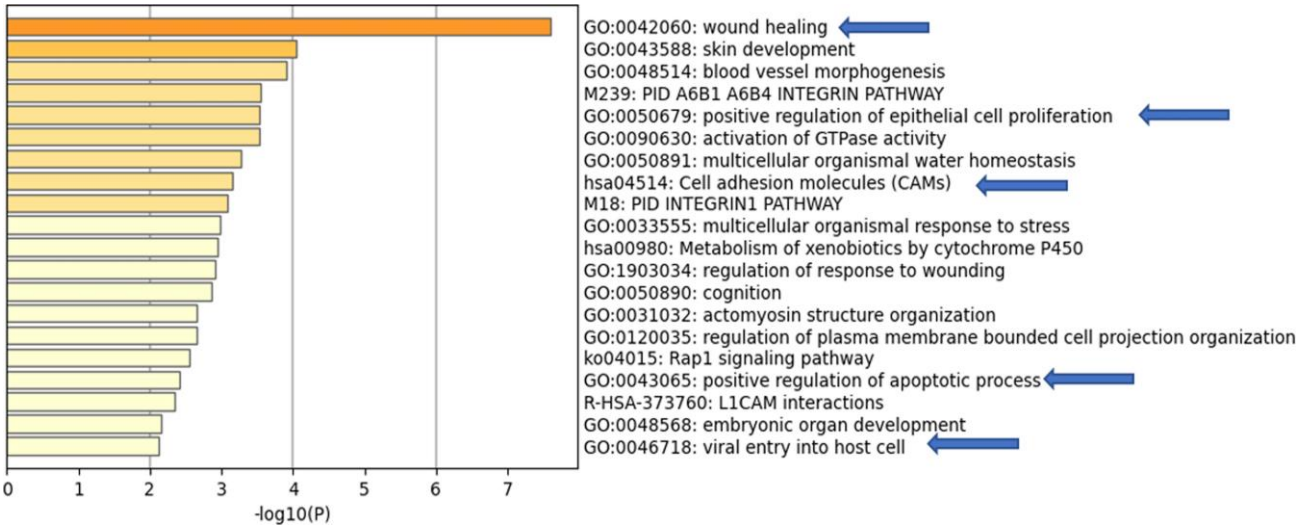

Figure 26.Pathway analysis using Metascape on South Korean thyroid cancer samples. Dark yellow represents high enrichment scores, Pale yellow represents low enrichment scores.

10.4.6 Identification of FDA-approved Drugs Associated with Differentially Expressed Genes identified by Bioinformatics Analysis

A Drugbank database search using differentially expressed genes associated with PTC revealed many FDA-approved therapeutic targets used in metastatic thyroid cancer treatment. The drugs identified mainly were related to vascular EGFR (Table 23). The search also identified approved drugs associated with other genes linked to thyroid carcinomas that might be useful for prospective clinical trials concerning thyroid cancer treatments (Table 24). Additionally, a

population-specific drug search concerning the genes expressed in such populations revealed that only Brazil and Ukraine had some drugs targeting MAPK4 and CRABP1(Table 25).

Table 23. FDA-approved Drugs for Thyroid cancer treatment(2).

Drug Name	Targeted Gene	Thyroid cancer stage
Cometriq (Cabozantinib-S-Malate)(25, 41, 76, 88)	VEGFR	differentiated and spread; metastasized
Vandetanib (23, 43, 89-91)	VEGFR and EGFR inhibitor	Metastasized

Table 24.Drugs associated with Genes Involved in thyroid carcinoma (2).

Gene code	Targeting Drug	Associated conditions	Mode of Action
KCNQ1	Enflurane	General Anesthesia (7, 92)	Voltage-gated Potassium Channels inhibitor(93)
	Promethazine	Sedative therapy, Allergic conjunctivitis	Voltage-gated Potassium Channels inducer
CACNA1D (94, 95)	Isradipine (9)	Hypertension	Calcium channel blocker
PTK2B (96)	Genistein (97, 98)	Calcium deficiency	Unknown
	Leflunomide (99, 100)	Rheumatoid Arthritis	regulation of autoimmune lymphocytes
	Fostamatinib(73, 74, 101-113)	Chronic immune thrombocytopenia	Tyrosine kinase inhibitor
BCL-2	Navitoclax (114, 115) ENREF 91	Solid tumors	Targets BCL-2 family proteins

Table 25. List of Drugs Targeting the Genes Highly Upregulated in Population Specific Set(2)

Population	Gene	Drugs Known to Target the Gene	Conditions Associated	Mode of action
Ukraine	CRABP1	Alitretinoin, Tretinoin(116)	Vit A deficiency, eczema	Activates retinoid receptors
Brazil	MAPK4	Fostamatinib(73, 74, 101, 102, 104-106, 108-110, 112, 113)	Chronic immune thrombocytopenia	Inhibitor of spleen tyrosine kinase
South Korea	LAMB3	—	—	—

10.5 Transcriptomic Analysis of UAE- based Archival Papillary Thyroid Cancer Samples

10.5.1 Identification of Differentially Expressed Genes in Early and late Papillary TC Archival Biopsies

To investigate differential gene expression between early and late PTC, whole transcriptomic analyses were performed using next-generation sequencing of formalin-fixed PTC biopsies of patients hospitalized in UHS. Three were early-stage, and three were aggressive late-stage. The transcriptomic analysis (with a cut-off of $P < 0.05$) identified 250 overexpressed genes of interest in early-stage and 361 genes in aggressive late-stage. A further stringent cut-off of $P < 0.01$ identified 44 differentially expressed genes of interest, primarily overexpressed in later stage PTC samples, as indicated by the clustering in Figure. An interesting gene identified in the cluster was MAPK6 ($p < 0.001$), which plays a vital role in MAP kinase signalling pathways associated with papillary thyroid carcinomas. Figure 27. shows that the normalized transcriptomic data obtained by DESeq2 separate the different grades and variants of TC. Early stages in samples T1, T2, and T3 clustered together, whereas late-stage samples T4 and T5 clustered together. Additionally, the separation in clustering between papillary thyroid cancer variants was observed between the follicular variant in sample T4 and the rest of the classic variants in samples T1, T2, T3, T5, and T6. This finding confirmed the heterogeneity of RNA-seq data of PTC samples, which was further observed via principal component analysis (PCA), as shown in Figure 28.

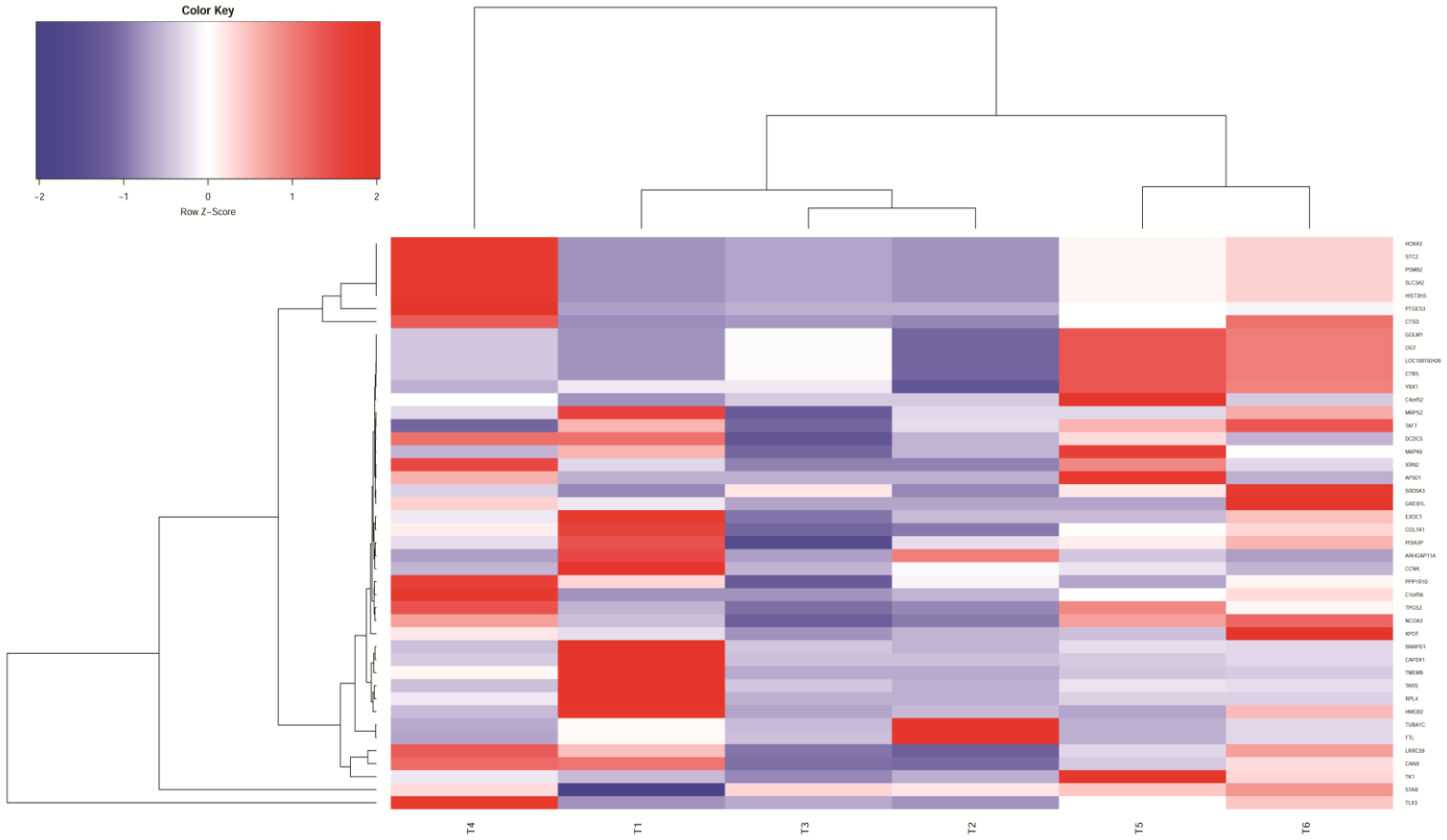

Figure 27 .Hierarchical Clustering of the 44 differentially expressed genes obtained by transcriptomic analysis of PTC archival biopsies in UAE.T1, T2, T3; early PTC sampleS.T4, T5; late PTC samples.T4; follicular variant of PTC.Red represents higher expression, and blue represents lower expression

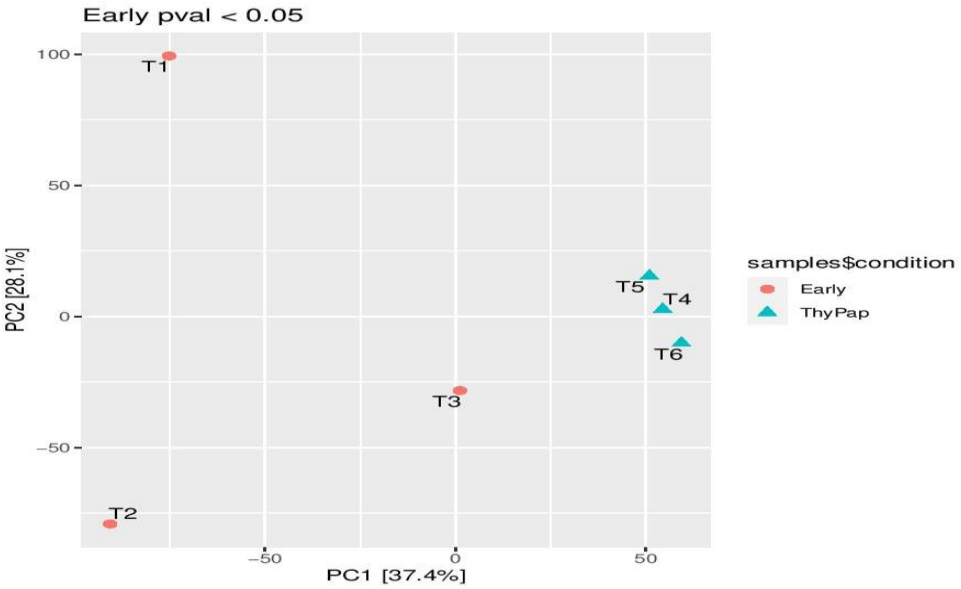

Figure 28. PCA of the transcriptomic data of early and late papillary thyroid cancer patients. The cancer stage is indicated using red circles (early) and blue triangles (late). The clustering direction indicates similarity in gene expression.

10.5.2 Late versus Early PTC single-sample Gene Set Enrichment Analysis related to biological processes of Signalling Pathways (ssGSEA)

To generate the enrichment profile of gene sets regarding their biological and molecular related to signalling pathways, we performed ssGSEA on normalized RNA-seq data. Resultant enrichment scores represent the activity level of specific biological processes in which those gene sets are up or downregulated (Figure 29 and Table26).

Table 26. Top molecular signatures of up/downregulated gene set enrichment analysis

Hallmarks of Upregulated Gene set	Hallmarks of Down-regulated gene sets
PANCREAS_BETA_CELLS	PI3K AKT MTOR MTORC1 SIGNALING
KRAS_SIGNALING_DN	MTORC1 SIGNALING SIGNALING
WNT_BETA_CATENIN_SIGNALING	CHOLESTEROL HOMEOSTASIS
ANGIOGENESIS	UNFOLDED PROTEIN RESPONSE
KRAS_SIGNALING_UP	OXIDATIVE PHOSPHORYLATION
NOTCH_SIGNALING	ADIPOGENESIS
TNFA_SIGNALING_VIA_NFKB	GLYCOLYSIS
APICAL_SURFACE	MYC TARGETS V1
EPITHELIAL_MESENCHYMAL_TRANSITION	MYC TARGETS V2
INTERFERON_GAMMA_RESPONSE	E2F TARGETS
UV_RESPONSE_DN	G2M CHECKPOINT
ESTROGEN_RESPONSE_EARLY	ALLOGRAFT REJECTION
MYOGENESIS	IL6 JAK STAT3 SIGNALING
HYPOXIA	INFLAMMATORY RESPONSE
	INTERFERON

	ALPHA RESPONSE
	BILE ACID METABOLISM
	PEROXISOME
	FATTY ACID METABOLISM
	COAGULATION
	COMPLEMENT
	ESTROGEN RESPONSE LATE

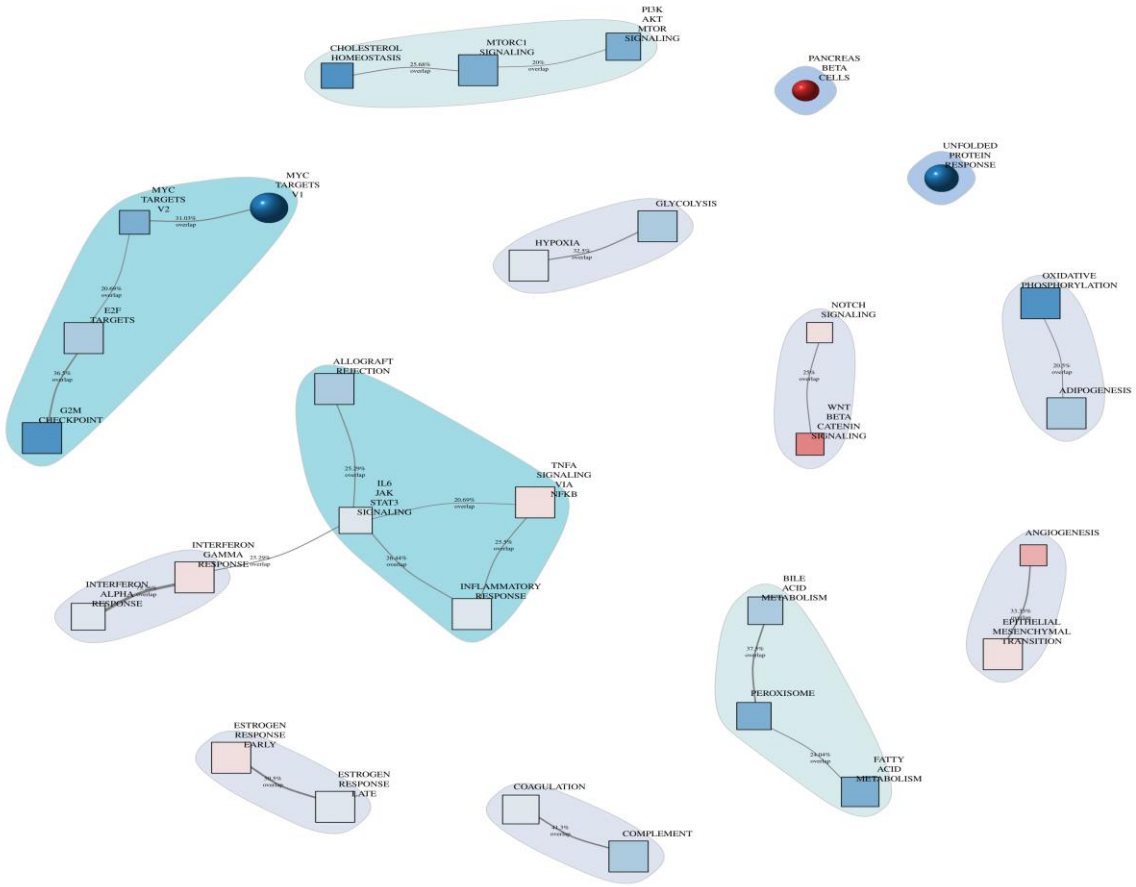

Figure 29 Late versus early ssGSEA of PTC regarding their biological functions related to signaling pathways. Nodes and squares represent enriched gene sets concerning molecular signatures. Size reflects the number of genes within the gene set. The line connecting objects represents the number of genes overlapping between enriched gene sets. Red represents upregulated gene sets. Blue represents underregulated gene sets. The intensity of color reflects activity/enrichment scores. Colors in between reflect lower enrichment scores compared to solid red and blue nodes.

10.5.3 Identification of Differentially Expressed Pathways in Early and Late PTC Biopsies

10.5.3.1 KEGG Pathway Analysis using Metascape in Early PTC

Data obtained from whole mRNA sequencing of PTC archival biopsies were analysed using the Metascape online analysis tool. KEGG pathway enrichment analysis results indicated that 21 differentially expressed pathways of early PTC were enriched in the negative regulation of protein phosphorylation, cranial nerve morphogenesis, steroid hormone biosynthesis, skeletal system morphogenesis, regulation of signalling receptor activity, acute–phase response, telencephalon development, response to glucocorticoids, positive regulation of fat cell differentiation, neuronal action potential, cellular response to amino acid stimulus, bone mineralization, detection of biotic stimulus, vitamin D receptor pathways, axoneme assembly, antigen processing, ubiquitination and proteasome degradation, execution phase of apoptosis, nephrotic syndrome, Rett syndrome-causing genes, neutrophil degranulation, and establishment of an endothelial barrier (Figure 30).

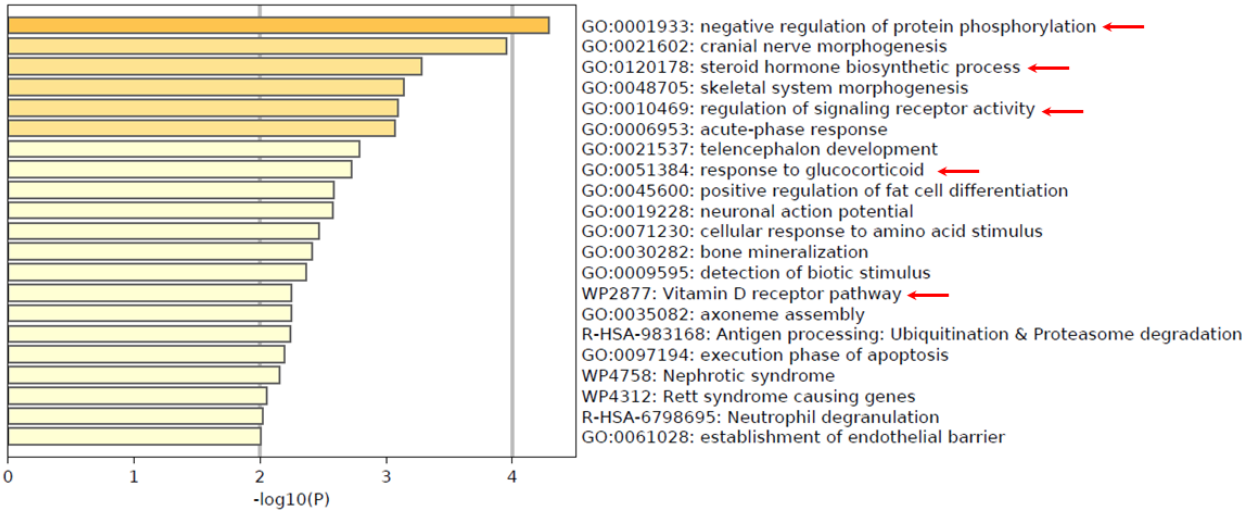

Figure 30 .Heatmap of KEGG-enriched differentially expressed pathways of early PTC biopsies. Colors represent P values. Arrows represent the most important pathways related to the PTC hallmark.

10.5.3.2 KEGG Pathway Enrichment Analysis using Metascape in late PTC

Using the Metascape analysis tool, Figure 31 shows the top differentially expressed pathways enriched in late PTC biopsies. Interestingly, the most enriched pathways were related to PTC hallmarks, including the cell cycle, sustaining proliferation, resisting cell death, angiogenesis and invasion, and metastasis (Figure 31).

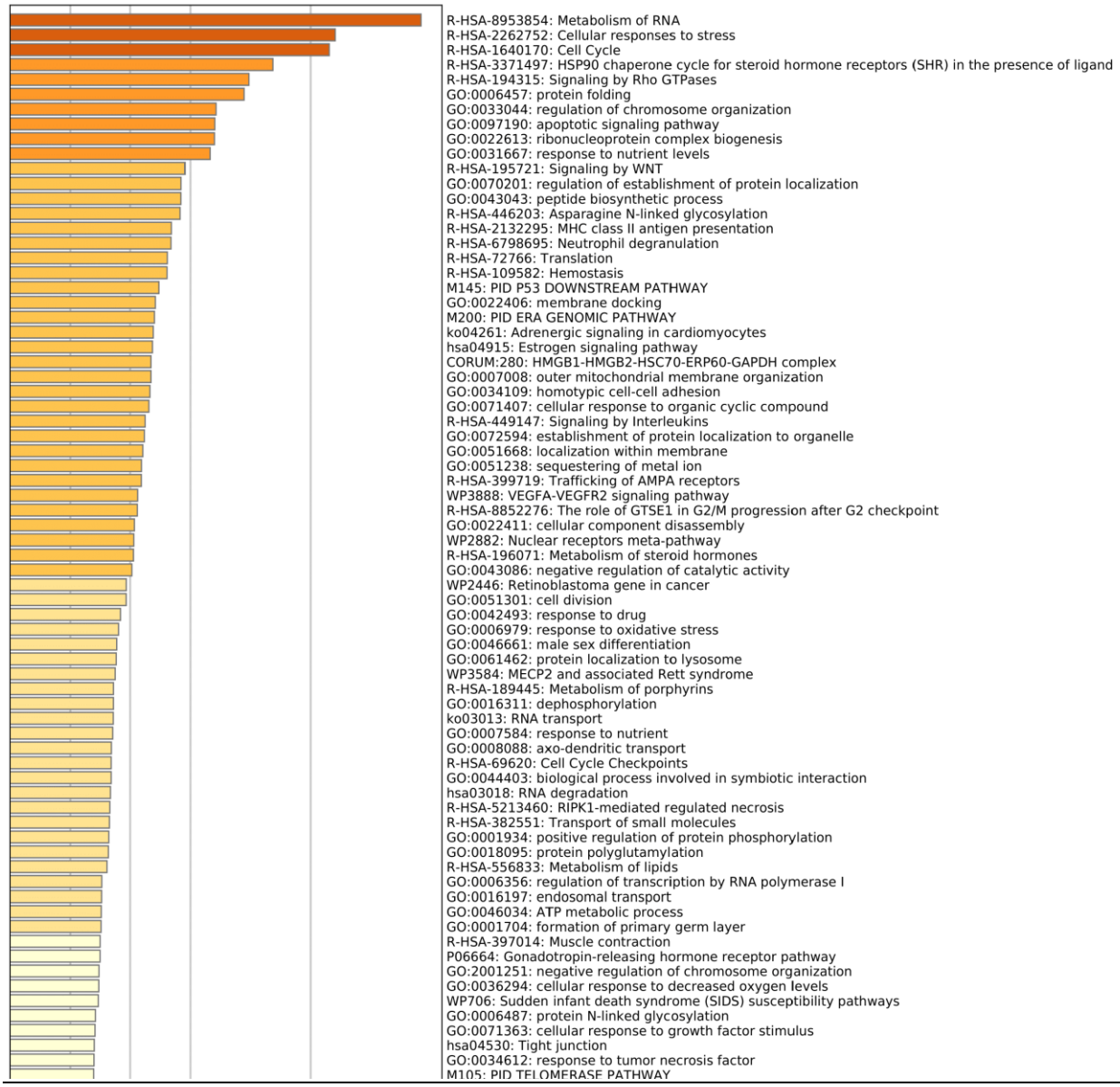

Figure 31.KEGG enrichment analysis by Metascape. Heatmap of KEGG-enriched differentially expressed pathways of late PTC biopsies. Colors represent P values.

10.5.4 Pathway –Responsive Gene Expression Signatures using (PROGENy)

To cross-validate the pathway enrichment analysis results obtained in the previous steps, we used variance stabilizing transformation (DESeq2 package, BioConductor) to normalize the gene expression matrix into the pathway score matrix. A total of 14 well-curated pathways were identified, strongly associated with its responsive gene expression. Key pathways activated in PTC are shown in (Figure 32).

10.5.5 Late vs. Early PTC Transcriptional Factors (TF) Activity Analysis using DoRothEA

We used the DoRothEA method coupled with VIPER on normalized mRNA-seq data of patients' biopsies to infer PTC transcriptional factors activity scores associated with molecular pathogenesis. A total of 12 differentially expressed transcription factors were found among PTC patients, including ETS2, six2, ZNF639IRF4, USF1, ETV1, JUN, AR, FOXK2, IRF2, E2F4, and MYC (Figure 33).

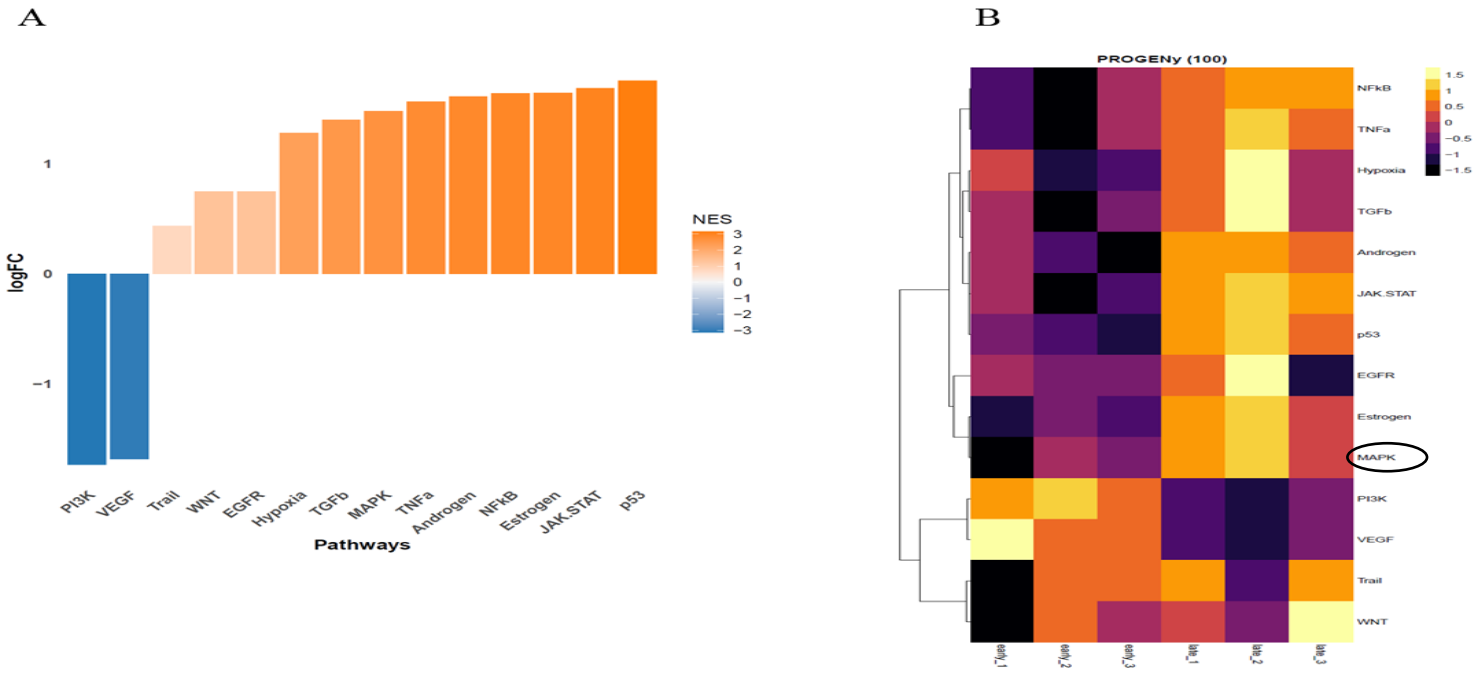

Figure 32 .A) PROGENy analysis of differentially expressed pathways. B) Differentially expressed pathways across the early and late PTC per sample activity score of corresponding pathway.NES: Normalized enrichment scores represented as shades of blue for downregulated pathways and orange for upregulated pathways.

10.5.6 PTC Large Signalling Contextualization using CARNIVAL

To determine the upstream processes that regulate the signaling network in PTC between late and early stages, we used previous data on pathway expression obtained by PROGENy and transcription factor activity scores obtained using DoRothEA. Figure 32 shows a putative number of predicted signalling pathways and protein activities with more activation of the MAP kinase pathway(Figure34).

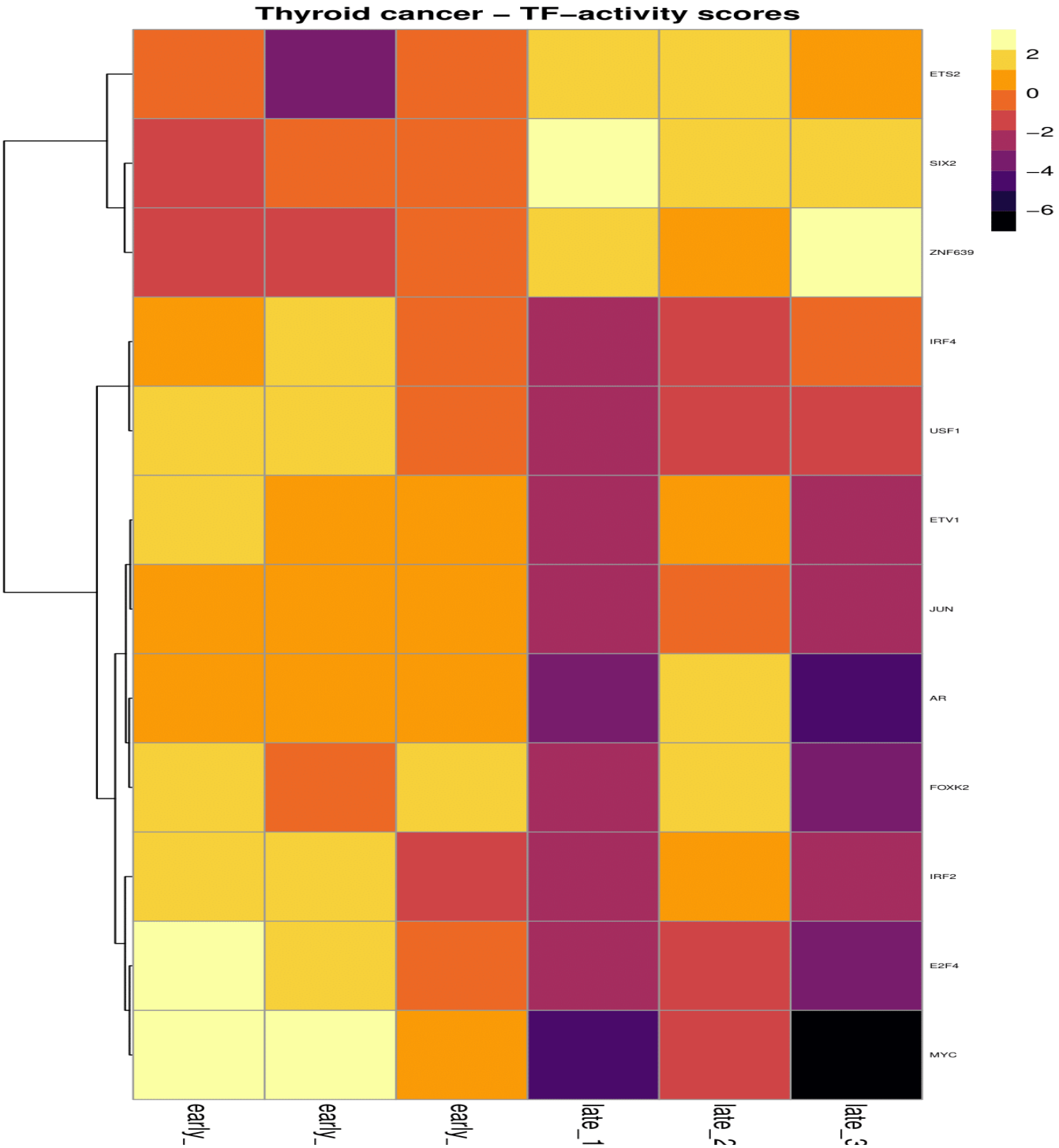

Figure 33 Late versus early PTC clustering of transcription factors activity scores using DoRothEA. TF activity scores are based on transcriptomic expression profiles of early- and late-stage patient samples

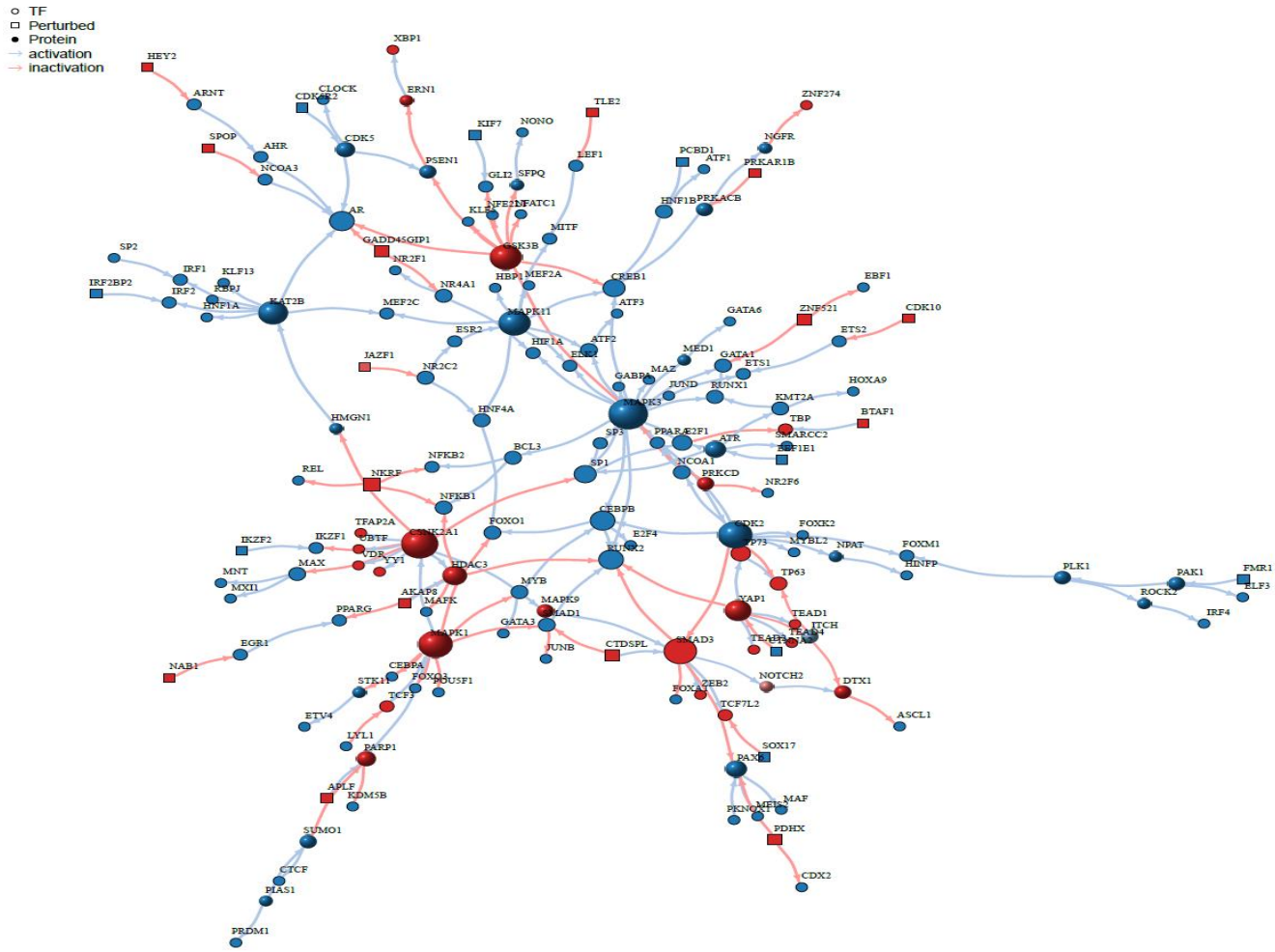

Figure 34. Network of architectural signaling cascade using prior knowledge of protein-protein interactions, differential pathway activation, and transcription factor activity, based on patients' mRNA gene expression. Nodes represent different proteins: red represents activation and blue represents inactivation. For edge arrows, red represents inactivation and blue represents activation. Interestingly, MAP kinase pathways appeared putatively in three activities with different interactions

10.6 Functional Transfection of MAPK6 Gene into PTC Cell Lines

10.6.1 In-vitro Validation of MAPK6 in PTC Cell Lines

Prior to next-generation sequencing analysis and to determine if MAPK was likely to be involved in PTC pathogenesis, cancerous (TPC-1) and normal Nthy-Ori-3-1 (Nthy) cell lines were transiently infected with a pcDNA-MAPK6 vector, and followed by validation techniques for expression as follows:

10.6.2 Effect of MAPK6 Transfection on TPC-1 Thyroid Cancer Cell Line by Transcriptomic Analysis

Using RNA sequencing analysis, Figure 35. shows that normal thyroid (NTHY) and thyroid cancer (TPC-1) showed higher expression when compared to untransfected normal and thyroid cancer cell lines.

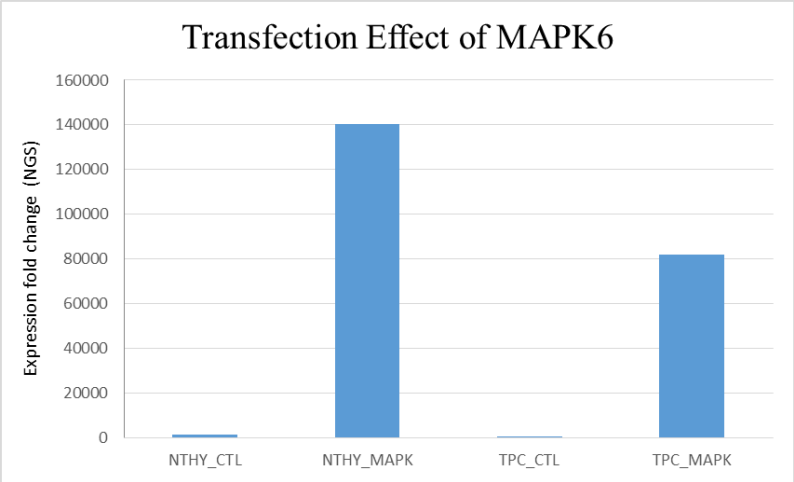

Figure 35 . Bar graph showing the expression fold change of MAPK 6 obtained via next-generation sequencing. NYTH: normal thyroid cell line; NYTH_MAPK: normal thyroid cell lines infected with MAPK6 vector; TPC: thyroid cancer cell lines; TPC_MAPK: thyroid cancer cell lines transfected with MAPK6 vector; NTHY_CTL: untransfected normal thyroid cell lines.

10.6.3 Characterization of transfected (TPC-1 tumor and Normal (Nthy)) cell lines using qRT-PCR

To confirm that (TPC-1) and (Nthy) cell lines were characterized for MAPK expression at the mRNA level, qRT-PCR was conducted, as shown in Figure. MAPK6 expression was shown to be higher in both normal (Nthy) and cancer (TPC-1) cell lines compared to the basal level of MAPK6 expression in untransfected and Viafect-treated cells. Figure A shows a cultured TPC-1 cell line under a microscope (Figure36).

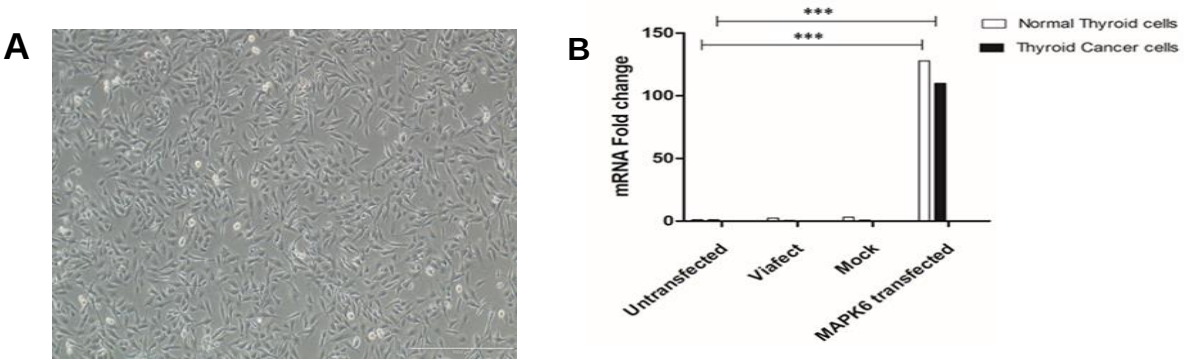

Figure 36 Figure 35. A) morphology of tumor TPC-1 cell line maintained in culture after four days of incubation at 37 °C and magnified at 10x inverted microscope: B) qRT-PCR of mRNA expression in transfected thyroid tumor and normal cell lines. *** P < 0.001

10.6.1 Validation of MAPK6 Protein Expression in Transfected (TPC-1 tumor and Normal (Nthy)) Cell lines using Western Blotting

Figure 37 indicates the protein expression of MAPK6 on tumor and normal thyroid cell lines compared to untransfected cells or cells treated with Viafect. MAPK6 with a molecular weight of 63 kDa in tumor and normal thyroid cell lines show high protein expression values for control or Viafect cells.

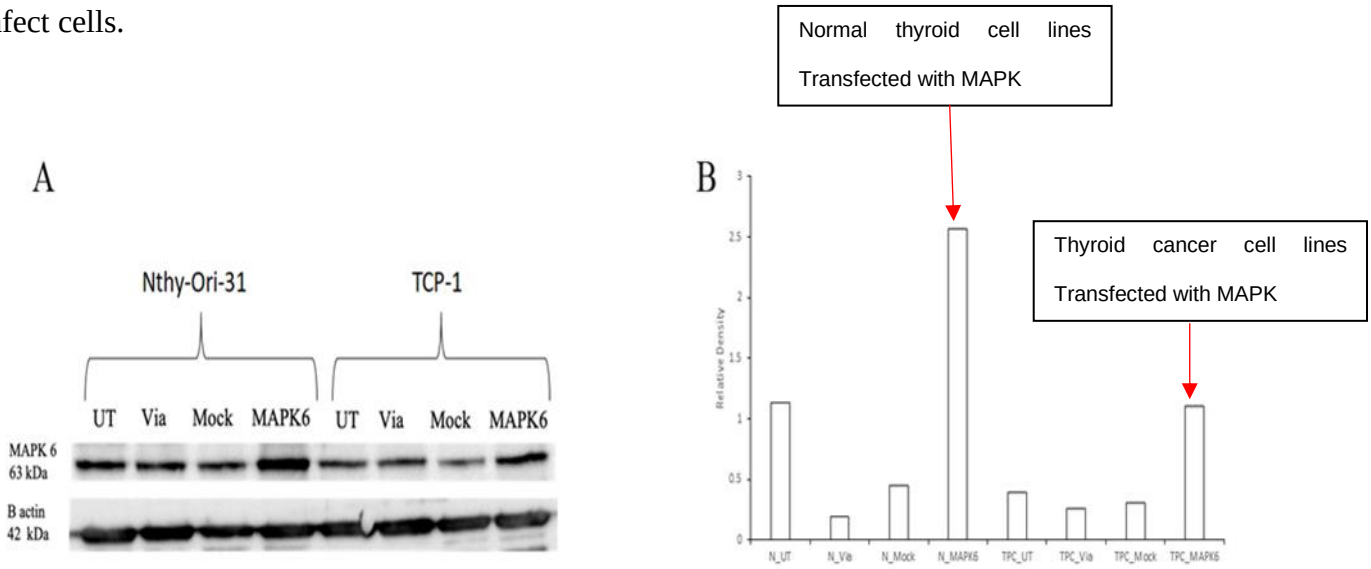

Figure 37. A) western blotting of MAPK 6 transfected normal and tumor thyroid cell lines. Nthy-ori-31: normal thyroid cell line; TPC-1: thyroid cancer cell line; UT: untransfected; Via: Viafect transfection reagent to transfect DNA into tumor cell lines; mock: transfected cells with a medium in place of pcDNA3-MAPK6 recombinant DNA to monitor the effect of the transfecting agent without DNA; MAPK6: transfection with recombinant DNA pcDNA3-MAPK6 into the cell lines. B) Densitometric analysis of MAPK6 relative expression in transfected normal thyroid (Nthy) and tumor (TPC-1) cell lines.

10.6.1 Identification of Differentially Expressed Pathways between Normal and Thyroid Cancer Cell Lines (untransfected)

10.6.1.1 KEGG Pathway Analysis using Metascape in Normal Thyroid Cell lines(Nthy)(untransfected)

A Metascape analysis showed that several differentially expressed pathways were enriched in thyroid cancer cell lines, as shown in Figure 38. Pathways of interest in normal thyroid cell lines were related to Interferon alpha/beta signaling, peripheral nervous system development, vitamin D receptor pathways, response to estrogen, and Type I diabetes mellitus.

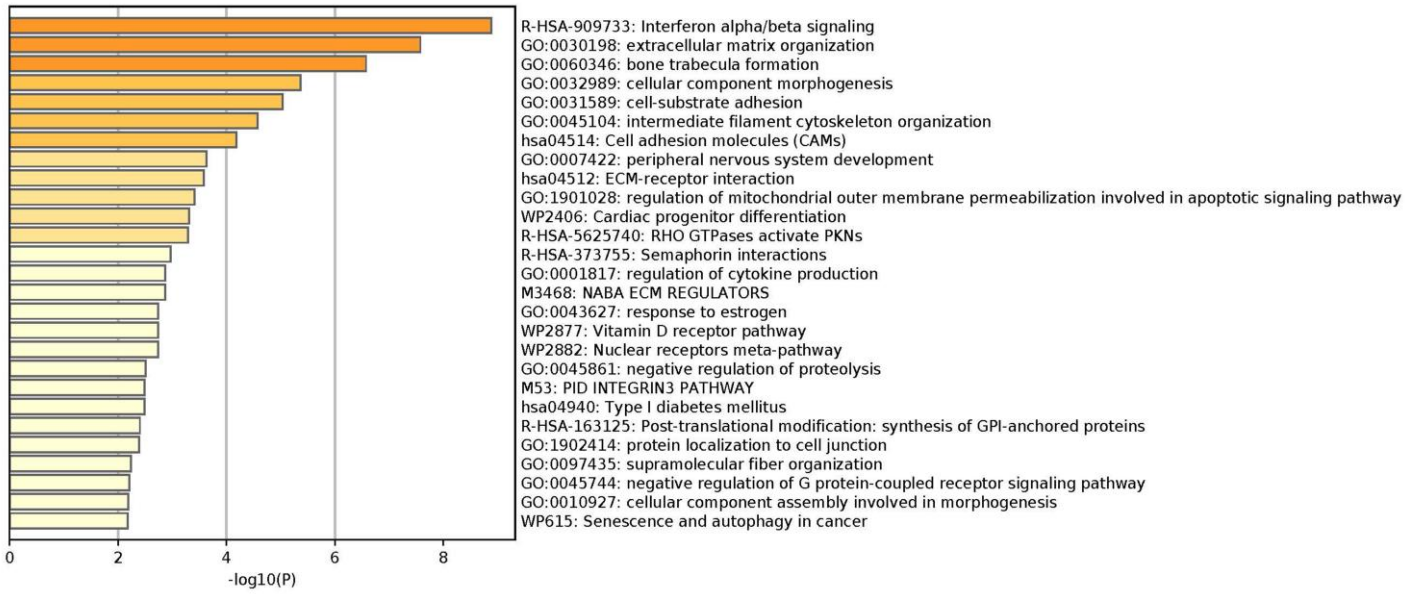

Figure 38. Analysis of Differentially expressed pathways in Normal thyroid cell lines by Metascape. Colors represent p values. Arrows represent the most important pathways related to the PTC hallmark. Orange color represents higher expression value; pale yellow represents lower expression value.

10.6.1.2 KEGG Pathway Analysis using Metascape in Thyroid Cancer Cell lines(TPC-1)(untransfected)

Data obtained from whole mRNA sequencing of normal thyroid cell lines were analyzed using the Metascape analysis tool. KEGG enrichment analysis showed that several pathways were enriched, as shown in Figure. Pathways of interest in normal thyroid cell lines were more related to the positive regulation of cell death, transcriptional regulation by TP53, positive regulation of proteolysis, signaling by receptor tyrosine kinases, P53 downstream pathways, cell growth, intrinsic apoptotic signaling pathway by p53 class mediator, DNA repair, cell division, and positive regulation of the apoptotic signaling pathway, as shown in Figure 39.

10.6.2 Identification of Differentially Expressed Pathways in MAPK6 Transfected Thyroid Cancer Cells

10.6.2.1 Pathways Activated in MAPK6 Transfected TPC-1

Figure 40 shows that several cancer hallmark pathways were enriched, such as cell cycle, ESR-mediated signalling, apoptotic signalling pathways, positive regulation of apoptotic processes, signalling by receptor tyrosine kinases, cell division, DNA repair, transcriptional regulation by TP53, and many more.

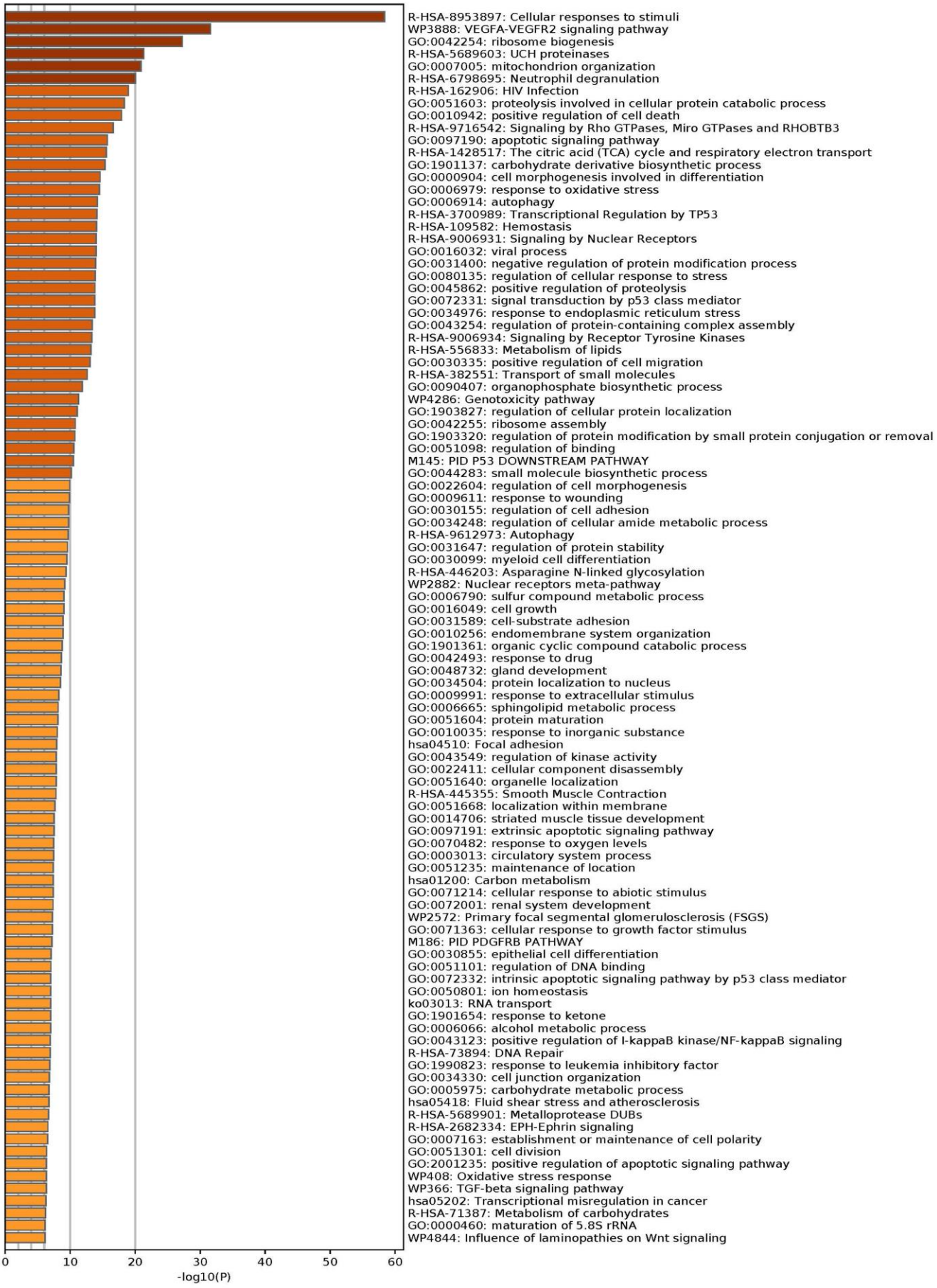

Figure 39. Differentially expressed pathways in thyroid cancer cell lines (TPC-) by Metascape

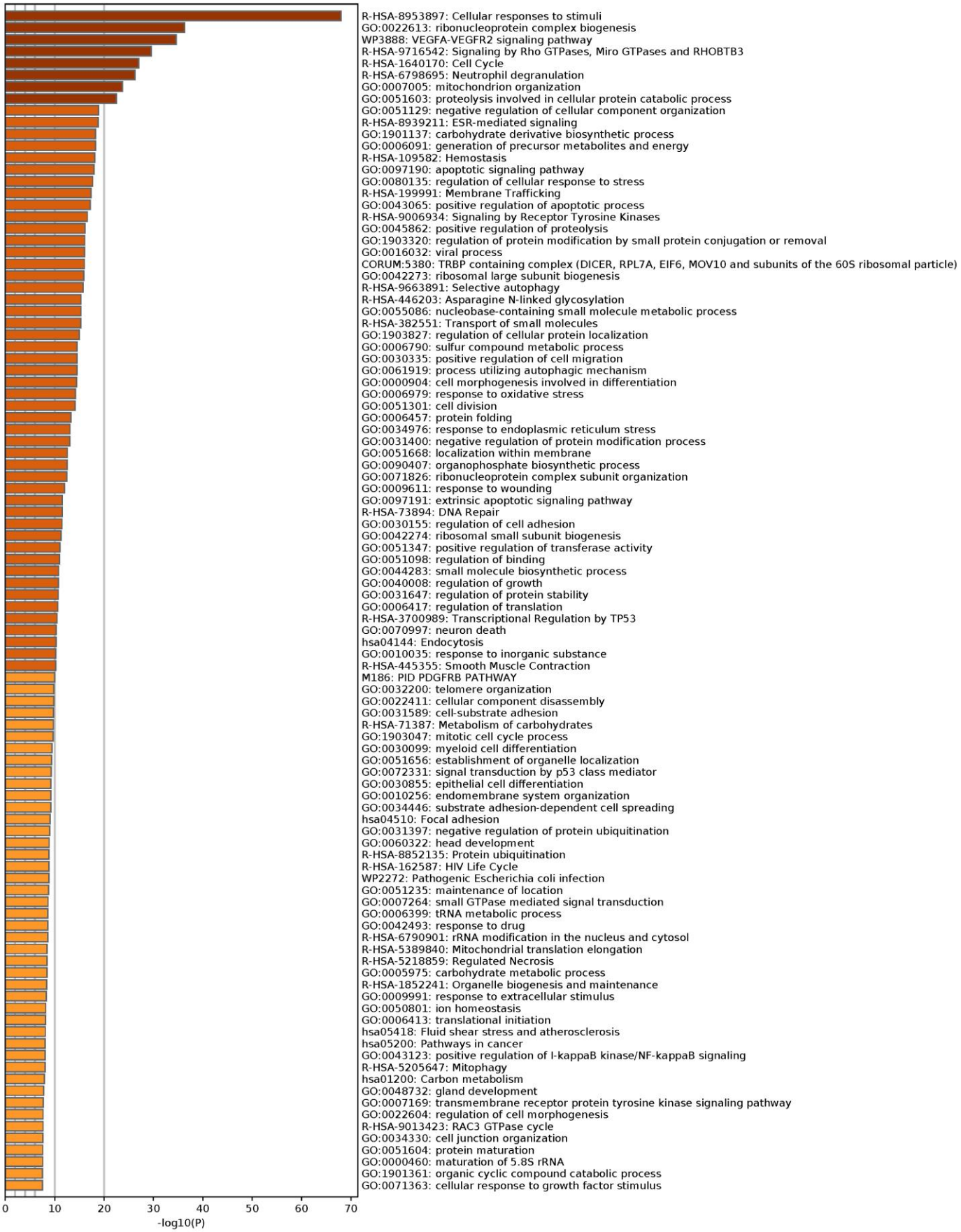

Figure 40 . Pathways activated in MAPK6 transfected thyroid cancer cells compared to thyroid cancer

10.6.2.2 Pathways Activated in Normal Thyroid Cell Line compared to MAPK6 Transfected Thyroid Cancer Cell Line TPC-1

Figure 41 shows that differentially expressed pathways were enriched in the metabolism of vitamins and cofactors, positive regulation of cell death, MAPK signaling pathway, Vitamin D pathway, and many important pathways.

10.6.2.3 Pathways Activated in Untransfected Cancer Cell Line (TPC-1) compared to MAPK6 Transfected Thyroid Cancer Cell Line TPC-1

Figure 42 shows that differentially expressed pathways in untransfected thyroid cancer cells were associated with Interferon alpha/beta signaling, TNF signaling pathways, PID AP pathways, regulation of steroid biosynthesis processes, vitamin B12 metabolism, signaling by ALK in cancer, PID AFT2 pathways, negative regulation of phosphatase activity, pyruvate metabolism, and many more.

10.7 Integration of Differentially Expressed Pathways in PTC Cell Lines.

Transcriptomic analysis has provided different gene sets which are differentially expressed for each cell line. Table 27 shows that the number of differentially expressed genes is reduced with MAPK6 overexpression.

Table 27. Differentially expressed genes exist across different combinations of thyroid cancer and normal cell lines. Nthy: normal thyroid cell line; TPC-1: thyroid cancer cell line; TPC-1+MAPK6: thyroid cancer cell line transfected with MAPK6 vector (86).

Experimental Description	Overexpression	Number of differentially expressed genes
Nthy v TPC-1	Overexpressed genes in Nthy	3660
Nthy v TPC-1	Overexpressed genes in TPC-1	2514
Nthy v TPC-1+MAPK6	Overexpressed genes in Nthy	3464
Nthy v TPC-1+MAPK6	Overexpressed genes in TPC-1 with MAPK6 overexpression	2671
TPC-1 v TPC-1+MAPK6	Overexpressed genes in TPC-1	318
TPC-1 v TPC-1+MAPK6	Overexpressed genes in TPC-1 MAPK6 overexpression	165

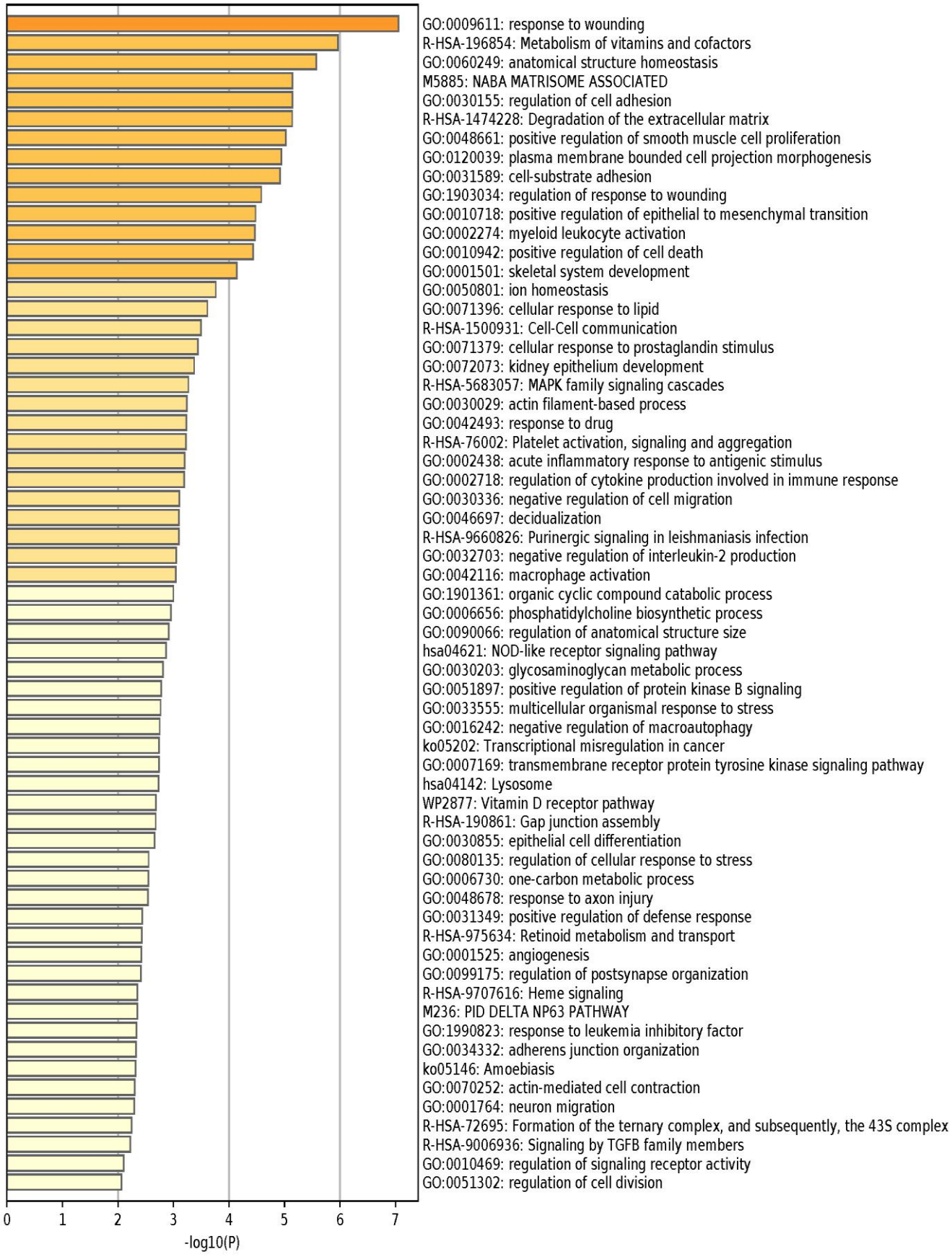

Figure 41. Pathway analysis between normal thyroid cell line and MAPK6 transfected cancer cell line.

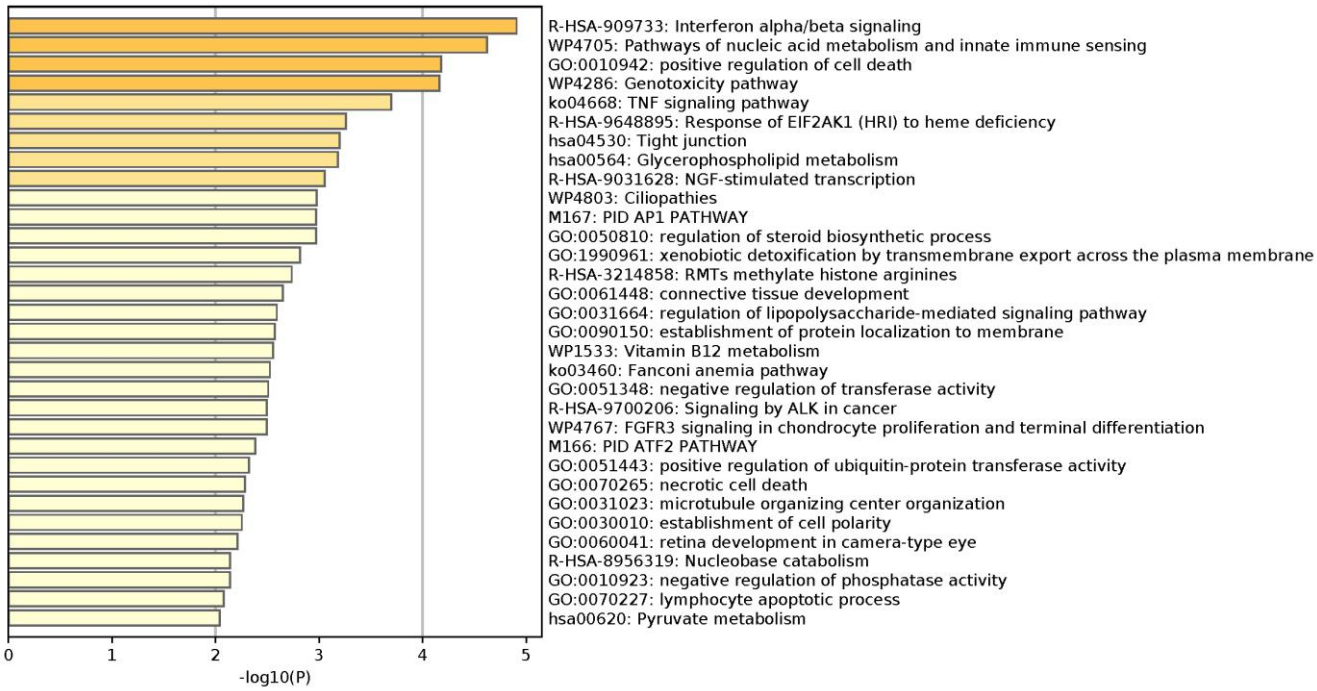

Figure 42 Differentially expressed pathways in cancer cell lines in comparison to MAPK 6 transfected thyroid cancer cell lines.

10.7.1 The Overall Expression of MAPK6 in Normal Thyroid and TC Cohort Patients Sets

By using TNM plotter, Figure 43. shows that MAPK6 is significantly differentially expressed ($P < 0.0001$), with higher expression in thyroid cancer patients compared to normal thyroid patients.

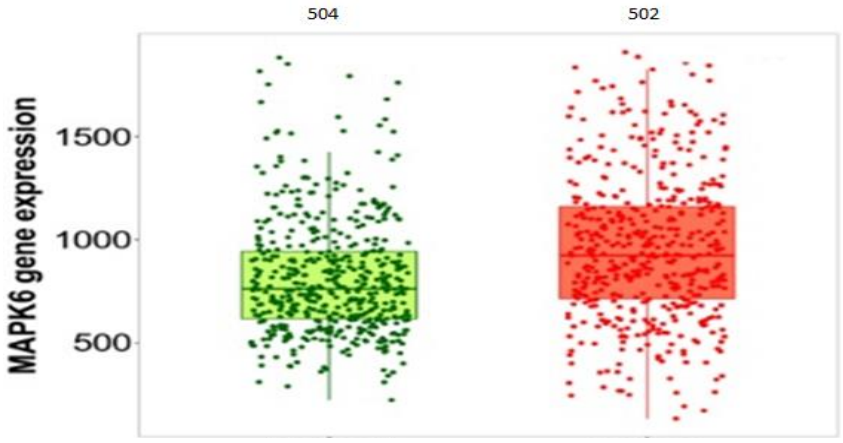

Figure 43. Expression of MAPK6 across normal (N = 504 patients) and thyroid cancer (N = 502 patients) using TNM plotter. Results are significant if P < 0.0001.

10.8 In vivo validation of MAPK6 Overexpression on independent cohort samples

10.8.1 Effect of MAPK6 Overexpression across Normal, Tumour, and Metastatic Thyroid Cancer Cohort Samples

Figure 44. shows that MAPK6 is significantly differentially expressed ($P < 0.05$), with higher expression in tumour than normal thyroid samples and lower expression of MAPK6 in metastatic thyroid patients.

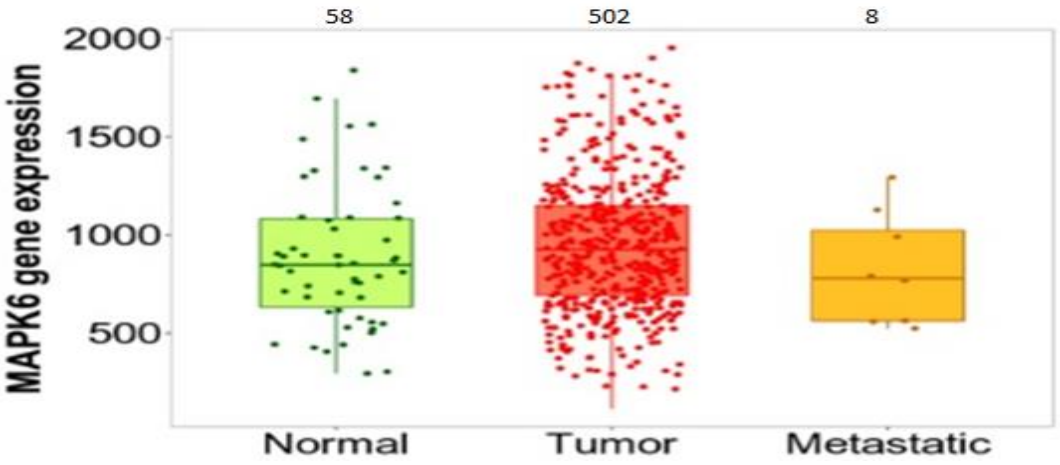

Figure 44 . MAPK6 expression representation among a group of 58 normal thyroid patients, 502 tumor thyroid patients, and eight metastatic thyroid patients.

10.8.2 Effect of MAPK6 Overexpression on Patients' Survival by using Kaplan Meier Survival Analysis

An independent cohort of 502 patient samples (375 low-MAPK6 and 127 high MAPK6) was analyzed using the Kaplan Meier survival tool. The analysis revealed that overexpression of MAPK6 is linked to poor survival in PTC patients, as shown in Figure 45. Additionally, the hazard ratio of 2.57 strengthened the association between overexpression and poor survival (Table 28).

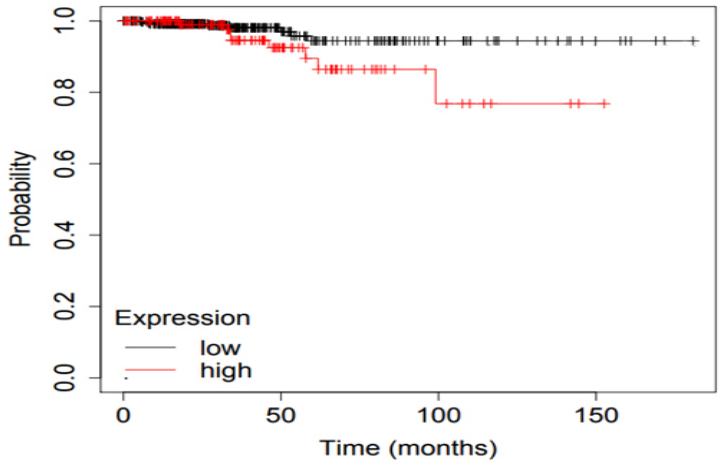

Figure 45. Kaplan Meier survival analysis of independent cohort PTC patients. At the time point of 50 months, patients with higher MAPK6 expression began to show poorer survival than patients with low MAPK6 expression. The same effect was observed at around 90-98 months from the initial diagnosis.

Table 28. Survival analysis based on the level of MAPK6 expression for the validation cohort (N = 502). Patients with higher MAPK6 expression survived less than patients with low expression over different time intervals.

MAPK-6 Expression	Patients Frequency	Number of patients Survived at 50 months	Number of patients Survived at 100 months	Number of patients Survived at 150 months
low	375	89	26	6
High	127	39	8	1

11 Discussion

11.1 Global Thyroid Cancer Incidence Demographics

The primary purpose of this study was to perform a comparative epidemiological analysis of thyroid cancer (TC) in UAE and other populations using data obtained from national and global cancer registries. To our knowledge, this study is the first to explore TC incidence covering the entire UAE region. This incidence in UAE increased from 4.37% in 2011 to 9.99% in 2017 (56). Earlier research supported the increasing rate of TC between 2011 and 2017 (33). In terms of continental incidence, our results revealed that Asia had the highest TC incidence rate in 2020 (349,897 per 100,000), and Oceania had the lowest rate (5062 per 100,000). UAE's TC incidence rate follows a steady global trend, which is still low (405 per 100,000). The predictive models used in this study from 2020–2040 also showed a relatively low global rate of change in TC incidence when compared to other cancers. The Asian continent will be most affected by the increasing rate (4665), followed by Africa (3885) and Latin America (1002.8). UAE showed a low rate of change of 15.2, whereas Europe had a negative rate of change (-84.3) past 2020. Moreover, the predicted TC incidence in UAE between 2020 and 2040 dropped from 8.40 in 2020 to 6.95 in 2040. As per the UAE-NCR, a total of 2036 newly diagnosed thyroid carcinoma cases were diagnosed between 2011 and 2017, out of which 14020 were expats, and 634 were Emiratis.

11.2 Gender and Age Association with Thyroid Cancer

The association between TC incidence and gender was further investigated to reveal that the TC incidence rate was higher in females across all continents, at an average of 3 times higher than in males. This finding was supported by previous research investigating the global burden of TC attributes (117). The highest incidence of TC was observed in Polynesia, and the lowest was found in Africa. In UAE, 2011 scored the highest female to male ratio of 12.0 for Emiratis and

the year 2016 for expats, with a ratio of 3.92. Therefore, our study supports that TC is associated with gender both globally and locally. Females are more susceptible to this disease due to hormonal fluctuations at puberty, whereas the possibility of developing such cancer declines as women get closer to menopause (118). Estrogen is not only associated with the prognosis of breast cancer but is also linked to the pathogenesis of papillary thyroid carcinoma. Recent studies have revealed that females are 3–4 times more likely to develop TC during pregnancy or have a high reoccurrence of such cancer due to pregnancy (119). The results obtained by these studies supported the role of estrogen and its receptors in thyroid carcinoma pathogenesis (120). In UAE, although the incidence rate is considered low compared to other regions, the prevalence in UAE females increased between 2011 and 2017(32, 33, 116, 121-125). The higher incidence in females may be associated with a hormonal influence, as was found to be the case for other female populations around the globe, in addition to exposure to environmental toxins, obesity, smoking, lack of exercise, and a sedentary lifestyle(55, 59).

This study also demonstrated that age is another risk factor for TC pathogenesis. The highest peak of TC incidence among both genders tends to be at the age of 35–39 years. Moreover, the highest peak of incidence in females was observed in 2016 among Emiratis and expats in the 30–34-year age group. The association between age and TC development might be explained by the fact that, as aforementioned, the younger generation has adopted significant lifestyle changes, including increased fast-food consumption, a diet poor in iodine, and increased exposure to environmental toxins. However, further investigations should be conducted to confirm such associations. In addition, this study also showed that the peak incidence of TC occurs during the third-fourth decade of life, which is a decade behind neighboring Gulf countries(36). The study's strengths include establishing the first data platform in UAE related to TC cases diagnosed in 2011–2017 and providing malignancy predictions for future monitoring. In addition, the epidemiological method, including predictions, could be used to investigate other complex diseases and cancers in UAE. Some significant limitations of this

study include a lack of detailed clinicopathological data about patients, such as BMI, family history, pre-existing medical conditions, and treatment history.

In conclusion, the study showed a small but steady increase in TC incidence per year, following global incidence rates. It also identified that age and gender are risk factors for TC pathogenesis. Not only does UAE have a high female-to-male ratio, but females are more susceptible than males worldwide. The majority of the disease's contribution accounts for UAE expats due to the larger population. In addition, our study revealed that the most affected age group was above 30 years and below 40 years. Interestingly, by applying predictive models, the future trend of TC in Europe was different than the other continents, diverting towards a declining rate of occurrence.

11.3 Cellular Pathways' Association with PTC in Selected Populations

The secondary aim of the study was to identify cellular pathways related to PTC pathogenesis between NAG and metastatic stages in different populations, such as Korea, Ukraine, and Brazil. This work was performed through in-silico transcriptomic analysis of PTC biopsies using Bioinformatics tools, followed by validation using independent cohorts of PTC patients. Cellular pathways specific to non-aggressive and corresponding metastatic PTC and those commons between the two types were uncovered in this research. Both clinical groups shared several genes and pathways, including potassium and calcium transmission and tyrosine and phosphatase pathways. Cell signaling linked to hormonal control was more strongly associated with the NAG group. In contrast, the research found more prevalence of MAPK activation and other cancer characteristic pathways, such as apoptosis and proliferation regulation, to be more significant in the metastatic pathways.

By employing pathway analysis to examine the differentially expressed genes across various populations, it was discovered that MAPK is active in various populations, including Ukraine, South Korea, and Brazil. On the other hand, each group has a distinct set of active cellular

pathways. Patients from Ukraine have more significant pathways associated with hormone response and metabolic activities. Patients from Brazil showed pathways related to environmental stimuli, such as the reaction to inorganic chemicals and vitamin A metabolism, indicating that pollution and a poor diet may have played a role in developing PTC cases(126, 127). Cancer hallmark pathways, including apoptosis and progress, appear to be more active in South Korean patients, as evidenced by the activation of viral entry into the cell corridors, proposing possible hereditary predispositions within Korean populations that contribute to persistent inflammatory responses that, if not cured promptly, may result in PTC.

Overall, the analysis demonstrated that PTC is a highly complex illness with significant levels of *intra-tumoral heterogeneity*, as illustrated by the instigation of diverse cellular pathways across various populations with the highest prevalence of MAPK-associated pathways. The genetic diversity across multiple populations may explain the variation in pathways activated in each population. TP53 mutations, which may cause tumors in various tissues and are shown in Li-Fraumeni patients(128), are common in the Brazilian population, for example. The DNA repair genes BRCA1 and BRCA2(129) are also commonly mutated in Brazilian people, whereas a mutation to the DNA repair gene called RAD5124(130) is more common among Ukrainians. There is a correlation between mutational deletion in *Sialic Acid Binding Ig Like Lectin 14 (SIGLEC14)(131)* and macrophage inflammasome activation (132). However, this mutation is more prevalent in the South Korean population. Taken together, the diversity in mutations in the studied populations may have contributed to varying transcriptomic profiles for each population. GSEA pathway analysis for each studied population had distinct genes elevated: CRABP1 for Ukrainians, MAPK4 for Brazilians, and LAMB3 for South Koreans. Additionally, a DrugBank search employing the identified genes found CRABP1 retinoid receptor treatments for eczema, including Tretinoine and Alitretinoine, the MAPK4 inhibitor Fostamatinib(2), which is used to treat chronic immunological thrombocytopenia, was also identified. The transcriptome analysis showed that various medications linked to the identified genes might be repurposed in different groups for TC treatment.

When comparing the immune response in NAG and metastatic thyroid samples, the study found a disparity in the tumor's microenvironment, where NAG samples had more inflammatory-related pathways than metastatic ones. This observation may be explained partially by the fact that NAG contains both an inactive and active NK segment and a larger reminiscence; naive B-cell ratio, as metastatic cancer did not, suggesting that the disease phase moved from the inflammatory NAG to a metastatic stage. According to previous research, NK cell penetration in the early phases of PTC is increased compared to PTC's metastatic stages(133), which supports this conclusion. Additionally, The M1/M2 ratio was found to be imbalanced in the NAG and MET stages of PTC, with a marginally more significant proportion in the metastatic phase, suggesting that the metastatic stage can potentially have a diverse PTC mechanism of pathogenesis, meriting additional research of the genes associated with M1 and M2 divergence in TC(60).

11.4 Genes Associated with PTC Carcinogenesis

This research also found that *BCL2, CACNA1D, KCNQ1, KCNN4, EGFR, and PTK2B* were all associated with the initiation and development of PTC. The BCL2 (B cell lymphoma 2) anti-apoptotic protein is essential for suppressing cellular suicide, often referred to as apoptosis (134). A study by Aksoy et al. revealed that reduced BCL2 expression in early TC stages promotes the anticipated development of oncolytic neoplasms by preventing tumor cell death(135). In our study, BCL2 overexpression was observed in both the NAG and metastatic sets, agreeing with Aksoy and colleagues' study. Additionally, few studies linked BCL2 involvement in early PTC. They mainly indicated that BCL2 manifestation declines in microcarcinomas of PTC, implying that it is perhaps not a reliable prognostic factor because it is convoluted in the early stages of PTC and persists in the metastatic stage(136). However, Navitoclax31 and other PTC-related medications, such as Navitoclax, may be effective in some PTC cases(72).

Ion transport, notably the transfer of calcium and potassium, is one of the often active pathways discovered by our study. Many genes associated with calcium and potassium transport have been found. As part of the alpha-1 subunit of the CaV1.3 channel in the adrenal gland, the CACNA1D gene regulates positively charged CaV1.3 channels across cell membranes, where calcium ions may pass via these subunits that function as channels. Blood pressure and fluid balance are also maintained by aldosterone production, which this gene regulates (118, 137). Adrenal aldosterone-producing adenomas have somatic CACNA1D mutations linked to tumor genesis (137). Interestingly, it was also shown that cancer cells might convert from an apoptosis-prompting Ca+ influx route to a proliferative Ca+ influx pathway, resulting in an oncogenic switch that promotes cancer cell proliferation and apoptosis susceptibility. In our study, the stimulation of calcium ion carriage pathways in both metastatic PTC and NAG was also successfully validated by pathway analysis. Overall, our research found that CACNA1D is more commonly expressed in the metastatic PTC and sometimes in the NAG than in healthy controls, which suggests that it may have a role in PTC development. Even though Isradipine and other CACNA1D-targeting medicines treat hypertension by controlling calcium ion transport (9). Besides, the results of our study show that these medications could be used in treating some PTC cases.

The KCNQ1 gene, part of a family responsible for developing potassium channels, is also involved in PTC progression. KCNQ1-formed channels are primarily found in the innermost ear, heart, kidney, colon, and stomach. Researchers have revealed voltage-gated K+ channels as novel prognostic markers(138). Many disorders, including cardiovascular disease, perinatal death, and cancer, may be caused by somatic mutations in the potassium ion transport gene KCNQ1 and specifically through the methylation of its promoter that results in the silencing of genes and disrupted regulation of K-ion transport(139-142). According to our findings, KCNQ1 was the most commonly expressed gene in cellular pathways associated with NAG PTC. However, our study also showed that Promethazine and Enflurane, two sedative medications targeting KCNQ1, may be potential targets for future studies seeking possible PTC treatments.

The *Potassium Calcium-Activated Channel Subfamily N Member 4 (KCNN4)*, a well-known oncogene found to be elevated in our results, has since been recommended as an investigative and prognostic indicator for PTC(143). Additionally, it has been shown that patients with KCNN4 deficiency have a worse prognosis, drug resistance, and a shorter lifespan than those with normal levels of KCNN4(144-146). The KCNN4 gene was highly prevalent, with an expression increase of approximately twofold in our current investigation. Therefore, targeting potassium calcium-activated channels may inhibit PTC development to the metastatic phase. In short, next-generation sequencing and the TNM plot of our clinical biopsy indicated that KCNN4 is considerably overexpressed in metastatic and NAG compared to normal PTC ($p < 0.001$), which is an exciting finding.

Epidermal growth factor receptor (EGFR) has also been linked to TC. EGFR has been shown to have a role in cell propagation and survival signaling cascades. *Transmembrane tyrosine kinase* receptors may be found in various cancerous tissues, including thyroid carcinomas, glioblastomas, breast cancer, osteosarcoma, and lung cancer(147). Following somatic mutations, gene intensification, and protein over-expression, EGFR signaling pathways undergo alterations in human malignancies, contributing to worse prognosis and poor survival(70). Our findings revealed that EGFR is the most often differentially expressed gene in metastatic PTC and is also present in half of the non-aggressive group, showing that EGFR plays a vital role in PTC development and metastasis. Moreover, a DrugBank search for TC treatment drugs yielded multiple FDA-approved therapies that target EGFR, such as Vandetanib and Cabozantinib-S-Malate, which can be used for PTC patients(88, 148). To recapitulate, RNA-seq on the clinical samples in our study demonstrated that EGFR was considerably overexpressed in metastatic and NAG PTC compared to control thyroid samples ($p < 0.05$).

(PTK2B), Another gene identified in our study refers to protein tyrosine kinase 2 beta, the encoded proteins involved in Ca+channel regulation and MAPK signaling pathway activation. PTK2B harboring mutations linked to differential overexpression may contribute to of Pyk2/c-Src complex formation, c-Src pathway initiation, and ERK/MAPK signaling pathway activation.

The activated ERK/MAPK signaling cascade was known to regulate the activation of more than 160 transcriptional factors downstream signaling proteins involved in tumor progression(149). ERK/MAPK regulates cellular development, survival, invasion, and progression(150). Our study's clinical samples' RNA-seq revealed that the PTK2B gene exhibits significant overexpression in both NAG and metastatic samples compared to normal thyroid ($p < 0.05$). Consequently, because PTK2B is associated with CA+ regulation and activation of the MAPK signaling pathway, PTK2B-targeting drugs, including Genistein (CA+ deficiency treatment)(97, 98), Fostamatinib (chronic immune thrombocytopenia treatment)(151), and Leflunomide (rheumatoid Arthritis) may be used for some PTC cases after further investigations(117). Only a few studies explored the association between PTK2B and EGFR genes. A recent study by Selemetjev et al. revealed that overexpression of FA kinases and EGFR is associated with more aggressive forms of PTC and metastasis into the lymph nodes(152) . It was also found that PTK2B, which is a member of the FA kinase group, is known to be linked with pathogenesis and metastasis to lymph nodes in PTC patients. Thus, the use of a combinational treatment protocol comprising Crizotinib (tyrosine kinase targeting drug) and erlotinib (EGFR targeting drug) was effective for treating triple-negative breast cancer, with a noticeable reduction in tumor size(153). PTK2B was also found to be a favorable target point for Crizotinib, a well-known drug used for treating several cancer types(154, 155).

Our study revealed that the PTK2B gene was overexpressed in both NAG and metastatic PTC in addition to EGFR, the MAPK signaling pathway, and Ca+ ion transport pathways. Therefore, a combinational therapy approach that targets all of these immune components could represent an attractive therapeutic point for treating PTC, particularly in cases associated with poor survival. Briefly, gene set enrichment of activated cellular pathways in PTC has shown that enriched pathways overlap between NAG and metastatic samples. Encoded regulatory proteins involved in PTC pathogenesis are primarily associated with protein tyrosine kinase receptors, Ca+-induced channels, K+ channels, and MAP/ERK kinases. Furthermore, overexpressed genes identified among NAG and metastatic genes are hot spots for potential drug discoveries targeting PTC.

11.5 Genes and Cellular Pathways Association with PTC Progression in UAE-Based Archival Samples

The third aim of this study was to identify co-differentially expressed genes and cellular pathways associated with TC pathogenesis. A whole transcriptomic analysis of 6 UAE-based TC FFPE was performed to achieve this aim. At a cut-off of $p < 0.05$, the differential gene expression analysis identified 250 genes that are over-expressed in early PTC and 361 that are over-expressed in late PTC. Further use of a more stringent cut-off of $p < 0.01$ identified 44 differentially significantly expressed genes between early and late PTC. In addition, pathway analysis identified several cellular pathways activated as the disease transitions from early to late stages, including MAP kinase pathways, estrogen, NFkB, PI3K, vitamin D, and VEGF. The analysis also revealed a panel of interesting genes involved in PTC, such as MAPK 6, HOXA3, TLX3, OGT, HIST3H3, ADAM9, and GREB1 signaling cascades.

11.5.1 MAPK6 Gene

Mitogen-activated protein kinase 6 (MAPK6) is a protein-coding gene that regulates extracellular signaling mechanisms in the nucleus. Proteins encoded by the MAPK6 gene are Ser/Thr, members of the protein kinase family-related closely to mitogen-activated protein kinase (MAPK pathway) (156). The MAPK6 gene is activated by a series of complex phosphorylation events, which begin at Ser-189 of the S-E-G motif, where atypical interaction of MAPKAPK5 at T182(157) and MAPK6 takes place and, in turn, leads to phosphorylation of ERK3/MAPK6, tyrosyl DNA phosphodiesterase 2 (TDP2), receptor coactivator 3 (SRC-3) (158), and MAPK/Akt, all of which in combination promote cell cycle entry and downstream signaling cascades(158). MAPK 6 is also known to promote tumor growth, cell invasion, and migration. In addition, MAPK6 mRNA is associated with poor patient survival in many types of cancer(159). In our study, we discovered that MAPK6 is overexpressed in late PTC. This result is also consistent with a study by Trevino et al. that suggested that MAPK6 plays a role in thyroid

carcinogenesis. With respect to the few studies conducted to discover the molecular function of the MAPK protein family in different cancers, MAPK6's precise role in thyroid tumor genesis remains understudied.

11.5.2 HOXA3 Gene

HomeboxA3 (HOXA3) is a transcription factor, the expression of which is spatially regulated during embryogenesis. This gene is found to be part of chromosome 7's cluster A and is associated with gene expression and differentiation regulation via DNA-binding transcriptional factors(160). Furthermore, the expression of HOX3 genes is found to be involved in angiogenesis of endothelial cells (161), transcriptional regulation by RNA polymerase II, and positive regulation of cellular proliferation(162). In our study, we observed that the HOXA3 gene is overexpressed in PTC tumor samples, agreeing with the results of Jiang et al. (2019), who noted via an *in vivo* experiment in a mouse model that PTC tumor growth was promoted by HOXA3 overexpression. Moreover, that study showed that HOXA-AS2/miR-15a-5p/HOXA3, along with the non-coding RNA complex, promotes carcinogenesis and progression in PTC via modulation of the HOXA3 gene. The authors also noted that HOXA-A2 knockdown suppresses PTC cell proliferation, migration, and invasion and promotes tumor cell apoptosis contrastingly. Interestingly, the study also mentioned that the HOXA-AS2/miR-15a-5p/HOXA3 axis activates the Wnt/β-catenin signaling pathway, which contributes to PTC tumor progression. Similarly, both overexpression of HOXA3 and wnt signaling activation were observed in our results, suggesting a potential role of the HOXA3 axis in regulating Wnt/β-catenin signaling and, therefore, promoting PTC progression.

11.5.3 TLX3 Gene

T-cell leukemia homebox3 (TLX3) is a DNA-binding transcription factor associated with T-cell leukemia in adults and pediatric patients (162). The TLX3 gene is known to be methylated in bladder cancer cells harboring resistance to the chemotherapeutic drug cisplatin (163). Aberrant methylation of DNA is a well-known epigenetic mechanism in cancer cells that involves

deactivating tumor suppressor genes via a hypermethylated CpG island promotor (164). However, very little is known about the molecular function of TLX3 genes in thyroid cancer. Our results showed that the TLX3 gene is significantly differentially expressed, following a study by Kikuchi et al., who demonstrated that aberrantly methylated TLX3 is associated with a BRAF/RAS mutation in PTC (165). Additionally, the same study supported our findings of HIST3H3 differential expression in PTC, noting aberrant methylation in the HIST3H3 gene encodes nuclear proteins located on the histone cluster on chromosome 6p22-p21.3 (160)is associated with PTC carcinogenesis related to BRAF/RAS mutations.

11.5.4 OGT Gene

O-Linked N-Acetylglucosamine transferase (OGT) is a glycosyltransferase responsible for adding single N-acetylglucosamine to serine/threonine proteins in the cytoplasm. OGT regulates its cellular mechanism via an alternating loop of glycosylation and phosphorylation essential in tumor progression and metastasis (162). Our findings show that OGT is differentially expressed in PTC, agreeing with a recent study revealing that the upregulation of OGT and O-GlcNAcylation (O-GlcNAc) is linked to PTC(166). In addition, the study explained that acylation of YAP Ser109 O-GlcN was responsible for promoting malignant PTC phenotypes via YAP Ser127 phosphorylation. These findings confirmed that OGT is essential in the transcriptional coactivating Hippo-YAP kinase pathways required for PTC growth and metastasis. Additional genes related to PTC include metalloproteinase domain-containing protein 9 (ADAM9), which plays a vital role in shedding ectodomains of membrane-bound heparin/EGF growth factor and releasing molecular integrins such as EPHB4, VCAM1, TEK, and CD40, all of which are necessary for angiogenesis and tumor genesis (162). Another study revealing a similar association between ADAM9 and PTC tumor genesis was conducted by Chen et al. (167). The authors noted that the overexpression of lncRNA CASC9 leads to subsequent activation of miR-488-3p/ADAM9 and EGFR-Akt signaling pathways, therefore promoting malignant phenotypes of

PTC. Furthermore, Xiong et al. showed a tumor-suppressing effect of over-expressed miR-126-632 3p on thyroid tumor cell migration and metastasis associated with aggressive PTC (168).

Additional to the abovementioned genes, GREB1 was identified among the differentially expressed gene panel. GREB1 is an estrogen receptor that plays a vital role in the estrogen-receptor regulating cascade and hormone-dependent growth in prostate and breast cancer (80). A recent study by Alaswad et al. (2021) that explored the effect of thyroid hormone on estrogen-mediated growth of breast cancer ER^+ showed that TH+E2 promoted the overexpression of GREB1, subsequently promoting tumor genesis(169). These findings support the results obtained by our study, where both estrogen-induced signaling pathways and GREB1 were activated. Our research suggests that thyroid hormone and estrogen-induced pathways can drive oncogenic pathways related to tumor genesis.

11.5.5 MAPK Signaling Pathway Association with Papillary Thyroid Carcinoma Pathogenesis

The MAPK and mitogen-activated protein kinase signaling pathways have been well established as being associated with PTC progression due to genetic alterations(2, 14, 44, 65, 91, 120, 157-159, 170-178). Changes in such pathways can result from rearrangement or point mutations of the RET, RAS, and BRAF genes. The signaling cascade begins with growth factors binding to tyrosine kinase receptors such as RET and NTRK, resulting in autophosphorylation of tyrosine molecules and receptor activation. The activated receptor (RET/ NTRK), coupled with adaptor proteins, activates RAS on the inner side of the plasma membrane. Activated RAS proteins bind to BRAF proteins, activating BRAF receptors (93, 170). This activated BRAF receptor phosphorylates ERK/MEK protein kinase and subsequently causes ERK activation. The activated ERK receptor undergoes translocation into the nucleus, where genes involved in cell proliferation, differentiation, and survival are regulated(91). In our study, MAPK pathways were found to be activated in PTC, with a higher overexpression in the late PTC stage. Our results

agree with the findings of Nikiforov et al., who noted that the MAPK kinase pathway is significantly activated in papillary thyroid carcinoma.

11.5.6 Estrogen Pathway

In the thyroid gland, three mitogenic pathways operate in the growth regulation of thyroid cells. These pathways include the h-receptor–Gq–phospholipase C pathway, hormone R–tyrosine-protein kinase cascade, and hormone receptor–Gs–adenylyl cyclase–cAMP-dependent protein kinase system (93). In TC and under the influence of genetic alterations of BRAF, RET/PTC, and tyrosine kinase receptors,(178) estrogen stimulates the tyrosine kinase signaling cascade, PI3K–Akt, and Ras/Raf/MAPK pathways. These estrogen-dependent signaling molecules target the mitogenic pathways to divert growth regulation to favor thyroid carcinogenesis(179).

In our study, we discovered that the activated estrogen pathway is linked to thyroid tumor genesis and also explains the association between the higher prevalence in females than males. Our results are in line with previous studies (37, 120, 151, 178-184)reporting a higher incidence in females than in males, which may be attributed to the high level of estrogen and estrogen receptors (E2) in mediating genomic and nongenomic pathways(175). Although estrogen is a remarkable growth factor for malignant and benign thyroid tumors, its association with MAPK activation has been reported in few studies. In addition, earlier results in our study indicated that the highest TC incidence was mainly observed among the child-bearing age group (<40 years). This finding is supported by an earlier study by Kimura et al. (1990) that linked thyroid tumor growth during pregnancy to higher estrogen levels, HCG effects, and iron deficiency(185). However, few studies assessed the effect of estrogen receptor overexpression on TC development. Taken together, the data obtained show that PI3K–Akt and Ras/Raf/MAPK pathways are critical components in thyroid cancer proliferation. Inhibition of these signaling cascades may prevent estrogen-induced tumor genesis and provide an opportunity for targeted therapies.

11.5.7 NFkB and MAPK Pathways Correlation in PTC

NFkB is a well-recognized transcription factor that acts as a central activator of anti-apoptotic signaling pathways when stimulated by intrinsic or extrinsic immune stimuli (186). The approximate interrelation between NFkB and oncogenes not only promotes thyroid carcinogenesis but also promotes tumor progression and metastasis. The results revealed that NFkB is activated in papillary thyroid carcinoma. This finding was consistent with several studies suggesting that NF-kB is associated with TC progression (187). Estrogen-mediated pathways activate not only the MAPK pathway but also mutant genes of the NF-kB cascade, such as BRAF v600E, RAS, and RET/PTC, which are well known to induce MAPK pathway activation (188-190). In addition, activated transcription controls related to the NF-kB cascade, such as matrix metalloproteinase 9 (MMP-9), ICAM-1, and Cox-2, were correlated to poor prognosis and poor prognosis survival and metastasis(191).

11.5.8 NF-Kb and PI36 Kinase Pathway Correlation in PTC

The PI36-kinase cascade is a vital signaling pathway that regulates apoptosis and cell survival. Upon stimulation with cytokines or growth factors, PI3k recruits membrane phosphatidylinositol 3,4,5-triphosphate, which then activates serine/threonine Akt/PBK kinase. The Akt/PBK compound initiates signals for several proteins involved in cellular proliferation, apoptotic resistance, and angiogenesis. The abnormal activation of Akt/PBK is found in thyroid tumors harboring *RET/PTC* rearrangements and Ras mutations. The pro-survival of abnormal Akt/PBK is complimented by an increase in NF-kB signaling activity(192-194). Our study revealed that both PI3K and MAPK are associated with TC progression, supporting the findings of Namba et al. The latter noted that activated NF-kB and PI36 p are associated with thyroid carcinogenesis, metastasis, poor survival, and prognosis(190, 194, 195).

11.5.9 VEGF Transcriptional Factor Association with PTC

Vascular endothelial growth factors are essential signaling proteins responsible for regulating the angiogenesis associated with thyroid cancer. Among other growth factors playing critical roles in the angiogenic cascade in different cancers, VEGF is most important for thyroid tumor development and progression (196).VEGF stimulates endothelial tyrosine kinase receptors(90, 101, 197), such as VEGFR-1/Flt-1 and VEGFR-2/KDR, differentially expressed in thyroid carcinoma.

Our results revealed that the VEGF signaling pathway was activated in papillary thyroid carcinoma, similar to Vieira and co-workers' (2005) research noting the role of VEGF signaling in thyroid tumor genesis. Another study supporting our findings was that of Jebreel et al. (2007), who confirmed the co-expression of VEGF and its receptors in benign and malignant human thyroid cell lines (NPA’87). Their study also showed that VEGF co-expression with its receptors was found in 50% of papillary thyroid tumors, 12% of anaplastic thyroid tumors, and 39% in the remaining differentiated forms of thyroid cancers. The expression of VEGF and its receptors has been found to mediate neovascularization and cellular proliferation of thyroid tumors’ endothelium (198). In fact, the autocrine/paracrine behavior of VEGF in thyroid carcinoma is regulated by several events, such as p53 deficiency, hypoxia, and Ras activation pathways(199). Moreover, the involvement of activated MAPK proteins, such as extracellular signal-regulated kinase (ERK) kinase and the (MEK)/ERK complex induced by *B-Raf* ^{V600E} mutation, eventually causes an increase in VEGF activity(200). In addition, higher VEGF expression in TC is associated with an increased likelihood of recurrence and invasion(198). Interestingly, Kieran and colleagues' (2012) work supports our results, noting that high VEGF mRNA expression is linked to increased tumorigenic behavior and plays a vital role in transitioning from lower- to higher-grade tumors(197), as was the case in our study. Taken together, VEGF induced pathways via its receptors VEGFR-1 and VEGFR, contributing to sustained tumor survival and angiogenesis in papillary thyroid carcinoma(62).

11.5.10 Vitamin D Pathways in PTC

The in-depth pathway analysis used in our study identified the activation of vitamin D pathways in the early stages of papillary thyroid carcinoma. Vitamin D has a potential role in tumor genesis by regulating several signaling pathways, including cell proliferation, differentiation, inflammation, invasion, and metastasis (201). Previous animal model research has demonstrated that vitamin D harbors pro-differentiative, pro-apoptotic, anti-proliferative, and anti-inflammatory roles in carcinomic thyroid cells. However, the association between TC and vitamin D remains controversial. In recent years, more attention has been placed on the role of vitamin D in regulating cancer-related signaling pathways. Despite the controversial relationship between vitamin D and cancer, several clinical studies have attempted to determine whether there is a clear link between vitamin D status and papillary thyroid carcinoma. Interestingly, a metanalysis of 14 articles by Zhao et al. (2019) noted a strong association between vitamin D deficiency and a 30% risk increase for TC development, supporting our study's results. Furthermore, Stepien et al. and Roskies et al. found that vitamin D deficiency is associated with advanced papillary TC staging(202). Another study by Clinckspoor et al. explored the role of vitamin D in bone metastases in PTC and identified a significant expression of vitamin D receptors and enzymatic D receptors in PTC patients prone to metastasis(203). This study suggested a strong antitumor role of vitamin D and also identified the link between the metastatic effect of PTC in down-regulating vitamin D's effect(204). The down-regulation pathway of vitamin D is performed by 25(OH)D-24-hydroxylase (CYP24A1) and VDR overexpression in the tumor microenvironment, therefore deactivating its anti-proliferative role (205). The aforementioned studies supported the link between vitamin D deficiency and PTC; other works by Bains et al. suggested not using vitamin D status as a prognostic marker for PTC(206).

In sum, our study and previous molecular research support the proposal that vitamin D deficiency is associated with papillary thyroid carcinoma. However, using vitamin D as a prognostic marker

for PTC remains elusive and requires further research to apply it as a clinical biomarker in patient care.

12 Conclusion

In conclusion, thyroid cancer is a rare disease, yet, it can be lethal if not diagnosed early. Our current study aims to provide the first insight into the molecular pathogenesis of papillary thyroid cancer in UAE. For that purpose, First, we conducted an epidemiological study to identify cancer trends and associations. Second, we conducted an in silico analysis study using bioinformatics techniques to identify molecular markers and pathways in selected populations and cross-validate them with independent cohort samples. Third, we performed transcriptomics and bioinformatics analysis on RNA-seq data of UAE clinical biopsies to identify the population's specific molecular biomarkers and cellular pathways involved. Finally, we performed an in vitro validation for the MAPK6 gene by using transfection methodology on normal and malignant thyroid cell lines to validate its protein expression in PTC pathogenesis. The results from epidemiological study showed that Thyroid cancer incidence is increasing steadily in UAE and worldwide.TC was found to be gender-dependent, where females are mostly affected than males with a ratio of 4:1 due to suggestive hormonal or reproductive factors. The female to male ratio of TC incidence is Higher in Emirati patients than in expats, even though expat incidence is higher in general due to larger population counts. Age was also associated with TC diagnosis, where more than one-third of UAE TC cases were diagnosed below 40. Predictive models showed that Asia would have the highest incidence per year, and Europe is the lowest. Results from our In-silico analysis of publicly available transcriptomic studies showed that pathways enriched in the non-aggressive stage of PTC were associated with Ca+ and K+ ion transport, hormone signaling, and protein tyrosine phosphatase, and Kinase activity. Enriched pathways in metastatic stages were more associated with apoptosis, MAPK activation, growth, and serine-threonine kinase activity. In selected populations (Ukraine, Brazil, South Korea), putative molecular biomarkers including PTK2B, KCNN4, BCL2, EGFR, CACNA1D, and KCNQ1 were identified that suggest a vital role in PTC pathogenesis and progression to metastatic stages. MAPK pathways were also found to be activated across different populations sets of PTC. In addition, a Drugbank search based on DEGs identified FDA-approved drugs currently in use for other medical conditions that may prove

helpful in treating PTC, such as Enflurane, Leflunomide, and Navitoclax. Our transcriptomic analysis of UAE-based archival FFPE biopsies identified the MAPK gene and its related pathway as a key component in driving PTC tumor genesis and metastasis. Furthermore, whole transcriptomic analysis on MAPK6 transfected cell lines identified several genes associated with later stages of PTC and poor overall survival, such as TLX3, OGT, HIST3H3, ADAM9, and GREB1. Overall, Pathway analysis sheds light on the role of MAPK pathway signaling cross-talk with other pathways such as PI3K, estrogen, vitamin D, VEGFR, and many others in initiating, progressing, and metastasizing PTC. Collectively, the results may provide useful information to explore further molecular inhibitors and prognostic markers for PTC patients.

13 Limitations

Our Research, as in other cancer research, faced several challenges, including Small sample size, minimal Tumor content, Nucleic acid quality, lack of previous epidemiological and translational studies in UAE, and a Lack of detailed Clinicopathological information on patients' records and understudied pathways and genes related to PTC. Overcoming limitations is described in Table 30.

Table 30. Current study limitations.

Limitations	Remarks	Overcoming Actions/Strategies
▪ Small sample size(n=6)	▪ Due to the rarity of the disease, most patients' Tissue blocks are either exhausted for molecular diagnosis or available outside UAE, where their diagnosis and treatment took place. ▪ Ethical approval challenges in obtaining samples from hospitals	▪ we used a larger independent cohort sample of 502 PTC patients to validate our results. ▪ Some hospitals resisted ethical approval to disclose tissue blocks, while others preferred to preserve blocks for future necessities, especially for patients with whole thyroidectomy.
Limitations	Remarks	Overcoming actions/strategies
▪ FFPE blocks tumor content	▪ Fine needle biopsies yield a minimal amount of tissues for diagnosis; by the time these blocks reach us, we had very little to no tumor content.	▪ Laser and manual microdissection under the microscope was employed to enhance tumor content and eliminate non-tumorous tissues.
▪ lack of previous PTC epidemiological and translational studies in the UAE	▪ Due to the rarity and complexity of the disease.	▪ Scientists need more ethical consideration and dedication to approach rare diseases instead of focusing only on classical and frequently occurring disorders.

▪ Lack of recent cancer data	▪ Due to the recent establishment of statistical platforms such as NCR, that needs improvement in collecting, interpreting, and representing numerical data.	▪ Regarding statistics: Implementing more stringent data collection laws that mandate health organizations to reasonably collect and analyze recent cancer data (Available data was only between 2011 and 2017). ▪ In addition, statistical disclosure of cancer incidence from some hospitals is restricted due to managerial policies and preservation acts.
▪ Lack of detailed Patients records	▪ Physicians' notes were missing information regarding hormonal levels, preexisting conditions, Reoccurrence, follow-ups, familial history of PTC, and many others, either to incompetent documentation practices or low-quality measures of auditing cycles.	▪ Enforcement of more frequent auditing cycles with stricter documentation practices for physicians.

14 Future directions

Results obtained from this study may provide further investigation opportunities such as assessment of the role of diet in developing TC per ethnicity, Exploration of the effect of environmental pollutants per geographic area in UAE, conducting more studies on females with different age groups to understand the role of thyroid hormones during puberty, gestations and menopause and finally investigate possible molecular targets of identified pathways to develop personalized therapies that may replace classical cancer treatments

15 Supplementary Index

Supplementary Table 1 . GSEA of Enriched Pathways in Non-Aggressive Samples in Comparison to Normal Thyroid Tissue (86)

Gene Set	Size	ES	NES	NOM p-val	FDR q-val	FWER p-val	Tag %	Gene %	Signal	glob.p.val
Go_regulation_of_ion_transport	298	0.489	2.09	<0.0001	0.004	0.048	0.292	0.184	0.246	0
Go_positive_regulation_of_nervous_system_development	287	0.478	2.147	<0.0001	0.002	0.026	0.401	0.287	0.295	0
Go_regulation_of_hormone_levels	240	0.517	2.272	<0.0001	0	0.002	0.354	0.209	0.288	0
Go_regulation_of_developmental_growth	179	0.471	1.995	<0.0001	0.008	0.141	0.413	0.3	0.295	0.001
Go_regulation_of_membrane_potential	173	0.542	2.333	<0.0001	0.001	0.001	0.318	0.159	0.273	0
Go_organic_acid_transport	168	0.478	2.118	<0.0001	0.003	0.032	0.327	0.214	0.262	0
Go_intracellular_receptor_signaling_pathway	161	0.416	1.835	<0.0001	0.02	0.449	0.366	0.294	0.263	0.002
Go_hormone_transport	156	0.469	2.056	<0.0001	0.005	0.078	0.308	0.209	0.248	0.001
Go_positive_regulation_of_growth	146	0.481	1.963	<0.0001	0.01	0.189	0.349	0.243	0.269	0.001
Go_regulation_of_blood_circulation	128	0.532	2.138	<0.0001	0.002	0.029	0.352	0.197	0.286	0
Go_peptide_hormone_secretion	128	0.489	2.084	<0.0001	0.004	0.055	0.312	0.197	0.254	0
Go_regulation_of_hormone_secretion	126	0.482	2.088	<0.0001	0.004	0.05	0.317	0.209	0.255	0
Go_insulin_secretion	110	0.502	2.149	<0.0001	0.002	0.026	0.327	0.197	0.266	0
Go_regulation_of_peptide_hormone_secretion	105	0.485	2.074	<0.0001	0.005	0.061	0.314	0.197	0.255	0
Go_cell_substrate_adhesion	236	0.455	1.857	0.002	0.017	0.4	0.297	0.198	0.244	0.001
Go_g_protein_coupled_receptor_signaling_pathway	345	0.477	1.933	0.002	0.011	0.233	0.31	0.203	0.257	0.001
Go_regulation_of_wnt_signaling_pathway	221	0.421	1.73	0.004	0.031	0.674	0.281	0.226	0.222	0.001
Go_transmembrane_receptor_protein_serine_threonine_kinase_signaling	198	0.471	1.846	0.004	0.018	0.424	0.379	0.261	0.286	0.002
Go_response_to_transforming_growth_factor_beta	161	0.437	1.72	0.006	0.032	0.69	0.466	0.352	0.307	0.001
Go_positive_regulation_of_apoptotic_signaling_pathway	130	0.406	1.694	0.008	0.036	0.741	0.308	0.249	0.234	0.001
Go_positive_regulation_of_map_kinase_activity	169	0.451	1.725	0.01	0.032	0.681	0.308	0.216	0.246	0.001
Go_positive_regulation_of_peptidyl_tyrosine_phosphorylation	106	0.487	1.696	0.012	0.036	0.738	0.34	0.199	0.275	0.001
Go_regulation_of_protein_serine_threonine_kinase_activity	330	0.401	1.601	0.012	0.055	0.866	0.264	0.212	0.215	0
Go_cell_cycle_arrest	141	0.374	1.63	0.014	0.049	0.837	0.348	0.331	0.236	0
Go_regulation_of_apoptotic_signaling_pathway	256	0.375	1.605	0.018	0.054	0.861	0.285	0.25	0.22	0
Go_positive_regulation_of_erk1_and_erk2_cascade	109	0.491	1.624	0.028	0.05	0.846	0.404	0.243	0.309	0

Abbreviations: ES, enrichment score; NES, normalized ES; NOM, nominal; FDR, false discovery rate; FWER, family-wise error rate; Tag%, the percentage of gene tags before (for positive ES) or after (for negative ES) the peak in the running enrichment score; gene %, the percentage of genes in the gene list before (for positive ES) of after (for negative ES) the peak in the running enrichment score; GO, gene ontology.

Supplementary Table 2. GSEA of Enriched Pathways in Metastatic Samples in Comparison to Normal Thyroid Tissue (86)

Gene Set	Size	ES	NES	NOM p-val	FDR q-val	FWER p-val	Tag %	Gene %	Signal	FDR (Median)	glob.p.val
Go_growth	563	0.429	1.893	<0.0001	0.014	0.3	0.329	0.26	0.259	0	0.001
Go_regulation_of_cell_development	525	0.447	1.948	<0.0001	0.01	0.19	0.417	0.31	0.305	0	0.001
Go_positive_regulation_of_transport	515	0.41	1.698	<0.0001	0.037	0.792	0.357	0.297	0.266	0.014	0.001
Go_cation_transport	511	0.439	2.008	<0.0001	0.008	0.1	0.399	0.306	0.293	0	0
Go_ion_transmembrane_transport	510	0.448	2.129	<0.0001	0.005	0.014	0.445	0.335	0.313	0	0.001
Go_g_protein_coupled_receptor_signaling_pathway	345	0.474	1.859	<0.0001	0.017	0.397	0.441	0.305	0.318	0	0.001
Go_cell_cell_signaling_by_wnt	311	0.385	1.635	<0.0001	0.05	0.882	0.334	0.284	0.248	0.023	0.001
Go_anion_transport	307	0.444	1.976	<0.0001	0.009	0.149	0.423	0.305	0.304	0	0.001
Go_regulation_of_ion_transport	298	0.469	1.951	<0.0001	0.01	0.187	0.436	0.306	0.313	0	0.001
Go_response_to_extracellular_stimulus	280	0.404	1.737	<0.0001	0.031	0.712	0.443	0.36	0.292	0.011	0.001
Go_regulation_of_transmembrane_transport	266	0.467	1.963	<0.0001	0.01	0.166	0.466	0.336	0.319	0	0.001
Go_organic_anion_transport	240	0.444	1.948	<0.0001	0.01	0.19	0.438	0.305	0.312	0	0.001
Go_cell_substrate_adhesion	236	0.483	1.872	<0.0001	0.016	0.366	0.39	0.259	0.296	0	0.001
Go_regulation_of_wnt_signaling_pathway	221	0.42	1.684	<0.0001	0.039	0.81	0.353	0.284	0.259	0.016	0.001
Go_positive_regulation_of_neuron_differentiation	215	0.448	1.904	<0.0001	0.013	0.28	0.433	0.319	0.301	0	0.001
Go_regulation_of_ion_transmembrane_transport	211	0.478	1.984	<0.0001	0.009	0.135	0.441	0.304	0.314	0	0.001
Go_canonical_wnt_signaling_pathway	197	0.427	1.689	<0.0001	0.038	0.803	0.365	0.284	0.267	0.015	0.001
Go_negative_regulation_of_cell_development	179	0.456	1.895	<0.0001	0.014	0.299	0.419	0.299	0.3	0	0.001
Go_regulation_of_membrane_potential	173	0.541	2.343	<0.0001	0	0	0.347	0.178	0.29	0	0
Go_regulation_of_cation_transmembrane_transport	165	0.489	1.952	<0.0001	0.01	0.187	0.467	0.304	0.33	0	0.001
Go_intracellular_receptor_signaling_pathway	161	0.418	1.797	<0.0001	0.023	0.555	0.292	0.223	0.231	0.006	0.001
Go_hormone_transport	156	0.46	2	<0.0001	0.007	0.112	0.41	0.307	0.289	0	0.001
Go_positive_regulation_of_growth	146	0.425	1.708	<0.0001	0.035	0.766	0.199	0.113	0.179	0.013	0.001
Go_calcium_ion_transmembrane_transport	153	0.424	1.813	0.002	0.021	0.522	0.366	0.294	0.263	0.005	0.001
Go_regulation_of_protein_localization_to_membrane	133	0.445	1.678	0.002	0.041	0.819	0.429	0.32	0.296	0.016	0.001
Go_transmembrane_receptor_protein_tyrosine_kinase_signaling	452	0.416	1.723	0.002	0.033	0.734	0.358	0.289	0.268	0.012	0.001
Go_positive_regulation_of_protein_serine_threonine_kinase	218	0.461	1.7	0.004	0.036	0.79	0.394	0.289	0.287	0.014	0.001
Go_regulation_of_mapk_cascade	434	0.438	1.708	0.008	0.035	0.767	0.366	0.27	0.28	0.013	0.001
Go_positive_regulation_of_map_kinase_activity	169	0.462	1.647	0.008	0.047	0.871	0.402	0.289	0.291	0.021	0.001
Go_regulation_of_peptidyl_tyrosine_phosphorylation	142	0.483	1.67	0.01	0.043	0.827	0.423	0.287	0.306	0.018	0.001
Go_response_to_wounding	381	0.427	1.655	0.012	0.046	0.861	0.399	0.312	0.286	0.02	0.001
Go_regulation_of_apoptotic_signaling_pathway	256	0.39	1.646	0.018	0.048	0.872	0.387	0.308	0.275	0.021	0.001
Go_extracellular_structure_organization	236	0.505	1.678	0.021	0.041	0.819	0.458	0.27	0.343	0.016	0.001

Abbreviations: ES, enrichment score; NES, normalized ES; NOM, nominal; FDR, false discovery rate; FWER, family-wise error rate; Tag%, the percentage of gene tags before (for positive ES) or after (for negative ES) the peak in the running enrichment score; gene %, the percentage of genes in the gene list before (for positive ES) of after (for negative ES) the peak in the running enrichment score; GO, gene ontology.

16 References

*Reproduced with modification and Permission

1. *Almansoori A, Busch H, Bendardaf R, Hamoudi R. Thyroid cancer incidence in the United Arab Emirates: a retrospective study on association with age and gender [version 2; peer review: 1 approved]. Adapted and originally published by and used with permission from F1000Research. 2022;11(338).
2. Almansoori A, Bhamidimarri PM, Bendardaf R, Hamoudi R. In silico Analysis of Publicly Available Transcriptomics Data Identifies Putative Prognostic and Therapeutic Molecular Targets for Papillary Thyroid Carcinoma. Int J Gen Med. 2022;15:3097-120. Epub2022/03/26. Adapted from International Journal of General Medicine 2022 153097-3120" originally published by and used with permission from Dove Medical Press Ltd.
3. Khan YS, Farhana A. Histology, Thyroid Gland. StatPearls. Treasure Island FL: © 2022, StatPearls Publishing LLC.; 2022.
4. Mohebati A, Shaha AR. Anatomy of thyroid and parathyroid glands and neurovascular relations. Clin Anat. 2012;25(1):19-31. Epub 2011/07/30.
5. Schneider DF, Chen H. New developments in the diagnosis and treatment of thyroid cancer. CA: a cancer journal for clinicians. 2013;63(6):374-94. Epub 2013/06/24.
6. Rosen RD, Sapra A. Embryology, Thyroid. StatPearls. Treasure Island FL: © 2022, StatPearls Publishing LLC.; 2022.
7. Ho WM, Wang YS, Tsou CT, Lin WH, Liao SQ, Hershman JM, et al. Thyroid function during isoflurane anesthesia and valvular heart surgery. J Cardiothorac Anesth. 1989;3(5):550-7. Epub 1989/10/01.
8. Köhrle J. Thyroid Hormones and Derivatives: Endogenous Thyroid Hormones and Their Targets. Methods Mol Biol. 2018;1801:85-104. Epub 2018/06/13.
9. Wegener JW, Lee M, Hofmann F. Hypothyroidism does not affect the dihydropyridine sensitivity of precontracted murine uterus. Can J Physiol Pharmacol. 2003;81(9):890-3. Epub 2003/11/14.
10. Krashin E, Piekiełko-Witkowska A, Ellis M, Ashur-Fabian O. Thyroid Hormones and Cancer: A Comprehensive Review of Preclinical and Clinical Studies. Front Endocrinol (Lausanne). 2019;10:59. Epub 2019/03/01.
11. Mousa SA, Hercbergs A, Lin H-Y, Keating KA, Davis PJ. Actions of Thyroid Hormones on Thyroid Cancers. Frontiers in Endocrinology. 2021;12.
12. Yeh NC, Chou CW, Weng SF, Yang CY, Yen FC, Lee SY, et al. Hyperthyroidism and thyroid cancer risk: a population-based cohort study. Exp Clin Endocrinol Diabetes. 2013;121(7):402-6. Epub 2013/04/26.
13. Yalcin M, Dyskin E, Lansing L, Bharali DJ, Mousa SS, Bridoux A, et al. Tetraiodothyroacetic acid (tetrac) and nanoparticulate tetrac arrest growth of medullary carcinoma of the thyroid. The Journal of clinical endocrinology and metabolism. 2010;95(4):1972-80. Epub 2010/02/06.
14. Bergh JJ, Lin HY, Lansing L, Mohamed SN, Davis FB, Mousa S, et al. Integrin alphaVbeta3 contains a cell surface receptor site for thyroid hormone that is linked to activation of mitogen-activated protein kinase and induction of angiogenesis. Endocrinology. 2005;146(7):2864-71. Epub 2005/04/02.
15. Yalcin M, Bharali DJ, Dyskin E, Dier E, Lansing L, Mousa SS, et al. Tetraiodothyroacetic acid and tetraiodothyroacetic acid nanoparticle effectively inhibit the growth of human follicular thyroid cell carcinoma. Thyroid. 2010;20(3):281-6. Epub 2010/03/02.
16. Vanderpump MP. The epidemiology of thyroid disease. Br Med Bull. 2011;99:39-51. Epub 2011/09/07.
17. Springer D, Jiskra J, Limanova Z, Zima T, Potlukova E. Thyroid in pregnancy: From physiology to screening. Crit Rev Clin Lab Sci. 2017;54(2):102-16. Epub 2017/01/20.
18. Skřivánek A, Lubuský M, Studničková M, Holusková I, Procházka M. [Disorders of the thyroid gland in pregnancy]. Ceska Gynekol. 2013;78(1):99-106. Epub 2013/04/24. Poruchy funkce štítné žlázy v těhotenství.

19. Derringer GA, Thompson LD, Frommelt RA, Bijwaard KE, Heffess CS, Abbondanzo SL. Malignant lymphoma of the thyroid gland: a clinicopathologic study of 108 cases. Am J Surg Pathol. 2000;24(5):623-39. Epub 2000/05/09.
20. Molto E, Sheldrick P. Paleo-oncology in the Dakhleh Oasis, Egypt: Case studies and a paleoepidemiological perspective. Int J Paleopathol. 2018;21:96-110. Epub 2018/03/04.
21. Carling T, Udelsman R. Thyroid cancer. Annu Rev Med. 2014;65:125-37. Epub 2013/11/28.
22. Filetti S, Durante C, Hartl D, Leboulleux S, Locati LD, Newbold K, et al. Thyroid cancer: ESMO Clinical Practice Guidelines for diagnosis, treatment and follow-up†. Ann Oncol. 2019;30(12):1856-83. Epub 2019/09/25.
23. Kebebew E, Clark OH. Medullary thyroid cancer. Curr Treat Options Oncol. 2000;1(4):359-67. Epub 2002/06/12.
24. Kaliszewski K, Diakowska D, Strutyńska-Karpińska M, Wojtczak B, Domosławski P, Balcerzak W. Clinical and histopathological characteristics of patients with incidental and nonincidental thyroid cancer. Archives of medical science : AMS. 2017;13(2):390-5. Epub 2016/04/27.
25. Schlumberger M, Elisei R, Müller S, Schöffski P, Brose M, Shah M, et al. Overall survival analysis of EXAM, a phase III trial of cabozantinib in patients with radiographically progressive medullary thyroid carcinoma. Ann Oncol. 2017;28(11):2813-9. Epub 2017/10/19.
26. Veiga L, Neta G, Aschebrook-Kilfoy B, Ron E, Devesa S. Thyroid cancer incidence patterns in Sao Paulo, Brazil and the U.S. SEER Program, 1997-2008. Thyroid : official journal of the American Thyroid Association. 2013;23.
27. Bai Y, Kakudo K, Jung CK. Updates in the Pathologic Classification of Thyroid Neoplasms: A Review of the World Health Organization Classification. Endocrinology and metabolism (Seoul, Korea). 2020;35(4):696-715. Epub 2020/12/02.
28. Cabanillas ME, McFadden DG, Durante C. Thyroid cancer. Lancet. 2016;388(10061):2783-95. Epub 2016/06/01.
29. Lloyd RV, Buehler D, Khanafshar E. Papillary thyroid carcinoma variants. Head Neck Pathol. 2011;5(1):51-6. Epub 2011/01/12.
30. Sung H, Ferlay J, Siegel RL, Laversanne M, Soerjomataram I, Jemal A, et al. Global Cancer Statistics 2020: GLOBOCAN Estimates of Incidence and Mortality Worldwide for 36 Cancers in 185 Countries. CA: a cancer journal for clinicians. 2021;71(3):209-49. Epub 2021/02/05.
31. Jemal A, Bray F, Center MM, Ferlay J, Ward E, Forman D. Global cancer statistics. CA: a cancer journal for clinicians. 2011;61(2):69-90. Epub 2011/02/08.
32. GLOBOCAN 2020: estimated cancer incidence, mortality and prevalence UAE in 2020. [database on the Internet]. 2020. Available from: https://gco.iarc.fr/today/data/factsheets/populations/784-united-arab-emirates-fact-sheets.pdf.
33. Cancer Incidence In United Arab Emirates Annual Report 2011-2017 [database on the Internet]. 2011-2017. Available from: https://smartapps.moh.gov.ae/ords/f?p=105:511.
34. Siraj AK, Bavi P, Abubaker J, Jehan Z, Sultana M, Al-Dayel F, et al. Genome-wide expression analysis of Middle Eastern papillary thyroid cancer reveals c-MET as a novel target for cancer therapy. J Pathol. 2007;213(2):190-9. Epub 2007/08/19.
35. Qari FA. Pattern of thyroid malignancy at a University Hospital in Western Saudi Arabia. Saudi medical journal. 2004;25(7):866-70. Epub 2004/07/06.
36. Hussain F, Iqbal S, Mehmood A, Bazarbashi S, ElHassan T, Chaudhri N. Incidence of thyroid cancer in the Kingdom of Saudi Arabia, 2000-2010. Hematology/oncology and stem cell therapy. 2013;6(2):58-64. Epub 2013/06/13.
37. Wahdan-Alaswad RS, Edgerton SM, Salem H, Kim HM, Tan AC, Finlay-Schultz J, et al. Exogenous Thyroid Hormone Is Associated with Shortened Survival and Upregulation of High-Risk Gene Expression Profiles in Steroid Receptor-Positive Breast Cancers. Clin Cancer Res. 2021;27(2):585-97. Epub 2020/10/25.
38. Vaccarella S, Franceschi S, Bray F, Wild CP, Plummer M, Dal Maso L. Worldwide Thyroid-Cancer Epidemic? The Increasing Impact of Overdiagnosis. The New England journal of medicine. 2016;375(7):614-7. Epub 2016/08/18.

39. Tuttle RM, Ball DW, Byrd D, Dilawari RA, Doherty GM, Duh QY, et al. Thyroid carcinoma. J Natl Compr Canc Netw. 2010;8(11):1228-74. Epub 2010/11/18.
40. Shah JP. Thyroid carcinoma: epidemiology, histology, and diagnosis. Clinical advances in hematology & oncology : H&O. 2015;13(4 Suppl 4):3-6. Epub 2015/10/03.
41. Sherman SI, Clary DO, Elisei R, Schlumberger MJ, Cohen EE, Schöffski P, et al. Correlative analyses of RET and RAS mutations in a phase 3 trial of cabozantinib in patients with progressive, metastatic medullary thyroid cancer. Cancer. 2016;122(24):3856-64. Epub 2016/08/16.
42. Kodama Y, Asai N, Kawai K, Jijiwa M, Murakumo Y, Ichihara M, et al. The RET proto-oncogene: a molecular therapeutic target in thyroid cancer. Cancer Sci. 2005;96(3):143-8. Epub 2005/03/18.
43. de Groot JW, Links TP, Plukker JT, Lips CJ, Hofstra RM. RET as a diagnostic and therapeutic target in sporadic and hereditary endocrine tumors. Endocr Rev. 2006;27(5):535-60. Epub 2006/07/20.
44. Xing M. BRAF Mutation in Papillary Thyroid Cancer: Pathogenic Role, Molecular Bases, and Clinical Implications. Endocrine Reviews. 2007;28(7):742-62.
45. Santoro M, Melillo RM, Carlomagno F, Vecchio G, Fusco A. Minireview: RET: Normal and Abnormal Functions. Endocrinology. 2004;145(12):5448-51.
46. Romei C, Ciampi R, Elisei R. A comprehensive overview of the role of the RET proto-oncogene in thyroid carcinoma. Nature Reviews Endocrinology. 2016;12(4):192-202.
47. Ron E, Lubin JH, Shore RE, Mabuchi K, Modan B, Pottern LM, et al. Thyroid cancer after exposure to external radiation: a pooled analysis of seven studies. Radiation research. 1995;141(3):259-77. Epub 1995/03/01.
48. Drozdovitch V. Radiation Exposure to the Thyroid After the Chernobyl Accident. Frontiers in Endocrinology. 2021;11(994).
49. Han MA, Kim JH. Diagnostic X-Ray Exposure and Thyroid Cancer Risk: Systematic Review and Meta-Analysis. Thyroid. 2018;28(2):220-8. Epub 2017/11/22.
50. Leung AM, Braverman LE, Pearce EN. History of U.S. iodine fortification and supplementation. Nutrients. 2012;4(11):1740-6. Epub 2012/12/04.
51. Papi G, Corsello SM, Pontecorvi A. Clinical concepts on thyroid emergencies. Front Endocrinol (Lausanne). 2014;5:102. Epub 2014/07/30.
52. Magreni A, Bann DV, Schubart JR, Goldenberg D. The effects of race and ethnicity on thyroid cancer incidence. JAMA Otolaryngol Head Neck Surg. 2015;141(4):319-23. Epub 2015/02/06.
53. Lim H, Devesa SS, Sosa JA, Check D, Kitahara CM. Trends in Thyroid Cancer Incidence and Mortality in the United States, 1974-2013. Jama. 2017;317(13):1338-48.
54. Lal G, Groff M, Howe JR, Weigel RJ, Sugg SL, Lynch CF. Risk of subsequent primary thyroid cancer after another malignancy: latency trends in a population-based study. Ann Surg Oncol. 2012;19(6):1887-96. Epub 2012/01/10.
55. Frauenhoffer CM, Patchefsky AS, Cobanoglu A. Thyroid carcinoma: a clinical and pathologic study of 125 cases. Cancer. 1979;43(6):2414-21. Epub 1979/06/01.
56. Al-Nuaim AR, Ahmed M, Bakheet S, Abdul Kareem AM, Ingmenson S, al-Ahmari S, et al. Papillary thyroid cancer in Saudi Arabia. Clinical, pathologic, and management characteristics. Clinical nuclear medicine. 1996;21(4):307-11. Epub 1996/04/01.
57. Nguyen QT, Lee EJ, Huang MG, Park YI, Khullar A, Plodkowski RA. Diagnosis and treatment of patients with thyroid cancer. American health & drug benefits. 2015;8(1):30-40.
58. Memon A, Varghese A, Suresh A. Benign thyroid disease and dietary factors in thyroid cancer: a case-control study in Kuwait. British journal of cancer. 2002;86(11):1745-50. Epub 2002/06/28.
59. Carcangiu ML, Zampi G, Rosai J. Papillary thyroid carcinoma: a study of its many morphologic expressions and clinical correlates. Pathology annual. 1985;20 Pt 1:1-44. Epub 1985/01/01.
60. Zhuang G, Zeng Y, Tang Q, He Q, Luo G. Identifying M1 Macrophage-Related Genes Through a Co-expression Network to Construct a Four-Gene Risk-Scoring Model for Predicting Thyroid Cancer Prognosis. Front Genet. 2020;11:591079. Epub 2020/11/17.
61. Nagy Á, Munkácsy G, Győrffy B. Pancancer survival analysis of cancer hallmark genes. Scientific reports. 2021;11(1):6047.

62. Abubaker J, Jehan Z, Bavi P, Sultana M, Al-Harbi S, Ibrahim M, et al. Clinicopathological analysis of papillary thyroid cancer with PIK3CA alterations in a Middle Eastern population. The Journal of clinical endocrinology and metabolism. 2008;93(2):611-8. Epub 2007/11/15.
63. Johnston LE, Tran Cao HS, Chang DC, Bouvet M. Sociodemographic Predictors of Survival in Differentiated Thyroid Cancer: Results from the SEER Database. ISRN Endocrinology. 2012;2012:384707.
64. Pontius LN, Oyekunle TO, Thomas SM, Stang MT, Scheri RP, Roman SA, et al. Projecting Survival in Papillary Thyroid Cancer: A Comparison of the Seventh and Eighth Editions of the American Joint Commission on Cancer/Union for International Cancer Control Staging Systems in Two Contemporary National Patient Cohorts. Thyroid. 2017;27(11):1408-16. Epub 2017/09/12.
65. Zhang H, Gao B, Shi B. Identification of Differentially Expressed Kinase and Screening Potential Anticancer Drugs in Papillary Thyroid Carcinoma. Disease Markers. 2016;2016:2832980.
66. Yu GP, Li JC, Branovan D, McCormick S, Schantz SP. Thyroid cancer incidence and survival in the national cancer institute surveillance, epidemiology, and end results race/ethnicity groups. Thyroid. 2010;20(5):465-73. Epub 2010/04/14.
67. Xing M. Molecular pathogenesis and mechanisms of thyroid cancer. Nature reviews Cancer. 2013;13(3):184-99.
68. Wells SA, Jr., Gosnell JE, Gagel RF, Moley J, Pfister D, Sosa JA, et al. Vandetanib for the treatment of patients with locally advanced or metastatic hereditary medullary thyroid cancer. J Clin Oncol. 2010;28(5):767-72. Epub 2010/01/13.
69. Tolcher AW, LoRusso P, Arzt J, Busman TA, Lian G, Rudersdorf NS, et al. Safety, efficacy, and pharmacokinetics of navitoclax (ABT-263) in combination with irinotecan: results of an open-label, phase 1 study. Cancer Chemother Pharmacol. 2015;76(5):1041-9. Epub 2015/10/03.
70. Roskoski R, Jr. The ErbB/HER family of protein-tyrosine kinases and cancer. Pharmacol Res. 2014;79:34-74. Epub 2013/11/26.
71. O'Donnell EF, Saili KS, Koch DC, Kopparapu PR, Farrer D, Bisson WH, et al. The anti-inflammatory drug leflunomide is an agonist of the aryl hydrocarbon receptor. PloS one. 2010;5(10). Epub 2010/10/20.
72. Nor Hisam NS, Ugusman A, Rajab NF, Ahmad MF, Fenech M, Liew SL, et al. Combination Therapy of Navitoclax with Chemotherapeutic Agents in Solid Tumors and Blood Cancer: A Review of Current Evidence. Pharmaceutics. 2021;13(9). Epub 2021/09/29.
73. Newland A, McDonald V. Fostamatinib: a review of its clinical efficacy and safety in the management of chronic adult immune thrombocytopenia. Immunotherapy. 2020;12(18):1325-40.
74. Moore DC, Gebru T, Muslimani A. Fostamatinib for the treatment of immune thrombocytopenia in adults. Am J Health Syst Pharm. 2019;76(11):789-94. Epub 2019/04/06.
75. Mohamad Anuar NN, Nor Hisam NS, Liew SL, Ugusman A. Clinical Review: Navitoclax as a Pro-Apoptotic and Anti-Fibrotic Agent. Front Pharmacol. 2020;11:564108. Epub 2021/01/01.
76. Krajewska J, Olczyk T, Jarzab B. Cabozantinib for the treatment of progressive metastatic medullary thyroid cancer. Expert Rev Clin Pharmacol. 2016;9(1):69-79. Epub 2015/11/05.
77. Thyroid Cancer Treatment (Adult) (PDQ®): Health Professional Version. PDQ Cancer Information Summaries. Bethesda MD2002.
78. Sherman SI. EVOLUTION OF TARGETED THERAPIES FOR THYROID CARCINOMA. Trans Am Clin Climatol Assoc. 2019;130:255-65. Epub 2019/09/14.
79. Cabanillas ME, de Souza JA, Geyer S, Wirth LJ, Menefee ME, Liu SV, et al. Cabozantinib As Salvage Therapy for Patients With Tyrosine Kinase Inhibitor-Refractory Differentiated Thyroid Cancer: Results of a Multicenter Phase II International Thyroid Oncology Group Trial. J Clin Oncol. 2017;35(29):3315-21. Epub 2017/08/18.
80. Brose MS, Robinson B, Sherman SI, Krajewska J, Lin CC, Vaisman F, et al. Cabozantinib for radioiodine-refractory differentiated thyroid cancer (COSMIC-311): a randomised, double-blind, placebo-controlled, phase 3 trial. Lancet Oncol. 2021;22(8):1126-38. Epub 2021/07/09.
81. Ancker OV, Krüger M, Wehland M, Infanger M, Grimm D. Multikinase Inhibitor Treatment in Thyroid Cancer. Int J Mol Sci. 2019;21(1). Epub 2019/12/22.

82. Cabanillas ME, Ryder M, Jimenez C. Targeted Therapy for Advanced Thyroid Cancer: Kinase Inhibitors and Beyond. Endocr Rev. 2019;40(6):1573-604. Epub 2019/07/20.
83. Bray F, Ferlay J, Soerjomataram I, Siegel RL, Torre LA, Jemal A. Global cancer statistics 2018: GLOBOCAN estimates of incidence and mortality worldwide for 36 cancers in 185 countries. CA: a cancer journal for clinicians. 2018;68(6):394-424. Epub 2018/09/13.
84. Bray F, Møller B. Predicting the future burden of cancer. Nat Rev Cancer. 2006;6(1):63-74. Epub 2005/12/24.
85. Ferlay J LM, Ervik M, Lam F, Colombet M, Mery L, Piñeros M, Znaor A, Soerjomataram I, Bray F Global Cancer Observatory: Cancer Tomorrow.: International Agency for Research on Cancer; 2020; Available from: https://gco.iarc.fr/tomorrow/en.
86. Almansoori A, Bhamidimarri PM, Bendardaf R, Hamoudi R. In silico Analysis of Publicly Available Transcriptomics Data Identifies Putative Prognostic and Therapeutic Molecular Targets for Papillary Thyroid Carcinoma. International Journal of General Medicine. 2022;Volume 15:3097-120.
87. Almansoori A, Bhamidimarri PM, Bendardaf R, Hamoudi R. Identifying Diagnostic and Prognostic Targets for Papillary Thyroid Carcinoma Through Mining Gene Expression BIG Datasets Using Adaptive Filtering and Advanced Bioinformatics Algorithms2021. 358-63 p.
88. Elisei R, Schlumberger MJ, Müller SP, Schöffski P, Brose MS, Shah MH, et al. Cabozantinib in progressive medullary thyroid cancer. J Clin Oncol. 2013;31(29):3639-46. Epub 2013/09/05.
89. Wells SA, Jr., Robinson BG, Gagel RF, Dralle H, Fagin JA, Santoro M, et al. Vandetanib in patients with locally advanced or metastatic medullary thyroid cancer: a randomized, double-blind phase III trial. J Clin Oncol. 2012;30(2):134-41. Epub 2011/10/26.
90. Fallahi P, Ferrari SM, Elia G, Ragusa F, Paparo SR, Ruffilli I, et al. Evaluating vandetanib in the treatment of medullary thyroid cancer: patient-reported outcomes. Cancer management and research. 2019;11:7893-907.
91. Nikiforov YE. Thyroid carcinoma: molecular pathways and therapeutic targets. Mod Pathol. 2008;21 Suppl 2(Suppl 2):S37-43. Epub 2008/06/24.
92. Park DS, Kim SS, Chung JD, Kim SD, Kim DK, Park JH. Effects of Enflurane Anesthesia and Surgery on Thyroid Function. Korean J Anesthesiol. 1982;15(2):144-9.
93. Hébrant A, Dom G, Dewaele M, Andry G, Trésallet C, Leteurtre E, et al. mRNA Expression in Papillary and Anaplastic Thyroid Carcinoma: Molecular Anatomy of a Killing Switch. PLoS One. 2012;7(10):e37807.
94. Scholl UI, Stölting G, Nelson-Williams C, Vichot AA, Choi M, Loring E, et al. Recurrent gain of function mutation in calcium channel CACNA1H causes early-onset hypertension with primary aldosteronism. eLife. 2015;4:e06315-e.
95. Baig SM, Koschak A, Lieb A, Gebhart M, Dafinger C, Nürnberg G, et al. Loss of Cav1.3 (CACNA1D) function in a human channelopathy with bradycardia and congenital deafness. Nature Neuroscience. 2011;14(1):77-84.
96. Jing Q-B, Tong H-X, Tang W-J, Tian S-D. Clinical Significance and Potential Regulatory Mechanisms of Serum Response Factor in 1118 Cases of Thyroid Cancer Based on Gene Chip and RNA-Sequencing Data. Medical science monitor : international medical journal of experimental and clinical research. 2020;26:e919302-e.
97. Zhang K, Wang Y, Ma W, Hu Z, Zhao P. Genistein improves thyroid function in Hashimoto's thyroiditis patients through regulating Th1 cytokines. Immunobiology. 2017;222(2):183-7. Epub 2016/10/13.
98. Marini H, Polito F, Adamo E, Bitto A, Squadrito F, Benvenga S. Update on genistein and thyroid: An overall message of safety. Frontiers in endocrinology. 2012;3:94.
99. Li EK, Tam LS, Tomlinson B. Leflunomide in the treatment of rheumatoid arthritis. Clin Ther. 2004;26(4):447-59. Epub 2004/06/11.
100. Mall JW, Myers JA, Xu X, Saclarides TJ, Philipp AW, Pollmann C. [Leflunomide reduces the angiogenesis score and tumor growth of subcutaneously implanted colon carcinoma cells in the mouse model]. Chirurg. 2002;73(7):716-20. Epub 2002/09/24. Leflunomid reduziert den Angiogenesescore und das Tumorwachstum subkutan implantierter Kolonkarzinomzellen im Mausmodell.

101. Skinner M, Philp K, Lengel D, Coverley L, Lamm Bergström E, Glaves P, et al. The contribution of VEGF signalling to fostamatinib-induced blood pressure elevation. British Journal of Pharmacology. 2014;171(9):2308-20.
102. Bussel J, Arnold DM, Grossbard E, Mayer J, Treliński J, Homenda W, et al. Fostamatinib for the treatment of adult persistent and chronic immune thrombocytopenia: Results of two phase 3, randomized, placebo-controlled trials. American Journal of Hematology. 2018;93(7):921-30.
103. Bussel J, Arnold DM, Grossbard E, Mayer J, Treliński J, Homenda W, et al. Fostamatinib for the treatment of adult persistent and chronic immune thrombocytopenia: Results of two phase 3, randomized, placebo-controlled trials. Am J Hematol. 2018;93(7):921-30. Epub 2018/04/27.
104. Duliege A-M, Arnold DM, Boccia R, Boxer M, Cooper N, Hill QA, et al. Two-Year Safety and Efficacy Outcomes with Fostamatinib in Adult Patients with Immune Thrombocytopenia (ITP): Open-Label Extension to Phase 3 Trial Program. Blood. 2018;132(Supplement 1):736-.
105. Markham A. Fostamatinib: First Global Approval. Drugs. 2018;78(9):959-63. Epub 2018/06/06.
106. McKeage K, Lyseng-Williamson KA. Fostamatinib in chronic immune thrombocytopenia: a profile of its use in the USA. Drugs Ther Perspect. 2018;34(10):451-6. Epub 2018/11/22.
107. Bussel JB, Arnold DM, Boxer MA, Cooper N, Mayer J, Zayed H, et al. Long-term fostamatinib treatment of adults with immune thrombocytopenia during the phase 3 clinical trial program. Am J Hematol. 2019;94(5):546-53. Epub 2019/02/21.
108. Chandar AK, Alaber OA, Farooq MZ, Dahash BA, Mangla A. Safety Profile of Fostamatinib, an Oral Spleen Tyrosine Kinase Inhibitor: A Meta-Analysis of Randomized Controlled Trials. Blood. 2019;134(Supplement_1):4890-.
109. Kang Y, Jiang X, Qin D, Wang L, Yang J, Wu A, et al. Efficacy and Safety of Multiple Dosages of Fostamatinib in Adult Patients With Rheumatoid Arthritis: A Systematic Review and Meta-Analysis. Frontiers in Pharmacology. 2019;10(897).
110. Boccia R, Cooper N, Ghanima W, Boxer MA, Hill QA, Sholzberg M, et al. Fostamatinib is an effective second-line therapy in patients with immune thrombocytopenia. Br J Haematol. 2020;190(6):933-8. Epub 2021/01/14.
111. Boccia R, Cooper N, Ghanima W, Boxer MA, Hill QA, Sholzberg M, et al. Fostamatinib is an effective second-line therapy in patients with immune thrombocytopenia. British Journal of Haematology. 2020;190(6):933-8.
112. Cooper N, Altomare I, Thomas MR, Nicolson PLR, Watson SP, Markovtsov V, et al. Assessment of thrombotic risk during long-term treatment of immune thrombocytopenia with fostamatinib. Ther Adv Hematol. 2021;12:20406207211010875. Epub 2021/05/18.
113. Paik J. Fostamatinib: A Review in Chronic Immune Thrombocytopenia. Drugs. 2021;81(8):935-43. Epub 2021/05/11.
114. Cleary JM, Lima CM, Hurwitz HI, Montero AJ, Franklin C, Yang J, et al. A phase I clinical trial of navitoclax, a targeted high-affinity Bcl-2 family inhibitor, in combination with gemcitabine in patients with solid tumors. Invest New Drugs. 2014;32(5):937-45. Epub 2014/06/12.
115. Gandhi L, Camidge DR, Ribeiro de Oliveira M, Bonomi P, Gandara D, Khaira D, et al. Phase I study of Navitoclax (ABT-263), a novel Bcl-2 family inhibitor, in patients with small-cell lung cancer and other solid tumors. J Clin Oncol. 2011;29(7):909-16. Epub 2011/02/02.
116. Al-Salam S, Sharma C, Abu Sa'a MT, Afandi B, Aldahmani KM, Al Dhaheri A, et al. Ultrasound-guided fine needle aspiration cytology and ultrasound examination of thyroid nodules in the UAE: A comparison. PloS one. 2021;16(4):e0247807. Epub 2021/04/08.
117. Alhefdhi A, Burke JF, Redlich A, Kunnimalaiyaan M, Chen H. Leflunomide suppresses growth in human medullary thyroid cancer cells. The Journal of surgical research. 2013;185(1):212-6. Epub 2013/06/19.
118. Azizan EA, Poulsen H, Tuluc P, Zhou J, Clausen MV, Lieb A, et al. Somatic mutations in ATP1A1 and CACNA1D underlie a common subtype of adrenal hypertension. Nat Genet. 2013;45(9):1055-60. Epub 2013/08/06.
119. Ashburner M, Ball CA, Blake JA, Botstein D, Butler H, Cherry JM, et al. Gene Ontology: tool for the unification of biology. Nature Genetics. 2000;25(1):25-9.

120. Derwahl M, Nicula D. Estrogen and its role in thyroid cancer. Endocr Relat Cancer. 2014;21(5):T273-83. Epub 2014/07/24.
121. Sulaiman N, Elbadawi S, Hussein A, Abusnana S, Madani A, Mairghani M, et al. Prevalence of overweight and obesity in United Arab Emirates Expatriates: the UAE National Diabetes and Lifestyle Study. Diabetol Metab Syndr. 2017;9:88. Epub 2017/11/10.
122. Radwan H, Hasan H, Ballout RA, Rizk R. The epidemiology of cancer in the United Arab Emirates: A systematic review. Medicine. 2018;97(50):e13618. Epub 2018/12/19.
123. Radwan H, Hasan H, Ballout RA, Rizk R. The epidemiology of cancer in the United Arab Emirates: A systematic review. Medicine. 2018;97(50):e13618-e.
124. Al-Zaher N, Al-Salam S, El Teraifi H. Thyroid carcinoma in the United Arab Emirates: perspectives and experience of a tertiary care hospital. Hematology/oncology and stem cell therapy. 2008;1(1):14-21. Epub 2008/01/01.
125. Al-Salam S, Sharma C, Afandi B, Al Dahmani K, Al-Zahrani AS, Al Shamsi A, et al. BRAF and KRAS mutations in papillary thyroid carcinoma in the United Arab Emirates. PloS one. 2020;15(4):e0231341. Epub 2020/04/22.
126. Benedetti M, Zona A, Contiero P, D'Armiento E, Iavarone I, Group AW. Incidence of Thyroid Cancer in Italian Contaminated Sites. International Journal of Environmental Research and Public Health. 2021;18(1):191.
127. Harach HR, Ceballos GA. Thyroid cancer, thyroiditis and dietary iodine: a review based on the Salta, Argentina model. Endocr Pathol. 2008;19(4):209-20. Epub 2008/08/13.
128. Achatz MI, Zambetti GP. The Inherited p53 Mutation in the Brazilian Population. Cold Spring Harb Perspect Med. 2016;6(12). Epub 2016/09/25.
129. Fernandes GC, Michelli RA, Galvao HC, Paula AE, Pereira R, Andrade CE, et al. Prevalence of BRCA1/BRCA2 mutations in a Brazilian population sample at-risk for hereditary breast cancer and characterization of its genetic ancestry. Oncotarget. 2016;7(49):80465-81. Epub 2016/10/16.
130. Oleksyk TK, Wolfsberger WW, Weber AM, Shchubelka K, Oleksyk OT, Levchuk O, et al. Genome diversity in Ukraine. Gigascience. 2021;10(1). Epub 2021/01/14.
131. Lee S, Seo J, Park J, Nam JY, Choi A, Ignatius JS, et al. Korean Variant Archive (KOVA): a reference database of genetic variations in the Korean population. Scientific reports. 2017;7(1):4287. Epub 2017/06/29.
132. Tsai CM, Riestra AM, Ali SR, Fong JJ, Liu JZ, Hughes G, et al. Siglec-14 Enhances NLRP3-Inflammasome Activation in Macrophages. J Innate Immun. 2020;12(4):333-43. Epub 2019/12/06.
133. Gogali F, Paterakis G, Rassidakis GZ, Kaltsas G, Liakou CI, Gousis P, et al. Phenotypical analysis of lymphocytes with suppressive and regulatory properties (Tregs) and NK cells in the papillary carcinoma of thyroid. The Journal of clinical endocrinology and metabolism. 2012;97(5):1474-82. Epub 2012/03/09.
134. Youle RJ, Strasser A. The BCL-2 protein family: opposing activities that mediate cell death. Nature Reviews Molecular Cell Biology. 2008;9(1):47-59.
135. Aksoy M, Giles Y, Kapran Y, Terzioglu T, Tezelman S. Expression of bcl-2 in papillary thyroid cancers and its prognostic value. Acta Chir Belg. 2005;105(6):644-8. Epub 2006/01/28.
136. Aksoy M, Giles Y, Kapran Y, Terzioglu T, Tezelman S. Expression of bcl-2 in Papillary Thyroid Cancers and its Prognostic Value. Acta chirurgica Belgica. 2005;105:644-8.
137. Scholl UI, Goh G, Stölting G, de Oliveira RC, Choi M, Overton JD, et al. Somatic and germline CACNA1D calcium channel mutations in aldosterone-producing adenomas and primary aldosteronism. Nat Genet. 2013;45(9):1050-4. Epub 2013/08/06.
138. Pardo LA, Contreras-Jurado C, Zientkowska M, Alves F, Stühmer W. Role of Voltage-gated Potassium Channels in Cancer. The Journal of Membrane Biology. 2005;205(3):115-24.
139. Huang L, Bitner-Glindzicz M, Tranebjaerg L, Tinker A. A spectrum of functional effects for disease causing mutations in the Jervell and Lange-Nielsen syndrome. Cardiovasc Res. 2001;51(4):670-80. Epub 2001/09/01.
140. Ellinor PT, Moore RK, Patton KK, Ruskin JN, Pollak MR, Macrae CA. Mutations in the long QT gene, KCNQ1, are an uncommon cause of atrial fibrillation. Heart. 2004;90(12):1487-8. Epub 2004/11/18.

141. Jespersen T, Grunnet M, Olesen SP. The KCNQ1 potassium channel: from gene to physiological function. Physiology (Bethesda). 2005;20:408-16. Epub 2005/11/17.
142. Melman YF, Um SY, Krumerman A, Kagan A, McDonald TV. KCNE1 binds to the KCNQ1 pore to regulate potassium channel activity. Neuron. 2004;42(6):927-37. Epub 2004/06/23.
143. Wen J, Lin B, Lin L, Chen Y, Wang O. KCNN4 is a diagnostic and prognostic biomarker that promotes papillary thyroid cancer progression. Aging (Albany NY). 2020;12(16):16437-56. Epub 2020/08/29.
144. Liu X, Wei L, Zhao B, Cai X, Dong C, Yin F. Low expression of KCNN3 may affect drug resistance in ovarian cancer. Mol Med Rep. 2018;18(2):1377-86. Epub 2018/06/15.
145. Jiang S, Zhu L, Yang J, Hu L, Gu J, Xing X, et al. Integrated expression profiling of potassium channels identifys KCNN4 as a prognostic biomarker of pancreatic cancer. Biochem Biophys Res Commun. 2017;494(1-2):113-9. Epub 2017/10/21.
146. Ibrahim S, Dakik H, Vandier C, Chautard R, Paintaud G, Mazurier F, et al. Expression Profiling of Calcium Channels and Calcium-Activated Potassium Channels in Colorectal Cancer. Cancers. 2019;11(4). Epub 2019/04/24.
147. Fisher KE, Jani JC, Fisher SB, Foulks C, Hill CE, Weber CJ, et al. Epidermal growth factor receptor overexpression is a marker for adverse pathologic features in papillary thyroid carcinoma. J Surg Res. 2013;185(1):217-24. Epub 2013/06/12.
148. Wang SX, Zhang XW, Wang XX, An CM, Zhang YB, Liu W, et al. [Efficacy and safety of vandetanib on advanced medullary thyroid carcinoma: single center result from a phase Ⅲ study]. Zhonghua Er Bi Yan Hou Tou Jing Wai Ke Za Zhi. 2019;54(6):439-44. Epub 2019/07/03.
149. Yoon S, Seger R. The extracellular signal-regulated kinase: multiple substrates regulate diverse cellular functions. Growth Factors. 2006;24(1):21-44. Epub 2006/01/06.
150. Schaller MD. Cellular functions of FAK kinases: insight into molecular mechanisms and novel functions. Journal of Cell Science. 2010;123(7):1007-13.
151. Dong W, Zhang H, Li J, Guan H, He L, Wang Z, et al. Estrogen Induces Metastatic Potential of Papillary Thyroid Cancer Cells through Estrogen Receptor α and β. International Journal of Endocrinology. 2013;2013:941568.
152. Selemetjev S, Bartolome A, Isic Dencic T, Doric I, Paunovic I, Tatic S, et al. Overexpression of epidermal growth factor receptor and its downstream effector, focal adhesion kinase, correlates with papillary thyroid carcinoma progression. Int J Exp Pathol. 2018;99(2):87-94. Epub 2018/04/18.
153. Xu Q, Song A, Xie Q. The Integrated Analyses of Driver Genes Identify Key Biomarkers in Thyroid Cancer. Technology in Cancer Research & Treatment. 2020;19:1533033820940440.
154. Linklater ES, Tovar EA, Essenburg CJ, Turner L, Madaj Z, Winn ME, et al. Targeting MET and EGFR crosstalk signaling in triple-negative breast cancers. Oncotarget. 2016;7(43):69903-15. Epub 2016/09/23.
155. You KS, Yi YW, Cho J, Park JS, Seong YS. Potentiating Therapeutic Effects of Epidermal Growth Factor Receptor Inhibition in Triple-Negative Breast Cancer. Pharmaceuticals (Basel). 2021;14(6). Epub 2021/07/03.
156. Coulombe P, Meloche S. Atypical mitogen-activated protein kinases: structure, regulation and functions. Biochim Biophys Acta. 2007;1773(8):1376-87. Epub 2006/12/13.
157. Seternes OM, Mikalsen T, Johansen B, Michaelsen E, Armstrong CG, Morrice NA, et al. Activation of MK5/PRAK by the atypical MAP kinase ERK3 defines a novel signal transduction pathway. EMBO J. 2004;23(24):4780-91. Epub 2004/12/04.
158. Long W, Foulds CE, Qin J, Liu J, Ding C, Lonard DM, et al. ERK3 signals through SRC-3 coactivator to promote human lung cancer cell invasion. The Journal of clinical investigation. 2012;122(5):1869-80.
159. Cai Q, Zhou W, Wang W, Dong B, Han D, Shen T, et al. MAPK6-AKT signaling promotes tumor growth and resistance to mTOR kinase blockade. Sci Adv. 2021;7(46):eabi6439. Epub 2021/11/13.
160. O'Leary NA, Wright MW, Brister JR, Ciufo S, Haddad D, McVeigh R, et al. Reference sequence (RefSeq) database at NCBI: current status, taxonomic expansion, and functional annotation. Nucleic Acids Res. 2016;44(D1):D733-45. Epub 2015/11/11.

161. Chung N, Jee BK, Chae SW, Jeon YW, Lee KH, Rha HK. HOX gene analysis of endothelial cell differentiation in human bone marrow-derived mesenchymal stem cells. Mol Biol Rep. 2009;36(2):227-35. Epub 2007/11/01.
162. Stelzer G, Rosen N, Plaschkes I, Zimmerman S, Twik M, Fishilevich S, et al. The GeneCards Suite: From Gene Data Mining to Disease Genome Sequence Analyses. Curr Protoc Bioinformatics. 2016;54:1 30 1-1 3. Epub 2016/06/21.
163. Tada Y, Yokomizo A, Shiota M, Tsunoda T, Plass C, Naito S. Aberrant DNA methylation of T-cell leukemia, homeobox 3 modulates cisplatin sensitivity in bladder cancer. Int J Oncol. 2011;39(3):727-33. Epub 2011/05/28.
164. Esteller M. Aberrant DNA methylation as a cancer-inducing mechanism. Annu Rev Pharmacol Toxicol. 2005;45:629-56. Epub 2005/04/12.
165. Kikuchi Y, Tsuji E, Yagi K, Matsusaka K, Tsuji S, Kurebayashi J, et al. Aberrantly methylated genes in human papillary thyroid cancer and their association with BRAF/RAS mutation. Frontiers in Genetics. 2013;4(271).
166. Li X, Wu Z, He J, Jin Y, Chu C, Cao Y, et al. OGT regulated O-GlcNAcylation promotes papillary thyroid cancer malignancy via activating YAP. Oncogene. 2021;40(30):4859-71. Epub 2021/06/23.
167. Chen Y, Li Y, Gao H. Long noncoding RNA CASC9 promotes the proliferation and metastasis of papillary thyroid cancer via sponging miR-488-3p. Cancer Med. 2020;9(5):1830-41. Epub 2020/01/17.
168. Xiong Y, Kotian S, Zeiger MA, Zhang L, Kebebew E. miR-126-3p Inhibits Thyroid Cancer Cell Growth and Metastasis, and Is Associated with Aggressive Thyroid Cancer. PloS one. 2015;10(8):e0130496-e.
169. Wahdan-Alaswad RS, Edgerton SM, Salem H, Kim HM, Tan AC, Finlay-Schultz J, et al. Exogenous Thyroid Hormone Is Associated with Shortened Survival and Upregulation of High-Risk Gene Expression Profiles in Steroid Receptor–Positive Breast Cancers. Clinical Cancer Research. 2021;27(2):585-97.
170. Zafon C, Obiols G. [The mitogen-activated protein kinase (MAPK) signaling pathway in papillary thyroid cancer. From the molecular bases to clinical practice]. Endocrinol Nutr. 2009;56(4):176-86. Epub 2009/07/25. Vía de señalización dependiente de la proteincinasa de activación mitogénica en el carcinoma papilar de tiroides. De las bases moleculares a la práctica clínica.
171. Wefers B, Hitz C, Hölter SM, Trümbach D, Hansen J, Weber P, et al. MAPK signaling determines anxiety in the juvenile mouse brain but depression-like behavior in adults. PloS one. 2012;7(4):e35035. Epub 2012/04/25.
172. Sun CK, Man K, Ng KT, Ho JW, Lim ZX, Cheng Q, et al. Proline-rich tyrosine kinase 2 (Pyk2) promotes proliferation and invasiveness of hepatocellular carcinoma cells through c-Src/ERK activation. Carcinogenesis. 2008;29(11):2096-105.
173. Lim MS, Nam SH, Kim SJ, Kang SY, Lee YS, Kang KS. Signaling pathways of the early differentiation of neural stem cells by neurotrophin-3. Biochem Biophys Res Commun. 2007;357(4):903-9. Epub 2007/05/01.
174. Dhillon AS, Hagan S, Rath O, Kolch W. MAP kinase signalling pathways in cancer. Oncogene. 2007;26(22):3279-90.
175. Creighton CJ, Hilger AM, Murthy S, Rae JM, Chinnaiyan AM, El-Ashry D. Activation of mitogen-activated protein kinase in estrogen receptor alpha-positive breast cancer cells in vitro induces an in vivo molecular phenotype of estrogen receptor alpha-negative human breast tumors. Cancer Res. 2006;66(7):3903-11. Epub 2006/04/06.
176. Burotto M, Chiou VL, Lee JM, Kohn EC. The MAPK pathway across different malignancies: a new perspective. Cancer. 2014;120(22):3446-56. Epub 2014/06/21.
177. Bardwell L, Shah K. Analysis of mitogen-activated protein kinase activation and interactions with regulators and substrates. Methods (San Diego, Calif). 2006;40(3):213-23.
178. Atanaskova N, Keshamouni VG, Krueger JS, Schwartz JA, Miller F, Reddy KB. MAP kinase/estrogen receptor cross-talk enhances estrogen-mediated signaling and tumor growth but does not confer tamoxifen resistance. Oncogene. 2002;21(25):4000-8. Epub 2002/05/31.

179. Manole D, Schildknecht B, Gosnell B, Adams E, Derwahl M. Estrogen Promotes Growth of Human Thyroid Tumor Cells by Different Molecular Mechanisms1. The Journal of Clinical Endocrinology & Metabolism. 2001;86(3):1072-7.
180. Rossouw JE, Anderson GL, Prentice RL, LaCroix AZ, Kooperberg C, Stefanick ML, et al. Risks and benefits of estrogen plus progestin in healthy postmenopausal women: principal results From the Women's Health Initiative randomized controlled trial. Jama. 2002;288(3):321-33. Epub 2002/07/19.
181. Rajoria S, Suriano R, Shanmugam A, Wilson YL, Schantz SP, Geliebter J, et al. Metastatic phenotype is regulated by estrogen in thyroid cells. Thyroid. 2010;20(1):33-41. Epub 2010/01/14.
182. Rahbari R, Zhang L, Kebebew E. Thyroid cancer gender disparity. Future oncology (London, England). 2010;6(11):1771-9.
183. Hachim MY, Hachim IY, Elemam NM, Hamoudi RA. Toxicogenomic analysis of publicly available transcriptomic data can predict food, drugs, and chemical-induced asthma. Pharmgenomics Pers Med. 2019;12:181-99. Epub 2019/11/07.
184. Bayliss J, Hilger A, Vishnu P, Diehl K, El-Ashry D. Reversal of the estrogen receptor negative phenotype in breast cancer and restoration of antiestrogen response. Clin Cancer Res. 2007;13(23):7029-36. Epub 2007/12/07.
185. Kimura M, Amino N, Tamaki H, Mitsuda N, Miyai K, Tanizawa O. Physiologic thyroid activation in normal early pregnancy is induced by circulating hCG. Obstetrics and Gynecology. 1990;75:775-8.
186. Barkett M, Gilmore TD. Control of apoptosis by Rel/NF-kappaB transcription factors. Oncogene. 1999;18(49):6910-24. Epub 1999/12/22.
187. Visconti R, Cerutti J, Battista S, Fedele M, Trapasso F, Zeki K, et al. Expression of the neoplastic phenotype by human thyroid carcinoma cell lines requires NFkappaB p65 protein expression. Oncogene. 1997;15(16):1987-94. Epub 1997/11/19.
188. Fusco A, Grieco M, Santoro M, Berlingieri MT, Pilotti S, Pierotti MA, et al. A new oncogene in human thyroid papillary carcinomas and their lymph-nodal metastases. Nature. 1987;328(6126):170-2. Epub 1987/07/09.
189. Kimura ET, Nikiforova MN, Zhu Z, Knauf JA, Nikiforov YE, Fagin JA. High prevalence of BRAF mutations in thyroid cancer: genetic evidence for constitutive activation of the RET/PTC-RAS-BRAF signaling pathway in papillary thyroid carcinoma. Cancer Res. 2003;63(7):1454-7. Epub 2003/04/03.
190. Namba H, Gutman RA, Matsuo K, Alvarez A, Fagin JA. H-ras protooncogene mutations in human thyroid neoplasms. J Clin Endocrinol Metab. 1990;71(1):223-9. Epub 1990/07/01.
191. Baldwin AS. Control of oncogenesis and cancer therapy resistance by the transcription factor NF-kappaB. J Clin Invest. 2001;107(3):241-6. Epub 2001/02/13.
192. Vasko V, Saji M, Hardy E, Kruhlak M, Larin A, Savchenko V, et al. Akt activation and localisation correlate with tumour invasion and oncogene expression in thyroid cancer. J Med Genet. 2004;41(3):161-70. Epub 2004/02/27.
193. Kim D, Chung J. Akt: versatile mediator of cell survival and beyond. J Biochem Mol Biol. 2002;35(1):106-15. Epub 2005/10/27.
194. Jung HS, Kim DW, Jo YS, Chung HK, Song JH, Park JS, et al. Regulation of protein kinase B tyrosine phosphorylation by thyroid-specific oncogenic RET/PTC kinases. Mol Endocrinol. 2005;19(11):2748-59. Epub 2005/07/05.
195. Vasko V, Espinosa AV, Scouten W, He H, Auer H, Liyanarachchi S, et al. Gene expression and functional evidence of epithelial-to-mesenchymal transition in papillary thyroid carcinoma invasion. Proc Natl Acad Sci U S A. 2007;104(8):2803-8. Epub 2007/02/14.
196. Bartha A, Gyorffy B. TNMplot.com: A Web Tool for the Comparison of Gene Expression in Normal, Tumor and Metastatic Tissues. Int J Mol Sci. 2021;22(5). Epub 2021/04/04.
197. Kieran MW, Kalluri R, Cho YJ. The VEGF pathway in cancer and disease: responses, resistance, and the path forward. Cold Spring Harb Perspect Med. 2012;2(12):a006593. Epub 2012/12/05.
198. Mohamad Pakarul Razy NH, Wan Abdul Rahman WF, Win TT. Expression of Vascular Endothelial Growth Factor and Its Receptors in Thyroid Nodular Hyperplasia and Papillary Thyroid Carcinoma: A Tertiary Health Care Centre Based Study. Asian Pac J Cancer Prev. 2019;20(1):277-82. Epub 2019/01/27.

199. Arbiser JL. Molecular regulation of angiogenesis and tumorigenesis by signal transduction pathways: evidence of predicTable and reproducible patterns of synergy in diverse neoplasms. Semin Cancer Biol. 2004;14(2):81-91. Epub 2004/03/17.
200. Kranenburg O, Gebbink MF, Voest EE. Stimulation of angiogenesis by Ras proteins. Biochim Biophys Acta. 2004;1654(1):23-37. Epub 2004/02/27.
201. Kim D. The Role of Vitamin D in Thyroid Diseases. International journal of molecular sciences. 2017;18(9):1949.
202. Stepien T, Krupinski R, Sopinski J, Kuzdak K, Komorowski J, Lawnicka H, et al. Decreased 1-25 dihydroxyvitamin D3 concentration in peripheral blood serum of patients with thyroid cancer. Arch Med Res. 2010;41(3):190-4. Epub 2010/08/05.
203. Clinckspoor I, Verlinden L, Mathieu C, Bouillon R, Verstuyf A, Decallonne B. Vitamin D in thyroid tumorigenesis and development. Prog Histochem Cytochem. 2013;48(2):65-98. Epub 2013/07/31.
204. Viala M, Firmin N, Touraine C, Pouderoux S, Metge M, Rifai L, et al. Changes in vitamin D and calcium metabolism markers in patients undergoing adjuvant chemotherapy for breast cancer. BMC Cancer. 2021;21(1):815. Epub 2021/07/17.
205. Yavropoulou MP, Panagiotou G, Topouridou K, Karayannopoulou G, Koletsa T, Zarampoukas T, et al. Vitamin D receptor and progesterone receptor protein and gene expression in papillary thyroid carcinomas: associations with histological features. J Endocrinol Invest. 2017;40(12):1327-35. Epub 2017/06/08.
206. Bains A, Mur T, Wallace N, Noordzij JP. The Role of Vitamin D as a Prognostic Marker in Papillary Thyroid Cancer. Cancers (Basel). 2021;13(14). Epub 2021/07/25.

Asma Almansoori

Address : Sharjah, UAE

u17404342@sharjah.ac.ae

Work Experience

- Policy management Acting Senior officer, Sheikh Khalifa Hospital
- Graduate Medical education officer for Surgery, Opthalmology, and dermatology residency programs, Post Graduate medical education institute, Sheikh Khalifa Hospital
- Quality & Environmental health and safety link officer, Sheikh Khalifa Hospital
- Diabetic research officer, Abu Dhabi Diabetic center, Sheikh Khalifa hospital
- Medical liability officer, Emirates International Law Centre
- Braille and English sign language instructor, Cerebral Palsy, Visual and Auditory Disability section (RAK-special needs centre)
- Medical quality and patients' safety officer, Sheikh Khalifa Hospital
- Medical Innovations and Accreditation officer, Sheikh Khalifa Hospital

Education

- Pre-Med: BSc in Community Health Science and Biological Sciences, Canada
- Master of Science in Hospital management
- Post-graduate higher diploma in S. Government Consulting, Dubai
- Pre-Health Sciences, Canada
- Advanced English (General Art& Sciences program), Canada
- Advanced English, London, Ontario, Canada

Ongoing Education

- Ph.D. in Molecular Medicine
- Doctor of Dental Surgery (50credits-Recipient of MHE full scholarship)
- Current candidate for American board of medical quality Examination

Awards/Scholarships

- 2010 Full-year: Dean's Honor List, Faculty of Applied Health Sciences, Brock University, Canada.
- 2007 -2008: Honors Standing. Pre- Health Sciences, Niagara College, Canada.
- 2007 s: President's Honour Roll*, General Art& Sciences program, Niagara College, Canada.
- Recipient of Ministry of Higher education scholarship for academic excellence.UAE.
- Recipient of H.H.sheikh Sultan alQasimi full Ph.D. scholarship(Sharjah Government cabinets authority)

Skills

- Certified in GIS remote sensing for humanitarian actions
- Certified in ArcGIS for managing solutions
- Certified in professional healthcare quality

Professional memberships

- Member of American College of Medical Quality.
- Member of Society for Simulation in Healthcare, USA
- Member of National Commission on correctional health care
- Member of International Society for Quality in Health Care.
- Member of National Emergency Preparedness Operational Committee.Sheikh Khalifa Medical City, Abu Dhabi, UAE.
- Member of Clinical Competency Committee (American Accreditation for graduate medical residency programs) Skmc, Abu Dhabi, United Arab Emirates.
- SKMC medical Research Committee membership, Abu Dhabi, UAE

Languages

English, Arabic